

**ZOOPLANKTON COMMUNITY COMPOSITION AND GRAZING IN THE
AMAZON RIVER PLUME AND WESTERN TROPICAL NORTH ATLANTIC
OCEAN**

A Dissertation

Presented to

The Faculty of the School of Marine Science

The College of William and Mary in Virginia

In Partial Fulfillment

of the Requirements for the Degree of

Doctor of Philosophy

by

Brandon Judd Conroy

2016

APPROVAL SHEET

This thesis is submitted in partial fulfillment of
the requirements for the degree of
Doctor of Philosophy in Marine Science

Brandon J. Conroy

Approved August 1, 2016

Deborah K. Steinberg, Ph.D.
Committee Chair/Advisor

Deborah A. Bronk, Ph.D.

Rachel A. Foster, Ph.D.

Walker O. Smith, Jr., Ph.D.

Kam W. Tang, Ph.D.

TABLE OF CONTENTS

	<u>Page</u>
ACKNOWLEDGEMENTS	v
LIST OF TABLES	vi
LIST OF FIGURES	vii
ABSTRACT	x
CHAPTER 1	
Introduction to the dissertation	2
References.....	8
CHAPTER 2	
Mesozooplankton community composition in the Amazon River plume and western tropical North Atlantic Ocean	12
Abstract	13
1. Introduction.....	14
2. Methods.....	17
3. Results.....	20
4. Discussion	26
5. Conclusion	32
References.....	34
CHAPTER 3	
Meso- and microzooplankton grazing in the Amazon River plume and western tropical North Atlantic Ocean.....	65
Abstract	66
1. Introduction.....	67
2. Methods.....	71
3. Results.....	79
4. Discussion	84
5. Conclusion	92
References.....	94
CHAPTER 4	
Mesozooplankton grazing of cyanobacteria in the Amazon River plume and western tropical North Atlantic Ocean	114
Abstract	115
1. Introduction.....	116

2. Methods.....	120
3. Results.....	126
4. Discussion	130
5. Conclusion	138
References.....	140
CHAPTER 5	
Summary and Concluding Remarks	163
References.....	168
VITA.....	172

ACKNOWLEDGEMENTS

I am grateful to the many friends and family members that have supported me through my dissertation work. My advisor Debbie Steinberg has provided an outstanding example to follow in both my professional and personal life. I am thankful to my committee members for their interest and feedback in my research. I would also like to acknowledge funding support from the National Science Foundation (grants OCE-0934036 and DGE-0840804).

All of the former and current members of the Zooplankton Ecology Lab are an amazing family I'm proud to be a part of and am appreciative of the support and encouragement they provided. Even if it meant dealing with: Joe's grumblings, Lori's Pittsburgh cult membership, Miram's glitter and dubstep, Jeanna's...you were good, Josh's relentless birding, Jami's unwavering optimism, and Tricia's ear shattering goose honk, it was all worth it because I could rely on Kate's mom to be there for me anytime.

I would also like to thank all of my VIMS friends and family who have made VIMS and Gloucester Point an outstanding home while I pursued my degree. The student experience is what makes VIMS such a great place and I will always appreciate my time in GloPo.

Lastly, to my family, thank you for your support and encouragement while I pursued my degree. Even if you weren't sure what I was doing, I appreciated you listening to me ramble about plankton and marine life and without you I wouldn't be where I am today.

LIST OF TABLES

<u>Chapter 2</u>		<u>Page</u>
Table 1	Linear regressions for sea surface salinity vs. depth-integrated abundance of mesozooplankton taxonomic groups	43
Table S1	Spring (May-June) 2010 150m depth-integrated abundances for zooplankton taxa enumerated in this study.....	54
Table S2	Fall (Sept. – Oct.) 2011 150m depth-integrated abundances for zooplankton taxa enumerated in this study.....	58
<u>Chapter 3</u>		
Table 1	Average total mesozooplankton spring and fall depth-integrated grazing rates (mg Chl <i>a</i> equivalent m ⁻² day ⁻¹) by station category...	104
Table 2	Average mesozooplankton grazing impact from 0-150m and 0-25m for spring and fall by station category.....	105
<u>Chapter 4</u>		
Table S1	List of samples utilized in qPCR assays targeting het-1 (<i>Rhizosolenia</i> - <i>Richelia</i> DDA) and het-2 (<i>Hemiaulus</i> - <i>Richelia</i> DDA) and <i>Trichodesmium</i> spp with target amplifications reported..	156
Table S2	TaqMAN oligonucleotides used in qPCR assays.....	160
Table S3	Summary of samples and results from the next generation sequencing study.....	161

LIST OF FIGURES

<u>Chapter 2</u>		
		<u>Page</u>
Figure 1	Cruise maps of stations included in spring and fall mesozooplankton community composition analysis from the Amazon River plume and western tropical North Atlantic.....	44
Figure 2	Non-metric multidimensional scaling analysis (nMDS) ordination of spring and fall square root transformed, 150m depth-integrated mesozooplankton abundances.....	45
Figure 3	Average 150m depth-integrated abundance of major copepod order abundance compared between salinity categories and season.....	46
Figure 4	Surface salinity vs. total copepod abundance (0-150m integrated) regressions for spring and fall daytime and nighttime values.....	47
Figure 5	Spring daytime distribution of surface salinity and 150m depth-integrated abundances (individuals m ⁻²) for chaetognaths and copepod orders	48
Figure 6	Fall daytime distribution of surface salinity and 150m depth-integrated abundances (individuals m ⁻²) for chaetognaths and copepod orders	49
Figure 7	Spring daytime areal distribution of surface salinity and 150m depth-integrated abundances (individuals m ⁻²) for fish larvae, decapods, and euphausiids	50
Figure 8	Fall daytime areal distribution of surface salinity and 150m depth-integrated abundances (individuals m ⁻²) for fish larvae, decapods, and euphausiids	51
Figure 9	Day and night depth profiles for each station categories for calanoid copepods and decapod larvae representative of the two general vertical distributions observed in Amazon River plume waters	52
Figure 10	Vertical distributions of salinity, <i>Lucifer faxoni</i> , and chaetognaths in a fall plume transect	53
Figure S1	Surface salinity vs. total mesozooplankton abundance (0-150m integrated) regressions for spring and fall daytime and nighttime values	62

Figure S2 Spring daytime distribution of surface salinity and 150m depth-integrated abundances (individuals m⁻²) for selected non-copepod taxa 63

Figure S3 Fall daytime distribution of surface salinity and 150m depth-integrated abundances (individuals m⁻²) for selected non-copepod taxa 64

Chapter 3 Page

Figure 1 Stations sampled for mesozooplankton gut fluorescence and microzooplankton grazing in the Amazon River plume-Influenced waters and the western tropical North Atlantic 106

Figure 2 Daytime and nighttime surface salinity vs. mesozooplankton grazing (0–150 m integrated) during spring, and fall 107

Figure 3 Surface salinity and daytime grazing (0–150m integrated) areal distributions in the Amazon River plume region 108

Figure 4 Size-fractionated mesozooplankton daytime grazing (mg Chl-*a* equiv. m⁻³ day⁻¹) depth profiles in fall averaged by salinity category, size class, and depth interval 109

Figure 5 Vertical distributions of salinity and mesozooplankton community Grazing in a fall plume transect 110

Figure 6 Bulk phytoplankton growth vs. microzooplankton grazing rate across all salinity ranges in fall 111

Figure 7 Natural logarithm of photosynthetically active radiation (PAR) vs. bulk phytoplankton growth (A) and microzooplankton grazing (B) in fall 112

Figure 8 Instantaneous rates of change for phytoplankton growth (μ), microzooplankton grazing (m), and mesozooplankton total grazing (M_{TOT}) or daytime mesozooplankton (M_{DAY}) in fall 113

Chapter 4 Page

Figure 1 Cruise track from ANACONDAS cruise in May-June, 2010 with stations sampled for molecular analysis 151

Figure 2	Number of positive qPCR target hits for each primer target calanoid copepods (n=50 assays of pooled individuals), crab megalopae (n=2 assays), and the harpacticoid copepod <i>Macrosetella gracilis</i> 152
Figure 3	Principle coordinates analysis of 16S zooplankton microbial community shown by zooplankton taxonomic group 153
Figure 4	Bacterial community composition by phylum as determined by 16S next generation sequencing 154
Figure 5	Cyanobacteria sequence composition by taxonomic class as determined by 16S next generation sequencing 155

ABSTRACT

Large river plumes and frontal zones are important physical features influencing plankton distribution in the marine environment. In the western tropical North Atlantic Ocean (WTNA) the Amazon River plume may extend over an area reaching 1.5×10^6 km². The freshwater plume creates a low-density lens in the surface 25m and supplies silicon and phosphorus to the WTNA. These physical and chemical gradients create an ideal environment for large-scale blooms of diatom diazotroph associations (DDAs), a symbiotic relationship between nitrogen-fixing cyanobacteria and chain-forming diatoms. While the physical and chemical properties of the plume with regard to influences on phytoplankton have been reported, zooplankton distributions and the fate of enhanced primary production in the plume are largely unknown. I investigated mesozooplankton (>200 µm) composition and grazing in the Amazon River plume-influenced WTNA in spring (May-June 2010) and fall (Sept.-Oct. 2011). Changes in zooplankton distribution and grazing occurred over the sea surface salinity (SSS) gradient from low salinity and mesohaline plume waters to high salinity oceanic waters. Distinct communities were identified in each season along the salinity gradient with several taxa primarily constrained in the surface plume waters (e.g., *Lucifer faxonii*). The plume appears to function as an “extended estuary”, with a number of taxa (e.g., decapods, euphausiids, and fish larvae) utilizing the plume as a nursery habitat or dispersal mechanism for larval stages. Mesozooplankton grazing was elevated in plume waters compared to oceanic waters and was 2-3 times higher in the fall vs. spring. These patterns suggest a lag in the peak mesozooplankton abundance and grazing in response to the observed spring DDA bloom, at least in low salinity plume waters. Comparison of micro- and mesozooplankton grazing along the SSS gradient supported a transition from an “export” food web in waters with SSS < 33 where mesozooplankton grazing dominated and potential for export via fecal pellet production is higher, to a “retention” food web at SSS above 33 where microzooplankton grazing was highest and recycling of nutrients in surface waters is predicted. Using molecular techniques to investigate feeding on DDAs and other N-fixers, I found that copepods consumed DDAs (*Hemiallus-Richeliea* and *Rhizosolenia-Richeliea*, diatom-diazotroph respectively) as well as the colonial cyanobacterium *Trichodesmium*. Investigation of mesozooplankton grazing more broadly on other cyanobacteria with 16S rRNA sequencing revealed consumption of *Synechococcus*, *Prochlorococcus*, and the unicellular diazotroph UCYN-A Candidatus *Atelocyanobacterium thalassa*. Together, these results have important implications for our understanding of biogeochemical cycling in the WTNA, and other regions with abundant DDAs (e.g., the Mekong and Congo River plumes).

Brandon Judd Conroy

SCHOOL OF MARINE SCIENCE
THE COLLEGE OF WILLIAM AND MARY

**ZOOPLANKTON COMMUNITY COMPOSITION AND GRAZING IN THE
WESTERN TROPICAL NORTH ATLANTIC AND AMAZON RIVER PLUME**

CHAPTER 1

Introduction to the dissertation

The Amazon River plume-influenced western tropical North Atlantic Ocean

The Amazon River contributes approximately 20% of the total fresh water riverine input into the world oceans (Davis 1964). This massive outflow creates a seasonal plume that stretches approximately $1.5 \times 10^6 \text{ km}^2$ into the western tropical North Atlantic (WTNA) (Moller et al. 2010; Coles et al. 2013). The quantity and rate of river discharge forces mixing to occur on the continental shelf rather than in the coastal estuary as in most river deltas (Nittrouer and DeMaster 1996). Prior work investigating the influence of the physics and chemistry of the Amazon River plume on primary production indicates the plume supports increased productivity in the WTNA, driving a net sink of carbon from the atmosphere to the ocean (Cooley et al. 2007; Subramaniam et al. 2008). This biologically-mediated carbon sink is possible because of riverine input of nitrogen (N), phosphorus (P), and silica (Si). By the time plume waters reach offshore, particularly ‘mesohaline’ plume waters with sea surface salinity (SSS) between 30 and 35, riverine N has been removed yet there are still high concentrations of P and Si that supports high N₂-fixation by diatom-diazotroph associations (DDAs). (Carpenter et al. 1999; Subramaniam et al. 2008). The cyanobacterium *Richelia intracellularis* is an endosymbiont within the diatom hosts *Hemialus* spp. and *Rhizosolenia* spp. This symbiotic relationship provides the diatom host with fixed nitrogen (Foster et al. 2011), allowing the diatom to form significant blooms in the mesohaline region of the plume. Further offshore, the Si and P become depleted and there is a shift in the phytoplankton to typical oligotrophic species, and the dominant nitrogen fixer is the colonial cyanobacterium *Trichodesmium* (Carpenter et al. 2004; Capone et al. 2005; Foster et al. 2007; Subramaniam et al. 2008). While these patterns have been consistently observed

for phytoplankton in the Amazon River plume, influence of the plume on zooplankton abundance and community composition, and how grazing may affect the fate of enhanced primary production in the plume, are largely unknown.

Zooplankton community structure, grazing, and the biological pump

Region-specific zooplankton data for the Amazon River Plume-influenced WTNA is very limited. Information on zooplankton abundance and community composition in this region stems from a single study, which reported an increase in total zooplankton displacement volume and copepod abundance during the wet season (peak outflow of Amazon) compared to the fall dry season (Calef & Grice 1967). The taxonomic analysis was limited to copepod diversity, although it was noted that cladocera and decapod abundances in the surface 10m were associated with the low-salinity plume. The AmasSeds (A Multidisciplinary Amazon Shelf SEDiment Study) project results suggested zooplankton impact the distribution of biogenic silica and organic carbon by grazing on siliceous phytoplankton in Amazon-influenced waters (DeMaster et al. 1996). However, AmasSeds was restricted to the mouth of the Amazon River rather than the larger WTNA, and only total zooplankton abundance was reported and grazing was not measured.

While no prior studies have investigated zooplankton grazing in the WTNA, mesozooplankton grazing rates in the eastern tropical Atlantic were highest for the large size class ($> 1000 \mu\text{m}$) (Isla et al. 2004) and copepod community ingestion was highest around the Azores Front (Huskin et al. 2001). Our knowledge of grazing of cyanobacteria, and N₂ fixing populations such as DDAs or the colonial cyanobacterium *Trichodesmium*, for example, is also limited. Studies investigating grazing by *Trichodesmium* on

mesozooplankton suggest harpacticoid copepods are the main grazers (O’Neil and Roman 1994; O’Neil 1998), and that most other taxa avoid *Trichodesmium* due to its toxicity and unpalatability (Turner 2014). Given that DDA blooms have been observed in other large river plumes (e.g., the Mekong and Congo) and the global importance of *Trichodesmium* (Capone et al. 1997), understanding the role zooplankton play in the fate of both of these primary producers in the WTNA has important implications for both regional and global biogeochemical cycling.

Zooplankton play an integral role in the biological pump, grazing in surface waters and transporting carbon to the deep ocean via fecal pellet production and active transport by diel vertical migration (Ducklow et al. 2001; Steinberg et al. 2002; Turner 2015). Mesozooplankton repackage surface primary productivity into dense, fast sinking, fecal pellets (Landry et al. 1995; Legendre and Michaud 1998), while microzooplankton efficiently graze phytoplankton and regenerate nutrients and organic material in surface waters (Pomeroy et al. 2007). The efficiency by which organic material is transferred and sequestered in the deep ocean via the biological pump is dependent upon the regional planktonic community structure (Landry et al. 1995; Ducklow 2001). Open ocean environments are often characterized as retention food webs where small phytoplankton are efficiently grazed by microzooplankton, retaining nutrients and organic material in the surface waters. Conversely, export food webs common to upwelling or coastal regions, are distinguished by large phytoplankton and potentially shorter food webs, with phytoplankton sinking out in aggregates or grazed by large zooplankton producing rapidly sinking fecal pellets (Michaels and Silver 1988; Legendre and Michaud 1998). Enhanced primary production and differences in phytoplankton and zooplankton

community structure in river plumes may thus lead to regional changes in the biological pump.

Structure of dissertation

This dissertation is separated into three main chapters and presents results from two research cruises that were part of the Amazon INfluence on the Atlantic: CarbOn export from Nitrogen fixation by DiAtom Symbioses (ANACONDAS) project. The two cruises occurred May 22-June 24, 2010 aboard the *R/V Knorr* and September 3-October 8, 2011 aboard the *R/V Melville*, and were designed to provide a seasonal snapshot of plume biogeochemistry in the spring and fall, respectively.

In Chapter 2, I provide a detailed description of the mesozooplankton community composition along the plume salinity gradient. I discuss seasonal patterns in the context of the progression of the DDA bloom as well as highlight for several taxa the functioning of the plume as an “extended” estuary hundreds of kilometers into the WTNA and utilization of the plume as a nursery habitat.

In Chapter 3, I investigate both mesozooplankton and microzooplankton grazing within the plume and WTNA. I discuss these results with respect to seasonal progression of the bloom and the relative importance of mesozooplankton versus microzooplankton grazing in regards to structuring the food web and affecting export of carbon in the WTNA.

In Chapter 4, I investigate the direct grazing of mesozooplankton on DDAs and cyanobacteria using molecular methodology. I discuss the results of quantitative polymerase chain reaction (qPCR) for two DDAs and for the cyanobacteria

Trichodesmium. I then discuss the diversity of cyanobacteria in gut contents of mesozooplankton analyzed with 16S rRNA gene sequencing.

In Chapter 5, I provide a summary of results from my dissertation and suggestions for future research directions stemming from this research.

REFERENCES

- Carpenter EJ, Montoya JP, Burns J, Mulholland MR, Subramaniam A, Capone DG (1999) Extensive bloom of a N₂-fixing diatom/cyanobacterial association in the tropical Atlantic Ocean. *Marine Ecology Progress Series*, 185: 273-283
- Carpenter EJ, Subramaniam A,, Capone D.G. (2004) Biomass and primary productivity of the cyanobacterium, *Trichodesmium* spp, in the tropical N Atlantic Ocean. *Deep-Sea Research I* 51:173–203
- Capone, D. G., J. P. Zehr, H. W. Paerl, B. Bergman, and E. J. Carpenter. 1997. *Trichodesmium*, a Globally Significant Marine Cyanobacterium. *Science* **276**: 1221–1229. doi:10.1126/science.276.5316.1221
- Capone D, Burns JA, Montoya JP, Subramaniam A, Mahaffey C, Gunderson T, Michaels AF, Carpenter EJ (2005) Nitrogen fixation by *Trichodesmium* spp: An important source of new nitrogen to the tropical and subtropical North Atlantic Ocean. *Global Biogeochemical Cycles* 19: GB2024
- Coles, V. J., M. T. Brooks, J. Hopkins, M. R. Stukel, P. L. Yager, and R. R. Hood. 2013. The pathways and properties of the Amazon River Plume in the tropical North Atlantic Ocean: AMAZON RIVER PLUME. *J. Geophys. Res. Oceans* **118**: 6894–6913. doi:10.1002/2013JC008981
- Cooley SR, Coles VJ, Subramaniam A, Yager PL (2007) Seasonal variations in the Amazon plume-related atmospheric carbon sink. *Global Biogeochemical Cycles* 21: GB3014
- Dagg, M. J. 1995. Copepod grazing and the fate of phytoplankton in the northern Gulf of Mexico. *Cont. Shelf Res.* **15**: 1303–1317. doi:10.1016/0278-4343(94)00086-3

- Davis, LC (1964) The Amazon's rate of flow. *Natural History*, **73**:14-19
- Ducklow HW, Steinberg DK, Buesseler KO (2001) Upper ocean carbon export and the biological pump. *Oceanography* **14**: 50-58
- Flint, M. V., T. N. Semenova, E. G. Arashkevich, I. N. Sukhanova, V. I. Gagarin, V. V. Kremenetskiy, M. A. Pivovarov, and K. A. Soloviev. 2010. Structure of the zooplankton communities in the region of the Ob River's estuarine frontal zone. *Oceanology* **50**: 766–779. doi:10.1134/S0001437010050139
- Govoni, J. J., D. E. Hoss, and D. R. Colby. 1989. The spatial distribution of larvalfishes about the Mississippi River plume. *Limnol. Oceanogr.* **34**: 178–187. doi:10.4319/lo.1989.34.1.0178
- Grimes, C. B., and J. H. Finucane. 1991. Spatial distribution and abundance of larval and juvenile fish, chlorophyll and macrozooplankton around the Mississippi River discharge plume, and the role of the plume in fish recruitment. *Marine ecology progress series. Oldendorf* **75**: 109–119.
- Huskin I, Anadón R, Medina G, Head RN, Harris RP (2001) Mesozooplankton distribution and copepod grazing in the Subtropical Atlantic near the Azores: Influence of mesoscale structures. *Journal of Plankton Research* **23**: 671-691
- Isla JA, Llope M, Anadón R (2004) Size-fractionate mesozooplankton biomass, metabolism and grazing along a 50°N-30°S transect of the Atlantic Ocean. *Journal of Plankton Research* **26**: 1301-1313
- Foster RA, et al. (2007) Influence of the Amazon River plume on distributions of free-living and symbiotic cyanobacteria in the western tropical North Atlantic Ocean. *Limnology and Oceanography* **52**:517–532

Foster, R. A., A. Subramaniam, and J. P. Zehr. 2009. Distribution and activity of diazotrophs in the Eastern Equatorial Atlantic. *Environ Microbiol* **11**: 741–750.
doi:10.1111/j.1462-2920.2008.01796.x

Govoni, J. J., D. E. Hoss, and D. R. Colby. 1989. The spatial distribution of larvalfishes about the Mississippi River plume. *Limnol. Oceanogr.* **34**: 178–187.
doi:10.4319/lo.1989.34.1.0178

Grosse, J., D. Bombar, H. N. Doan, L. N. Nguyen, and M. Voss. 2010. The Mekong River plume fuels nitrogen fixation and determines phytoplankton species distribution in the South China Sea during low and high discharge season. *Limnology and Oceanography* **55**: 1668–1680. doi:10.4319/lo.2010.55.4.1668

Moller, G. S. F., E. M. L. d. M. Novo, and M. Kampel. 2010. Space-time variability of the Amazon River plume based on satellite ocean color. *Cont. Shelf Res.* **30**: 342–352. doi:10.1016/j.csr.2009.11.015

Morgan, C. A., A. De Robertis, and R. W. Zabel. 2005. Columbia River plume fronts. I. Hydrography, zooplankton distribution, and community composition. *Mar. Ecol.-Prog. Ser.* **299**: 19–31. doi:10.3354/meps299019

Nittrouer CA & DeMaster DJ (1996) The Amazon shelf setting: tropical, energetic, and influenced by a large river. *Continental Shelf Research* **16**: 553-573

Pomeroy, L., P. leB. Williams, F. Azam, and J. Hobbie. 2007. The Microbial Loop. *Oceanography* **20**: 28–33. doi:10.5670/oceanog.2007.45

Subramaniam A, Yager PL, Carpenter EJ, Mahaffey C, Bjorkman K, Cooley S, Montoya J, Sanudo-Wilhelmy S, Shipe R, Capone DG (2008) Amazon River enhances diazotrophy and carbon sequestration in the tropical North Atlantic Ocean.

Proceedings, National Academy of Sciences 105: 10460-10465 DOI

10.1073/pnas.0710279105

Steinberg, D. K., S. A. Goldthwait, and D. A. Hansell. 2002. Zooplankton vertical migration and the active transport of dissolved organic and inorganic nitrogen in the Sargasso Sea. Deep Sea Research Part I: Oceanographic Research Papers **49**: 1445–1461.

Turner, J. T. 2014. Planktonic marine copepods and harmful algae. Harmful Algae **32**: 81–93. doi:10.1016/j.hal.2013.12.001

Turner, J. T. 2015. Zooplankton fecal pellets, marine snow, phytodetritus and the ocean's biological pump. Progress in Oceanography **130**: 205–248.
doi:10.1016/j.pocean.2014.08.005

CHAPTER 2

**Mesozooplankton community composition in the Amazon River plume and
western tropical North Atlantic Ocean**

ABSTRACT

River plumes and associated fronts are physical features that may increase abundance and influence taxonomic composition of zooplankton due to a response of enhanced primary production or via physical aggregation. We measured epipelagic mesozooplankton community composition along the Amazon River plume salinity gradient in the western tropical North Atlantic (WTNA). Sampling occurred in spring (May-June) 2010 during the peak outflow of the Amazon River and in fall (September-October) 2011 during the plume seasonal retroflection. Total mesozooplankton and total copepod abundances were positively correlated with sea surface salinity (SSS) in the spring, but both were negatively correlated with SSS in the fall. These trends were driven by seasonal abundance changes in oceanic ($SSS > 35$) and low salinity plume water ($SSS < 30$) rather than in the mesohaline waters ($30 < SSS < 35$). We also identified a number of zooplankton taxa, such as the coastal decapod shrimp *Lucifer faxoni*, as well as decapod and fish larvae, that utilize the Amazon River plume as a nursery habitat in much the same way as traditional coastal estuaries. Through aggregative physical effects from frontal zone development and strong density gradients associated with the plume, or behavioral traits of mesozooplankton, we suggest that for some mesozooplankton taxa the plume functions as an “extended” estuary, supporting development in early life history stages for a variety of taxonomic groups.

1. INTRODUCTION

As drifting organisms, planktonic communities are strongly impacted by the physical processes that shape water masses in the marine environment. Enhanced abundance and biomass of phytoplankton and zooplankton in physical features such as estuarine turbidity maxima (Roman et al. 2001; North and Houde 2003), river plumes (Subramaniam et al. 2008; Flint et al. 2010; Bombar et al. 2011), mesoscale eddies (Goldthwait and Steinberg 2008; Eden et al. 2009) and frontal regions (Hunt et al. 2002; Hernández-León et al. 2013) have important short- and long-term impacts on biogeochemical cycling and support of higher trophic levels (Benoit-Bird and McManus 2012; Woodson and Litvin 2015). The Amazon River plume at its maximum extent expands out over $1.5 \times 10^6 \text{ km}^2$ of the western tropical North Atlantic (WTNA) (Moller et al. 2010; Coles et al. 2013). The plume creates a gradient of physical and chemical properties that support varied communities of phytoplankton along the gradient, particularly diatom diazotroph associations (DDAs) (Carpenter et al. 1999; Foster et al. 2007; Goes et al. 2014). In the plume-influenced WTNA region, stable isotope analysis of mesozooplankton (i.e., zooplankton $> 0.2\text{mm}$) and particles (Loick-Wilde et al. 2016), and mesozooplankton grazing measurements using gut pigments (Conroy et al. 2016) and molecular probing of gut contents (Conroy et al. in prep) indicate zooplankton consume DDAs and other nitrogen fixers (e.g., *Trichodesmium* and UCYN-A), yet the taxonomic composition of the mesozooplankton community remains poorly known. This study investigates how mesozooplankton community composition varies along the salinity gradient associated with the Amazon River plume relative to the surrounding open ocean.

Reports of zooplankton biomass or community composition for the Amazon Plume and WTNA region are limited. An increase in zooplankton biomass was documented during the wet season (May-June peak outflow of Amazon River), and in the low salinity lens sampled in the top 10 m of the water column, the coastal cladocera *Evadne tergestina* and decapod *Lucifer faxoni* were two and five times more abundant, respectively, than total copepod abundance within the same surface layer (Calef and Grice 1967). All other taxonomic analysis in that study was limited to copepod diversity, and because there was no discrete depth sampling, limited conclusions could be made about zooplankton vertical structure with regards to the plume. Results from AmasSeds (A Multidisciplinary Amazon Shelf SEDiment Study) indicate copepods were the most abundant taxa near the mouth of the Amazon River in shallow water (< 200 m), with the highest abundances occurring in the late summer and fall (August and November, respectively) (DeMaster et al. 1996). Total zooplankton abundance was reported without detailed taxonomic information, although elevated numbers of crab larvae at some stations are mentioned, and the offshore regions of the plume and WTNA were not sampled. The remaining studies investigating zooplankton community composition in this region are limited to shallow Amazon River coastal estuaries (e.g. Magalhães et al. 2009; Costa et al. 2009).

There is also limited work on zooplankton abundance on a larger scale in the tropical North Atlantic. Piontkovski and Landry (2003) analyzed copepod composition data from former Soviet Union transects of the Atlantic from 1963 to 1989 to investigate a hypothesized inter-decadal change in species diversity due to shifts in atmospheric wind patterns or warming, but found no statistical evidence of long-term change. Piontkovski

and Castellani (2009) expanded upon that study by analyzing additional Soviet Union transects (1950 to 1989) as well data from the UK Atlantic Meridional Transect program (AMT) (1995 to 2000). They reported a ten-fold decline in zooplankton biomass from 1950-2000, which they attributed to a decrease in primary production from increased stratification of the water column and range expansion of tropical species into the subtropics. These findings are also supported by the works of Beaugrand et al. (2002) and Ivory et al. (in preparation), but highlight the need for more work in the tropical Atlantic to understand the patterns and processes affecting zooplankton distributions.

In this study we investigated the effect of the Amazon River plume salinity gradient on mesozooplankton community structure— from low salinity, turbid intermediate (mesohaline) salinity plume waters, to high salinity, oceanic, oligotrophic waters. We highlight distribution patterns for a variety of mesozooplankton taxa that support the importance of river plumes and frontal regions for enhanced abundance and zones of aggregation. Identifying if zooplankton aggregate at certain salinities across the plume as well as vertically within the plume will provide insights into how zooplankton affect the fate of primary production in the WTNA and have broader implications for biogeochemical cycling.

2. METHODS

2.1 Study Location

We sampled mesozooplankton throughout the Amazon River plume-influenced WTNA (between 0-13° N and 44-57°W) as part of the Amazon Influence on the Atlantic: CarbOn export from Nitrogen fixation by DiAtom Symbioses (ANACONDAS) project. The analysis of zooplankton includes data from two cruises which occurred May 22-June 24, 2010 aboard the *R/V Knorr* and September 3-October 8, 2011 aboard the *R/V Melville*. In 2010, hereafter referred to as “spring”, we sampled during peak Amazon River discharge (Fig. 1A) while in 2011, referred to as “fall” hereafter, we sampled during the plume retroreflection, when the Amazon extends southeastward and reaches its maximum areal expanse (Coles et al. 2013) (Fig. 1B). Station selection was determined largely by underway (within top ~2 m) sea surface salinity (SSS) and Chl *a* fluorescence measured underway (Goes et al. 2014), and plume indicators such as chromophoric dissolved organic matter (CDOM) measured with satellite imagery. We categorize sampling stations into three groups: stations with SSS < 30 were classified as “low salinity” plume, stations with SSS between 30 and 35 as “mesohaline” stations, and stations with SSS > 35 as “oceanic” (Subramaniam et al. 2008; Goes et al. 2014; Conroy et al. 2016).

2.2 Zooplankton sampling and enumeration

Zooplankton were collected with a 1-m² Multiple Opening and Closing Net and Environment Sensing System (MOCNESS; Wiebe et al. 1976) containing ten 202 µm mesh nets. We present data for the top 0-150m, sampled in depth intervals of 0-25m, 25-50m, 50-100m, and 100-150m in the spring, with an additional depth interval added in the surface waters in the fall to better characterize the plume so that we sampled 0-10m

and 10-25m. Day and night tows were performed between 1000 and 1400 h and 2200 and 0200 h (local time), respectively. Once onboard, nets were rinsed with seawater and cod-end contents were split using a Folsom plankton splitter. Depending on other additional analyses required, $\frac{1}{4}$ or $\frac{1}{2}$ of the sample for each depth interval was preserved in 4% borax buffered formaldehyde for analysis of community composition.

Zooplankton were enumerated with an Olympus SZX10 stereo dissecting microscope using dark and light field illumination. Samples were first size-fractionated through two nested sieves (200 and 2000 μm). The $>2000\ \mu\text{m}$ fraction was usually counted in its entirety; on occasion very high biomass samples were split using a Folsom plankton splitter resulting in enumeration of 1/64th to 1/8th of the total tow. The 200-2000 μm fraction was subsampled using a 5 mL Stempel pipette with a minimum of 200 individuals identified per subsample (Alden III et al. 1982; Eden et al. 2009).

Zooplankton were identified to major taxonomic group (e.g., calanoid, harpacticoid, cyclopoid, or poecilostomatoid copepod; euphausiid; chaetognath) with some highly abundant or conspicuous taxa identified to species (e.g., the coastal decapod *Lucifer faxoni* and harpacticoid copepod *Macrosetella gracillis*). Twenty-two broad taxonomic groups comprising a total of 65 taxa are represented in our analyses. Table S1 and S2 lists all taxa identified.

2.3 Statistical Analyses

Statistical analyses were performed using SigmaPlot 11.0. Sea surface salinity was averaged over the top 5 m using data from the corresponding MOCNESS tow for comparisons of sea surface salinity vs. 150 m depth-integrated taxon abundance. Inter-seasonal comparisons were made with unpaired t-tests while intra-seasonal comparisons

between station salinity categories were analyzed with one-way ANOVA. When data did not meet the requirements of equal variance and normality, they were analyzed using non-parametric tests including the Mann-Whitney rank sum test for inter-seasonal comparisons and the Kruskal-Wallis ANOVA on ranks for intra-seasonal comparisons.

To further investigate if zooplankton composition varied along the plume salinity gradient, similar to patterns seen in phytoplankton (Subramaniam et al. 2008; Goes et al. 2014), we performed non-metric multidimensional scaling analysis (nMDS) in PRIMER 7 (Clarke et al. 1993; Clarke 2015). In this analysis all 65 possible taxa were used, abundances were square root transformed, and a Bray-Curtis similarity matrix was calculated.

3. RESULTS

3.1 Broad grouping with salinity

In spring mesozooplankton could be divided into two groups, with low sea surface salinity (SSS) plume stations grouping together, and mesohaline plume and oceanic stations in a separate cluster (Fig. 2A). In fall stations grouped into three distinct clusters— one for each of the three station SSS categories (Fig. 2B). Below we describe patterns for the most abundant taxa and for those exhibiting significant relationships with the salinity gradient. (See Table S1 and S2 for abundances for all taxa counted for day and night across all station categories.)

3.2 Total mesozooplankton, copepod, and other taxon depth-integrated patterns with salinity

For both seasons in the surface 150 m, copepods were the most abundant taxa across all salinities for both day and night and were dominated by calanoid copepods (Fig. 3; Table S1 and S2). In spring total mesozooplankton abundance over the plume salinity gradient varied by an order of magnitude during the day ($9.7 - 90.4 \times 10^3$ ind. m^{-2}) while nighttime abundance was less variable ($34.8 - 81.0 \times 10^3$ ind. m^{-2}). Copepods accounted for an average of 80.3% (day) and 88.0% (night) of total mesozooplankton abundance. The only exception to the dominance of copepods occurred at one mesohaline plume station where total copepods constituted only 49.3% of total mesozooplankton abundance, while the abundance of the decapod shrimp *Lucifer faxoni* was similar to that of calanoid copepods (33.0% and 34.6% of total mesozooplankton abundance, respectively). In fall total mesozooplankton abundance ranged from $15.4 - 63.7 \times 10^3$ ind. m^{-2} in the daytime and $22.4 - 62.0 \times 10^3$ ind. m^{-2} at night. Copepods averaged 85.5% (day) and 85.0% (night)

of total mesozooplankton abundance. Total mesozooplankton abundance was significantly higher in springtime mesohaline stations compared to the fall, but there was no difference in total copepod abundance between seasons. Calanoid and poecilostomatoid copepod abundance was significantly higher in spring than fall in the oceanic regions, while harpacticoid copepod abundance was higher in spring than fall in the mesohaline plume (Fig. 3). The only copepod order exhibiting a significant difference between station surface salinity categories within the same season were the poecilostomatoids, which were higher in oceanic waters than low salinity plume waters in spring (Fig. 3).

Between the two seasons, opposite patterns occurred along the plume SSS gradient with respect to both total copepod and total mesozooplankton abundance in the upper 150 m. In spring total daytime copepod abundance was significantly and positively correlated with SSS ($p=0.006$, $r^2=0.551$; Fig. 4), as was total daytime mesozooplankton abundance ($p=0.019$, $r^2=0.436$; Fig. S1); the same trend was observed for nighttime, although was not significant for either total copepod (Fig. 4) or total mesozooplankton abundance (Fig. S1). In fall the pattern was reversed; total copepod and total mesozooplankton abundance were each negatively correlated with SSS (Fig. 4 and S1, respectively). This relationship was not statistically significant for either daytime or nighttime copepods (Fig. 4), but was significant for total mesozooplankton abundance (daytime $p=0.029$, $r^2=0.28$; nighttime $p=0.027$, $r^2=0.74$; Fig. S1). Similar patterns were seen for total copepod abundance in the shallowest surface layer sampled. In spring 0-25 m day and night total copepod abundance increased with salinity although were not significantly correlated. In fall 0-10 m daytime total copepod abundance significantly

decreased with increasing salinity ($p=0.001$, $r^2=0.52$), while nighttime abundance was not related to SSS.

A number of taxa followed this opposing salinity-abundance trend between seasons and were responsible for driving the overall patterns observed (Table 1). The positive correlation between SSS and daytime mesozooplankton abundance in spring was primarily driven by poecilostomatoid ($p=0.004$, $r^2=0.58$) and calanoid ($p=0.014$, $r^2=0.47$) copepods. Chaetognaths ($p=0.009$, $r^2=0.51$) and adult euphausiids ($p=0.038$ $r^2=0.36$) were the only non-copepod taxa to show a significant increase with increasing SSS in spring. In fall (daytime), poecilostomatoid copepods ($p=0.024$, $r^2=0.29$) were the only copepods with a significant negative correlation with SSS, which was driven by abundance in the *Oncaeidae* family ($p=0.029$, $r^2=0.28$). The decapod shrimp *L. faxoni* ($p=0.030$, $r^2=0.28$) and ostracods ($p=0.050$, $r^2=0.23$) were the only other taxa with a significant negative correlation with SSS. A comparatively high number of nighttime taxa (vs. day) abundances were strongly negatively correlated ($r^2 > 0.7$) with SSS (Table 1).

3.3 Areal distributions of selected taxa

An areal view of abundance patterns of a number of different taxa indicates distributions were not uniform over the plume region (Fig. 5-8). In spring calanoid copepods were elevated throughout plume waters but the highest abundances were found in the northwest and southeast mesohaline plume waters (~ 10°N 55°W and 6°N 51°W, respectively; Fig. 5B). Abundances were also high close to the transitional areas between plume-influenced waters and the open ocean. In fall calanoid copepods were most abundant in the low salinity plume waters in the vicinity of the previously observed spring peak density in the southeast region (~ 7°N 52-49°W; Fig. 6B). Poecilostomatoid

copepods were distributed similarly to calanoid copepods in the spring (Fig. 5C) and fall (Fig. 6C), although high poecilostomatoid copepod abundance also occurred in the northernmost mesohaline station in fall. In spring cyclopoid copepod abundance (Fig. 5D) was variable across the plume with highest concentration in the northern plume (north of 8°N); this can be compared to fall (Fig. 6D) where cyclopoid copepod abundance was high throughout the plume and peaked at the northernmost mesohaline station. Harpacticoid copepod abundance in the spring was highest in oceanic waters (Fig. 5E), while in the fall was elevated throughout the plume (Fig. 6E). Chaetognath distributions in spring were significantly higher ($p < 0.05$) in oceanic waters compared to low salinity plume waters (Fig. 5F), while in the fall were similar throughout the sampling region. Fall peak chaetognath abundance occurred in the low salinity and mesohaline plume stations (Fig. 6F), although it was not significantly different from abundance outside of the plume.

One taxonomic group with a strong association with plume waters was the decapods. The adult decapod shrimp *L. faxoni* (Fig. 7C, 8C) as well as decapod larvae (Fig. 7D, 8D) were found almost exclusively in plume-influenced waters in both seasons. While we did not identify most of the decapod larvae beyond life stage (e.g., zoea, megalopa; Tables S1 and S2), there were high abundances of decapod larvae from the *Solenoceridae* family, especially in the plume waters in fall (Fig. S2D, S3D). Fish larvae also showed a similar association with plume waters. In the spring, fish larvae were high in the plume with highest concentrations occurring along the transition from plume to ocean waters (Fig. 7B). In the fall larval fish were primarily constrained in the low salinity plume waters as well as the transitional regions between the plume and oceanic

waters (Fig. 8B). Euphausiid distributions varied seasonally and by life stage (i.e., larva vs. adult). In spring highest adult abundances were found in oceanic waters (Fig. 7E) while larvae were found in predominantly in northern plume-influenced waters (Fig. 7F). In fall adult euphausiid abundance was high in both plume-influenced waters and adjacent oceanic waters (Fig. 8E), while larvae were found throughout the plume but highest in the lowest salinity plume waters (Fig. 8F). Areal distributions of other taxa in the Amazon River-influence WTNA had less pronounced plume or oceanic distributions (Figs. S2 and S3).

3.4 Vertical distribution of mesozooplankton

Depth-stratified abundance patterns were also observed for multiple taxa in both seasons. Overall, abundance was higher in surface waters, with several taxa highly constrained in the low salinity surface plume waters (0-10 and 10-25 m). General patterns seen across taxa are exemplified by two different taxa in the fall (Fig. 9). Calanoid copepods (night and day) were concentrated in the top 25 m in the salinity plume with a deepening of, and decrease in, abundance in the mesohaline plume before further decreasing in abundance and becoming more uniformly distributed through the water column at oceanic stations (Fig. 9). In another variation of this high surface plume abundance pattern, decapod larvae at low salinity plume stations during the daytime were almost an order of magnitude more abundant in the surface layer compared to deeper strata (21.7 ± 7.83 individuals m^{-3} and 3.43 ± 2.46 individuals m^{-3} , respectively). Decapod larvae then showed a slight deepening of abundance in the mesohaline plume before being almost absent from the water column during the day at oceanic stations. Decapod larvae were more abundant in surface waters at night in the mesohaline plume

and oceanic waters, suggesting diel vertical migration further along the plume gradient (Fig. 9; bottom).

Vertical patterns of abundance are further highlighted in a transect through the plume (Fig. 10). Day- and nighttime (not shown) vertical distributions of *L. faxoni* are almost entirely constrained in the upper 25 m of the water column with high abundances found in the core of the plume (Fig. 10B). Almost no *L. faxoni* were present outside of plume waters. In contrast, chaetognaths were present throughout the water column and across the entire transect, although they were most abundant in the same low salinity plume waters where *L. faxoni* were abundant (Fig. 10C).

4. DISCUSSION

4.1 Mesozooplankton abundance patterns

Seasonal differences in salinity vs. abundance- In spring both copepod and mesozooplankton abundances (day and night) increased with increasing salinity, while in fall, both decreased with increasing salinity. This is the same trend observed for spring (day and night) and fall (night) mesozooplankton biomass (integrated in the upper 150 m150m) across the salinity gradient (Steinberg et al. in prep). This change in relationship of abundance with increasing salinity from positive (spring) to negative (fall) is influenced by a significant decrease in calanoid and poecilostomatoid copepod abundances at oceanic stations from spring to fall (Fig. 3), as well as an increase in calanoid, poecilostomatoid, and cyclopoid copepod abundances in low salinity plume waters (although this was not statistically different between seasons). In the mesohaline, total mesozooplankton abundance was significantly higher in spring compared to fall, yet only harpacticoid copepods showed the same significant trend. This is surprising given harpacticoid copepods were primarily *Macrosetella gracilis*, which utilizes the oceanic cyanobacterium *Trichodesmium* as a substrate (O’Neil 1998; Turner 2014). Harpacticoid elevation in the spring mesohaline is likely due to the mixing of mesohaline and oceanic waters which is supported by the observation of *Trichodesmium* at some mesohaline stations (Goes et al. 2014; Loick-Wilde et al. 2016). Furthermore, DDA blooms are thought to occur most frequently in mesohaline waters (Subramaniam et al. 2008), which was true for the spring cruise (Goes et al. 2014). Calanoid copepods, considered important grazers on diatoms in coastal environments (Leising et al. 2005; Bergkvist et al. 2012), were not significantly more abundant in spring in plume waters, as might be

predicted in response to the spring DDA bloom, than in fall (no DDA bloom). Conroy et al. (2016) suggested that elevated grazing rates along the plume salinity gradient in the fall compared to the spring was due to a lag response by mesozooplankton to a spring DDA bloom. This could explain the increase in copepod abundances from spring to fall in the low salinity plume, but not the relatively similar abundance of copepods in both seasons in the mesohaline plume.

Comparison to other studies of mesozooplankton in the Amazon River plume is limited to the work of Calef and Grice (1967), which focused primarily on copepod species composition from two cruises during what they term the wet season (May-June; ‘spring’ in this study) and dry season (Oct.-Nov.; slightly post ‘fall’ in this study). Their only seasonal comparison is for stations where the cruises overlapped (approximately 12-5°N and 48-58°W), which correspond primarily to mesohaline stations in our study. They observed almost a 3-fold increase in zooplankton displacement volume and abundance in the wet season compared to the dry, with calanoid copepods stated as being the most abundant taxon. This increase is higher than we observed between seasons, but the authors suggest that there is a seasonal pattern associated with the plume discharge.

Aggregative effects of the plume - River plumes and frontal regions act as aggregation areas for zooplankton (e.g., Roman et al. 2001; Albaina and Irigoien 2004; Morgan et al. 2005). In the WTNA the Amazon River plume frequently creates strong density fronts driven by salinity gradients that increase vertical shear and mixing (Coles et al. 2013). In the fall retroreflection period a strong front was observed at approximately 7°N, 50°W along the North Equatorial Counter Current (NECC). This front showed elevated vertical shear in plume-influenced waters compared to higher-salinity oceanic

waters, along with a distinct color change and a large amount of floating debris (Coles et al. 2013). This frontal region and adjacent pathway of the NECC (see Fig. 1 in Coles et al. 2013) is the same area where we observed the highest total mesozooplankton, calanoid and poecilostomatoid copepod, *L. faxoni*, and decapod larvae abundances in the fall (Fig. 6). Aggregation may be via physical entrapment or behavioral—there is evidence that calanoid copepods preferential associate along velocity gradients (Woodson et al. 2005; True et al. 2015) similar to those observed at convergent fronts. Aggregation at these fronts increases prey encounter rate and has been shown in many systems to enhance secondary production (Grimes and Finucane 1991; Grimes and Kingsford 1996; Chiba et al. 2001; Labat et al. 2002).

4.2 The Amazon River plume as an “extended” estuary and coastal nursery habitat

Coastal environments, and estuaries in particular, are often considered nursery habitats. Estuaries are commonly defined as a “semi-enclosed coastal body of water having a free connection with the open sea and within which sea-water is measurably diluted with fresh water derived from land drainage” (Pritchard 1967). Nittrouer and DeMaster (1996) reported “estuarine-like processes” occurred over the shelf rather than the semi-enclosed mouth of the Amazon River due to the high-energy discharge of the river and high turbidity at the mouth reducing primary production rates. Physical mixing of fresh and saltwater, high primary production, and sediment and carbon deposition occurred in deeper shelf waters (50-100 m) (DeMaster et al. 1986, 1996; DeMaster and Pope 1996; Nittrouer and DeMaster 1996; Smith Jr and Demaster 1996), and Goes et al. (2014) report an “estuarine type” phytoplankton assemblage on the shelf and slope around 4-7 °N approximately 400-700 km north of the river mouth. Thus, while not

‘semi-enclosed’, the Amazon River plume functions as an “extended” estuary into the WTNA, and we suggest that for a number of mesozooplankton taxa the plume provides a nursery habitat for both mero- and holoplankton.

Decapods—One broad taxonomic group that supports the “extended” estuary function of the Amazon River plume is the decapods. Decapod shrimp in the genus *Lucifer* have a cosmopolitan distribution in the oceans, found everywhere but the Southern Ocean (Vega-Pérez et al. 1996). The species *L. faxoni* is neritic and found regularly along the east coast of North and South America as well as the Gulf of Mexico (Omori 1975). In the Amazon River plume *L. faxoni* was the only organism with abundance comparable to calanoid copepods, and was largely restricted to the upper 25 m in both day and night, although *L. faxoni* is known to vertically migrate in other systems (Checkley et al. 1992). Modeled estimates of the age of plume water masses indicate waters with SSS between 28 and 32 average between 21 and 65 days old, respectively (Coles et al. in prep.). This would provide time for *L. faxoni* in plume waters to complete one or two reproductive cycles, given their life cycle of 30-40 days (Lee et al. 1992; Teodoro et al. 2012). Interestingly, the lack of vertical migration we observed suggests that either *L. faxoni* preferentially stays in the surface plume or is incapable of swimming through the surface plume density gradient. The latter response was observed when the copepods *Acartia tonsa* and *Temora longicornis* encountered a strong density gradient and swam along the boundary rather than passing through it, effectively confining them in their respective water mass (Woodson et al. 2005). Whether through active swimming or physical entrainment, it appears *L. faxoni* that originate in coastal waters are able to effectively utilize plume waters far from the coast as a habitat.

A wide variety of decapod larvae were also abundant in the surface layer of low salinity and mesohaline plume waters, although not restricted to there. It is likely that food availability and entrainment in the surface plume are responsible for the decapod larvae abundance patterns, particularly as many brachyuran zoea and megalopa are strong swimmers (Epifanio and Cohen 2016). An alternative (or related) explanation is the utilization of the plume for larval dispersal. Buoyancy-driven flow from water masses with different densities is an important factor for blue crab dispersal on the North American continental shelf (Epifanio and Garvine 2001) and Morgan et al. (2014) showed crustacean larval behavior (i.e., depth regulation) was important for dispersal from a coastal estuary into an adjacent upwelling system.

Euphausiids—The different distribution patterns observed between euphausiid life stages support potential use of coastal plume waters as a spawning and nursery habitat. Larval euphausiid abundances were 2-3 times higher than adult abundances in plume waters in spring, and 4-8 times higher than adults in fall. In fall adults occurred throughout the plume, and the high abundance of larvae was concentrated in the low salinity core of the plume (Fig. 8a,f). Similarly, euphausiid eggs, nauplii, larvae, and early stage juveniles have been observed to concentrate in surface waters of the Benguela Current (Pillar et al. 1989), an upwelling system that may have some physical or biological aggregation properties that parallel those of river plumes. We thus suggest that adults spawn in the plume and then disperse into oceanic waters throughout the WTNA, with early life history stages, including juveniles, remaining entrained in the productive surface waters.

Fish larvae— Distributions of fish larvae also support the Amazon River plume as an “extended” estuary and nursery habitat. Elevated larval fish abundance occurred in plume waters in both seasons (although abundance was also high in oceanic waters at night in spring), with particularly high abundances in fall around the above mentioned front observed at approximately 7°N, 49°W. Similar patterns have been observed for the Mississippi (Govoni et al. 1989; Grimes and Finucane 1991) and Columbia (Morgan et al. 2005) River plumes. In the Mississippi River plume, larval fish were 20 times more abundant in the plume frontal region compared to fronts along the Gulf of Mexico Loop Current (Richards et al. 1989), highlighting the importance of river plumes for aggregation relative to other physical features. Churchill and Grimes (1991) attributed elevated larval fish abundance in the Mississippi plume to enhanced production within the plume supporting better growth conditions and acting as an area for enhanced fish recruitment. In the Columbia River Morgan et al. (2005) suggest food availability in the plume supports enhanced zooplankton and highlight them as ephemeral, yet important, food resources for planktivorous fish.

5. CONCLUSION

Similar to studies investigating phytoplankton in the Amazon River plume influenced WTNA (e.g., Subramaniam et al. 2008; Goes et al. 2014), zooplankton composition shows distinct trends along the salinity gradient. Other studies in the region suggest a seasonal pattern in mesozooplankton community composition and grazing (Calef and Grice 1967; Conroy et al. 2016), and while we also saw seasonal changes in abundance and composition— in low salinity plume and oceanic waters, seasonality was not apparent in the highly productive mesohaline plume waters where DDA blooms occur. Physical properties of the plume interacting with the underlying WTNA current system (Coles et al. 2013) as well as zooplankton behavioral characteristics likely led to the areas of high mesozooplankton abundance, similar to those seen in the Columbia (Peterson and Peterson 2008) and Mississippi (Grimes and Finucane 1991) Rivers. Some taxa (e.g., *Lucifer faxoni*) are vertically constrained in the surface plume layer, which functions as an "extended" estuary hundreds of kilometers into the WTNA. The extension of the estuary into the WTNA supported decapod and fish larvae, as well as euphausiids. Future work should investigate if this nursery habitat for planktonic organisms likewise serves as an important food source for higher trophic level predators such as large migratory fishes. This is the first quantitative study of mesozooplankton composition in the WTNA and serves as an important baseline for comparison with future ocean conditions, and can be utilized to improve biogeochemical models (Coles and Hood 2007; Stukel et al. 2014) of the region. Furthermore, climate change predictions for the WTNA are that the Amazon hydrological cycle will intensify resulting in larger river discharge into the WTNA (Gloor

et al. 2013), impacting the distributions of both phytoplankton and zooplankton along the plume salinity gradient.

REFERENCES

- Albaina, A., and X. Irigoien. 2004. Relationships between frontal structures and zooplankton communities along a cross-shelf transect in the Bay of Biscay (1995 to 2003). *Mar. Ecol.-Prog. Ser.* **284**: 65–75. doi:10.3354/meps284065
- Alden III, R. W., R. C. Dahiya, and R. J. Young Jr. 1982. A method for the enumeration of zooplankton subsamples. *Journal of Experimental Marine Biology and Ecology* **59**: 185–206.
- Beaugrand, G., P. C. Reid, F. Ibañez, J. A. Lindley, and M. Edwards. 2002. Reorganization of North Atlantic Marine Copepod Biodiversity and Climate. *Science* **296**: 1692–1694. doi:10.1126/science.1071329
- Benoit-Bird, K. J., and M. A. McManus. 2012. Bottom-up regulation of a pelagic community through spatial aggregations. *Biology Letters* **8**: 813–816. doi:10.1098/rsbl.2012.0232
- Bergkvist, J., P. Thor, H. Henrik Jakobsen, S.-Å. Wängberg, and E. Selander. 2012. Grazer-induced chain length plasticity reduces grazing risk in a marine diatom. *Limnology and Oceanography* **57**: 318. doi:10.4319/lo.2012.57.1.0318
- Bombar, D., P. Moisander, J. Dippner, R. Foster, M. Voss, B. Karfeld, and J. Zehr. 2011. Distribution of diazotrophic microorganisms and nifH gene expression in the Mekong River plume during intermonsoon. *Marine Ecology Progress Series* **424**: 39–52. doi:10.3354/meps08976
- Calef, G. F., and G. D. Grice. 1967. Influence of the Amazon River Outflow on the

- Ecology of the Western Tropical Atlantic II. Zooplankton Abundance, Copepod Distribution, with Remarks on the Fauna of Low-Salinity Areas. *Journal of Marine Research* **25**: 84–92.
- Carpenter, E. J., J. P. Montoya, J. Burns, M. R. Mulholland, A. Subramaniam, and D. G. Capone. 1999. Extensive bloom of a N₂-fixing diatom/cyanobacterial association in the tropical Atlantic Ocean. *Marine Ecology Progress Series* **185**: 273–283.
- Checkley, D. M., S. Uye, M. J. Dagg, M. M. Mullin, M. Omori, T. Onbé, and M. – Zhu. 1992. Diel variation of the zooplankton and its environment at neritic stations in the Inland Sea of Japan and the north-west Gulf of Mexico. *J. Plankton Res.* **14**: 1–40. doi:10.1093/plankt/14.1.1
- Chiba, S., T. Ishimaru, G. W. Hosie, and M. Fukuchi. 2001. Spatio-temporal variability of zooplankton community structure off east Antarctica (90 to 160°E). *Mar Ecol Prog Ser* **216**: 95–108. doi:10.3354/meps216095
- Clarke, K. R. 1993. Non-parametric multivariate analyses of changes in community structure. *Australian Journal of Ecology* **18**: 117–143. doi:10.1111/j.1442-9993.1993.tb00438.x
- Clarke, K. R., R. N. Gorley, P. J. Somerfield, and R. M. Warwick 2015. Change in Marine Communities: An Approach to Statistical Analysis and Interpretation, 3rd ed. PRIMER-E.
- Coles, V. J., M. T. Brooks, J. Hopkins, M. R. Stukel, P. L. Yager, and R. R. Hood. 2013. The pathways and properties of the Amazon River Plume in the tropical North Atlantic Ocean: AMAZON RIVER PLUME. *Journal of Geophysical Research: Oceans* **118**: 6894–6913. doi:10.1002/2013JC008981

- Coles, V. J., and R. R. Hood. 2007. Modeling the impact of iron and phosphorus limitations on nitrogen fixation in the Atlantic Ocean. *Biogeosciences* **4**: 455–479.
- Conroy, B. J., D. K. Steinberg, M. R. Stukel, J. I. Goes, and V. J. Coles. 2016. Meso- and microzooplankton grazing in the Amazon River plume and western tropical North Atlantic. *Limnology and Oceanography* **61**: 825–840. doi:10.1002/lo.10261
- Costa, R. M., N. R. Leite, and L. C. C. Pereira. 2009. Mesozooplankton of the Curuçá Estuary (Amazon Coast, Brazil). *Journal of Coastal Research* 400–404.
- DeMaster, D. J., S. A. Kuehl, and C. A. Nittrouer. 1986. Effects of suspended sediments on geochemical processes near the mouth of the Amazon River: examination of biological silica uptake and the fate of particle-reactive elements. *Continental Shelf Research* **6**: 107–125.
- Demaster, D. J., and R. H. Pope. 1996. Nutrient dynamics in Amazon shelf waters: results from AMASSEDS. *Continental Shelf Research* **16**: 263–289.
- DeMaster, D. J., W. O. Smith, D. M. Nelson, and J. Y. Aller. 1996. Biogeochemical processes in Amazon shelf waters: chemical distributions and uptake rates of silicon, carbon and nitrogen. *Continental Shelf Research* **16**: 617–643.
- Eden, B. R., D. K. Steinberg, S. A. Goldthwait, and D. J. McGillicuddy. 2009. Zooplankton community structure in a cyclonic and mode-water eddy in the Sargasso Sea. *Deep Sea Research Part I: Oceanographic Research Papers* **56**: 1757–1776. doi:10.1016/j.dsr.2009.05.005
- Epifanio, C. E., and J. H. Cohen. 2016. Behavioral adaptations in larvae of brachyuran crabs: A review. *Journal of Experimental Marine Biology and Ecology* **482**: 85–105. doi:10.1016/j.jembe.2016.05.006

- Epifanio, C. E., and R. W. Garvine. 2001. Larval Transport on the Atlantic Continental Shelf of North America: a Review. *Estuarine, Coastal and Shelf Science* **52**: 51–77. doi:10.1006/ecss.2000.0727
- Flint, M. V., T. N. Semenova, E. G. Arashkevich, I. N. Sukhanova, V. I. Gagarin, V. V. Kremenetskiy, M. A. Pivovarov, and K. A. Soloviev. 2010. Structure of the zooplankton communities in the region of the Ob River's estuarine frontal zone. *Oceanology* **50**: 766–779. doi:10.1134/S0001437010050139
- Foster, R. A., A. Subramaniam, C. Mahaffey, E. J. Carpenter, D. G. Capone, and J. P. Zehr. 2007. Influence of the Amazon River plume on distributions of free-living and symbiotic cyanobacteria in the western tropical north Atlantic Ocean. *Limnology and oceanography* **52**: 517–532.
- Gloor, M., R. J. W. Brienen, D. Galbraith, and others. 2013. Intensification of the Amazon hydrological cycle over the last two decades: AMAZON HYDROLOGIC CYCLE INTENSIFICATION. *Geophysical Research Letters* **40**: 1729–1733. doi:10.1002/grl.50377
- Goes, J. I., H. do R. Gomes, A. M. Chekalyuk, and others. 2014. Influence of the Amazon River discharge on the biogeography of phytoplankton communities in the western tropical north Atlantic. *Progress in Oceanography* **120**: 29–40. doi:10.1016/j.pocean.2013.07.010
- Goldthwait, S. A., and D. K. Steinberg. 2008. Elevated biomass of mesozooplankton and enhanced fecal pellet flux in cyclonic and mode-water eddies in the Sargasso Sea. *Deep Sea Research Part II: Topical Studies in Oceanography* **55**: 1360–1377. doi:10.1016/j.dsr2.2008.01.003

Govoni, J. J., D. E. Hoss, and D. R. Colby. 1989. The spatial distribution of larvalfishes about the Mississippi River plume. Limnol. Oceanogr. **34**: 178–187.
doi:10.4319/lo.1989.34.1.0178

Grimes, C. B., and J. H. Finucane. 1991. Spatial distribution and abundance of larval and juvenile fish, chlorophyll and macrozooplankton around the Mississippi River discharge plume, and the role of the plume in fish recruitment. Marine ecology progress series. Oldendorf **75**: 109–119.

Grimes, C. B., and M. J. Kingsford. 1996. How do riverine plumes of different sizes influence fish larvae: do they enhance recruitment? Marine and Freshwater Research **47**: 191–208.

Hernández-León, S., P. Sangrà, P. Lehette, L. Lubián, C. Almeida, S. Putzeys, P. Bécognée, and M. P. Andrade. 2013. Zooplankton biomass and metabolism in the frontal zones of the Bransfield Strait, Antarctica. Journal of Marine Systems **111-112**: 196–207. doi:10.1016/j.jmarsys.2012.11.001

Hunt, B. P. V., E. A. Pakhomov, and C. D. McQuaid. 2002. Community structure of mesozooplankton in the Antarctic polar frontal zone in the vicinity of the Prince Edward Islands (Southern Ocean): small-scale distribution patterns in relation to physical parameters. Deep Sea Research Part II: Topical Studies in Oceanography **49**: 3307–3325. doi:10.1016/S0967-0645(02)00085-1

Labat, J. P., P. Mayzaud, S. Dallot, A. Errhif, S. Razouls, and S. Sabini. 2002. Mesoscale distribution of zooplankton in the Sub-Antarctic Frontal system in the Indian part of the Southern Ocean: a comparison between optical plankton counter and net

- sampling. Deep Sea Research Part I: Oceanographic Research Papers **49**: 735–749. doi:10.1016/S0967-0637(01)00076-0
- Lee, W. Y., M. Omori, and R. W. Peck. 1992. Growth, reproduction and feeding behavior of the planktonic shrimp, Lucifer faxoni Borradaile, off the Texas coast. J. Plankton Res. **14**: 61–69. doi:10.1093/plankt/14.1.61
- Leising, A. W., J. J. Pierson, C. Halsband-Lenk, R. Horner, and J. Postel. 2005. Copepod grazing during spring blooms: Does Calanus pacificus avoid harmful diatoms? Progress in Oceanography **67**: 384–405. doi:10.1016/j.pocean.2005.09.008
- Loick-Wilde, N., S. C. Weber, B. J. Conroy, D. G. Capone, V. J. Coles, P. M. Medeiros, D. K. Steinberg, and J. P. Montoya. 2016. Nitrogen sources and net growth efficiency of zooplankton in three Amazon River plume food webs. Limnol. Oceanogr. **61**: 460–481. doi:10.1002/lno.10227
- Magalhães, A., N. da R. Leite, J. G. Silva, L. C. Pereira, and R. M. da Costa. 2009. Seasonal variation in the copepod community structure from a tropical Amazon estuary, Northern Brazil. Anais da Academia Brasileira de Ciências **81**: 187–197. doi:<http://dx.doi.org/10.1590/S0001-37652009000200005>
- Moller, G. S. F., E. M. L. d. M. Novo, and M. Kampel. 2010. Space-time variability of the Amazon River plume based on satellite ocean color. Continental Shelf Research **30**: 342–352. doi:10.1016/j.csr.2009.11.015
- Morgan, C. A., A. De Robertis, and R. W. Zabel. 2005. Columbia River plume fronts. I. Hydrography, zooplankton distribution, and community composition. Mar. Ecol.-Prog. Ser. **299**: 19–31. doi:10.3354/meps299019
- Morgan, S. G., J. L. Fisher, S. T. McAfee, J. L. Largier, S. H. Miller, M. M. Sheridan,

- and J. E. Neigel. 2014. Transport of Crustacean Larvae Between a Low-Inflow Estuary and Coastal Waters. *Estuaries and Coasts* **37**: 1269–1283.
doi:10.1007/s12237-014-9772-y
- Nittrouer, C. A., and D. J. DeMaster. 1996. The Amazon shelf setting: tropical, energetic, and influenced by a large river. *Continental Shelf Research* **16**: 553–573.
doi:10.1016/0278-4343(95)00069-0
- North, E., and E. Houde. 2003. Linking ETM physics, zooplankton prey, and fish early-life histories to striped bass *Morone saxatilis* and white perch *M. americana* recruitment. *Marine Ecology Progress Series* **260**: 219–236.
doi:10.3354/meps260219
- Omori, M. 1975. The Biology of Pelagic Shrimps in the Ocean, p. 233–324. In F.S.R. and M. Yonge [ed.], *Advances in Marine Biology*. Academic Press.
- O’Neil, J. M. 1998. The colonial cyanobacterium *Trichodesmium* as a physical and nutritional substrate for the harpacticoid copepod *Macrosetella gracilis*. *Journal of plankton research* **20**: 43–59. doi:10.1093/plankt/20.1.43
- Peterson, J. O., and W. T. Peterson. 2008. Influence of the Columbia River plume (USA) on the vertical and horizontal distribution of mesozooplankton over the Washington and Oregon shelf. *ICES J. Mar. Sci.* **65**: 477–483.
doi:10.1093/icesjms/fsn006
- Piontkovski, S. A., and C. Castellani. 2009. Long-term declining trend of zooplankton biomass in the Tropical Atlantic. *Hydrobiologia* **632**: 365–370.
doi:10.1007/s10750-009-9854-1
- Piontkovski, S. A., and M. R. Landry. 2003. Copepod species diversity and climate

- variability in the tropical Atlantic Ocean. *Fisheries Oceanography* **12**: 352–359.
- Pritchard, D. W. 1967. What is an estuary: Physical Viewpoint.
- Roman, M., D. Holliday, and L. Sanford. 2001. Temporal and spatial patterns of zooplankton in the Chesapeake Bay turbidity maximum. *Marine Ecology Progress Series* **213**: 215–227. doi:10.3354/meps213215
- Smith Jr, W. O., and D. J. Demaster. 1996. Phytoplankton biomass and productivity in the Amazon River plume: correlation with seasonal river discharge. *Continental Shelf Research* **16**: 291–319.
- Stukel, M. R., V. J. Coles, M. T. Brooks, and R. R. Hood. 2014. Top-down, bottom-up and physical controls on diatom-diazotroph assemblage growth in the Amazon River plume. *Biogeosciences* **11**: 3259–3278. doi:10.5194/bg-11-3259-2014
- Subramaniam, A., P. L. Yager, E. J. Carpenter, and others. 2008. Amazon River enhances diazotrophy and carbon sequestration in the tropical North Atlantic Ocean. *PNAS* **105**: 10460–10465. doi:10.1073/pnas.0710279105
- Teodoro, S. de S. A., M. L. Negreiros-Franozo, S. M. Simões, M. Lopes, and R. C. da Costa. 2012. Population ecology of the planktonic shrimp Lucifer faxoni Borradale, 1915 (Crustacea, Sergestoidea, Luciferidae) of the southeastern coast of Brazil. *Brazilian Journal of Oceanography* **60**: 245–253.
- True, A. C., D. R. Webster, M. J. Weissburg, J. Yen, and A. Genin. 2015. Patchiness and depth-keeping of copepods in response to simulated frontal flows. *Mar Ecol Prog Ser* **539**: 65–76. doi:10.3354/meps11472
- Turner, J. T. 2014. Planktonic marine copepods and harmful algae. *Harmful Algae* **32**: 81–93. doi:10.1016/j.hal.2013.12.001

- Vega-Pérez, L. A., K. Ara, T. H. Liang, and M. M. Pedreira. 1996. Feeding of the planktonic shrimp Lucifer faroni Borradaile, 1915 (Crustacea: Decapoda) in the laboratory. *Revista Brasileira de Oceanografia* **44**: 1–8. doi:10.1590/S1413-77391996000100001
- Wiebe, P. H., K. H. Burt, S. H. Boyd, and A. W. Morton. 1976. A multiple opening/closing net and environmental sensing system for sampling zooplankton. *Journal of Marine Research* **34**: 313–326.
- Woodson, C. B., and S. Y. Litvin. 2015. Ocean fronts drive marine fishery production and biogeochemical cycling. *Proceedings of the National Academy of Sciences* **112**: 1710–1715. doi:10.1073/pnas.1417143112
- Woodson, C. B., D. R. Webster, M. J. Weissburg, and J. Yen. 2005. Response of copepods to physical gradients associated with structure in the ocean. *Limnol. Oceanogr.* **50**: 1552–1564. doi:10.4319/lo.2005.50.5.1552

Table 1. Linear regressions for sea surface salinity vs. depth-integrated abundance of mesozooplankton taxonomic groups. Only significant relationships ($p < 0.05$) listed. Spring is May-June, 2010 and fall is September-October, 2011. Shown are sample size (n), p-value, the correlation coefficient (r), the coefficient of determination (r^2), and the equation for each regression.

Season	Taxonomic Category	n	p-value	r	r^2	Regression Equation
Spring Daytime	Chaetognaths	12	0.009	0.71	0.51	$y = 133.6x - 2486$
	Calanoid Copepods	12	0.014	0.68	0.47	$y = 1210x - 16496$
	Poecilostomatoid Copepods (total)	12	0.004	0.76	0.58	$y = 534.9x - 9978$
	Corycaeid Copepods	12	0.025	0.64	0.41	$y = 256.3x - 4916$
	Oncaeid Copepods	12	0.035	0.61	0.37	$y = 275.5x - 5005$
	Adult Euphausiids	12	0.038	0.60	0.36	$y = 10.66x - 216.1$
Spring Nighttime	Hyperiid Amphipod	8	0.027	0.77	0.59	$y = 9.13x - 249.7$
	Chaetognaths	8	0.035	0.74	0.55	$y = 289.6x - 7374$
Fall Daytime	Poecilostomatoid Copepods (total)	17	0.024	0.54	0.29	$y = -666.1x + 26757$
	Oncaeid Copepods	17	0.015	0.58	0.33	$y = -543.4x + 20845$
	<i>Lucifer faxoni</i>	17	0.030	0.53	0.28	$y = -90.66x + 3256$
	Ostracods	17	0.050	0.48	0.23	$y = -51.33x + 2184$
Fall Nighttime	Barnacle Cyprids	6	0.002	0.97	0.93	$y = -255.6x + 9028$
	Calanoid Copepods	6	0.012	0.91	0.82	$y = -3647x + 144800$
	<i>Lucifer faxoni</i>	5	0.008	0.96	0.93	$y = -489.4x + 17210$
	Euphausiid Larvae	6	0.035	0.84	0.71	$y = -135.1x + 4807$
	Ostracods	6	0.014	0.90	0.81	$y = -97.00x + 3915$
	Polychaete worms	6	0.033	0.85	0.72	$y = -66.69x + 2396$
	Calycophoran Siphonophores (total)	6	0.025	0.87	0.75	$y = -33.47x + 1309$
	Diphyidae Siphonophores	6	0.017	0.89	0.80	$y = -34.02x + 1302$
	Doliolids	6	0.025	0.87	0.75	$y = -81.23x + 2933$

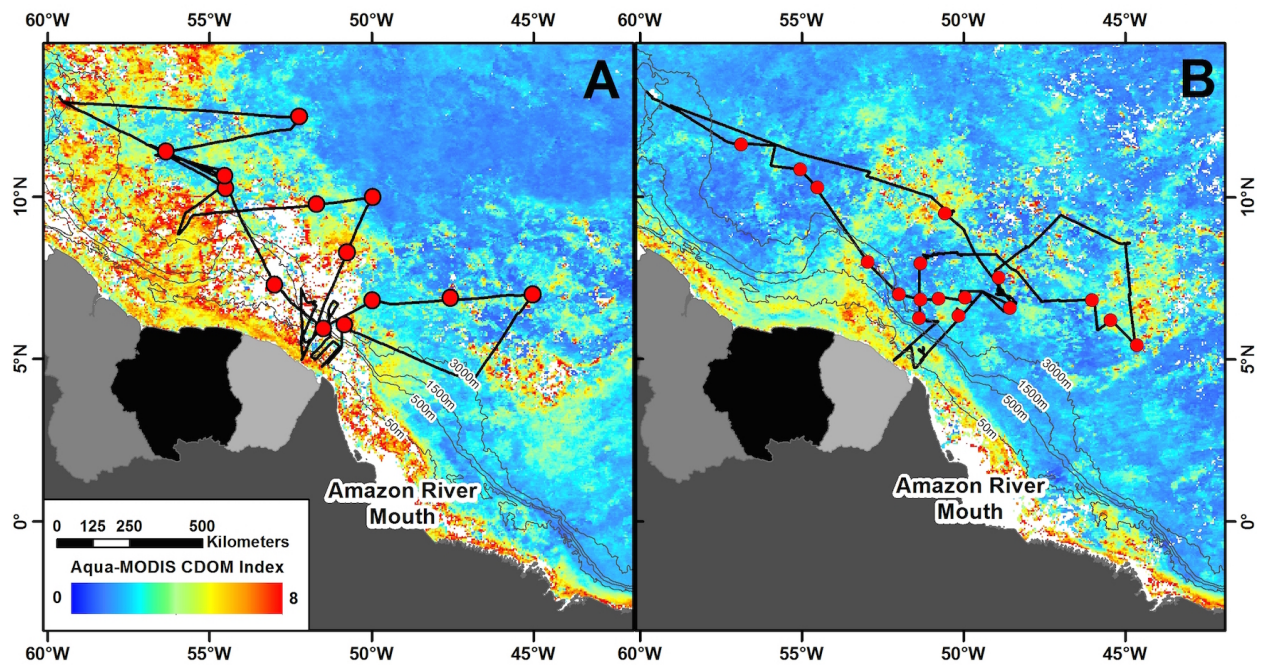
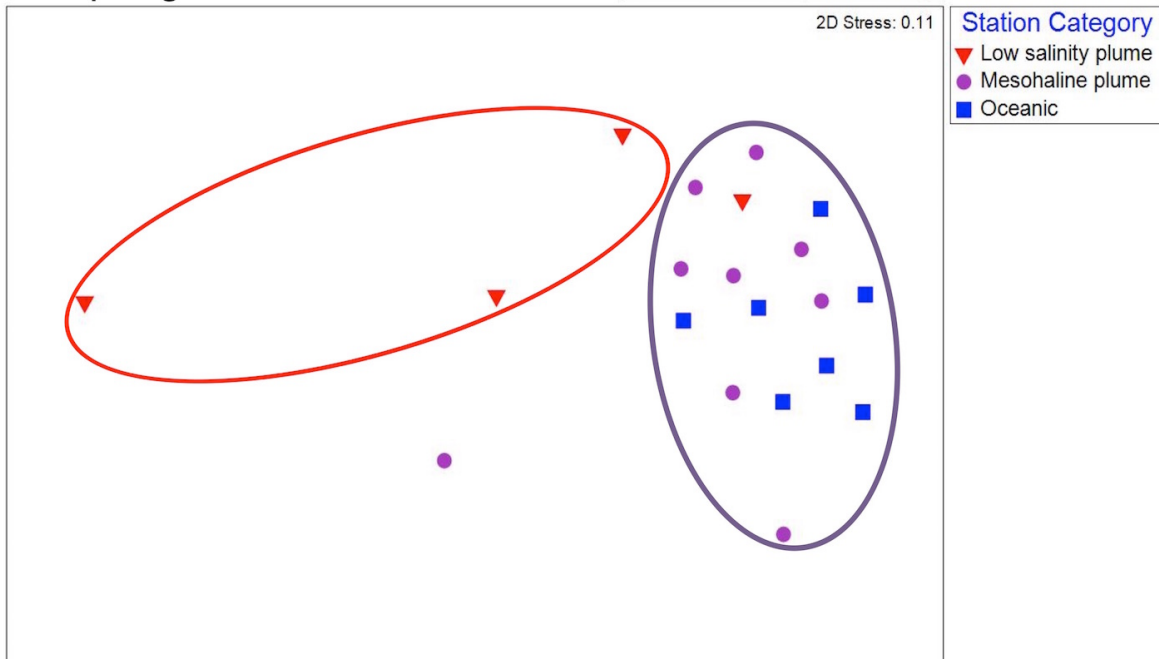


Fig. 1. Stations analyzed for mesozooplankton community composition analysis in the Amazon River plume-influenced waters and western tropical North Atlantic. Stations (red dots) and cruise track (black line) are overlaid on monthly averaged chromophoric dissolved organic matter (CDOM) concentration using Aqua-MODIS satellite data (oceancolor.gsfc.nasa.gov). (A) Stations sampled in spring (May-June) 2010 and (B) in fall (September-October) 2011. Bathymetry lines are shown in gray.

A. Spring



B. Fall

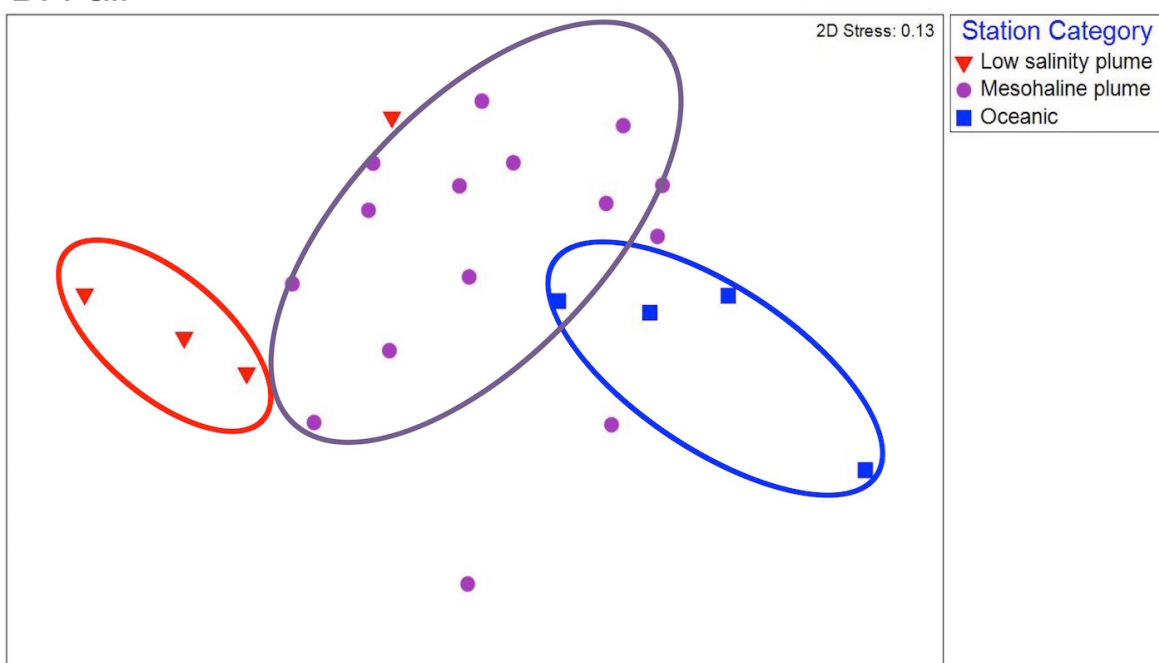


Fig. 2. Non-metric multidimensional scaling analysis (nMDS) ordination of spring (A) and fall (B) square root transformed, 150m depth-integrated mesozooplankton abundance. For spring (A) two clusters were identified consisting of low salinity stations (red circle) and a combination of mesohaline and oceanic stations (purple circle). In fall (B) three clusters were identified generally following the station categorization of low salinity plume (red circle), mesohaline plume (purple circle) and oceanic stations (blue circle).

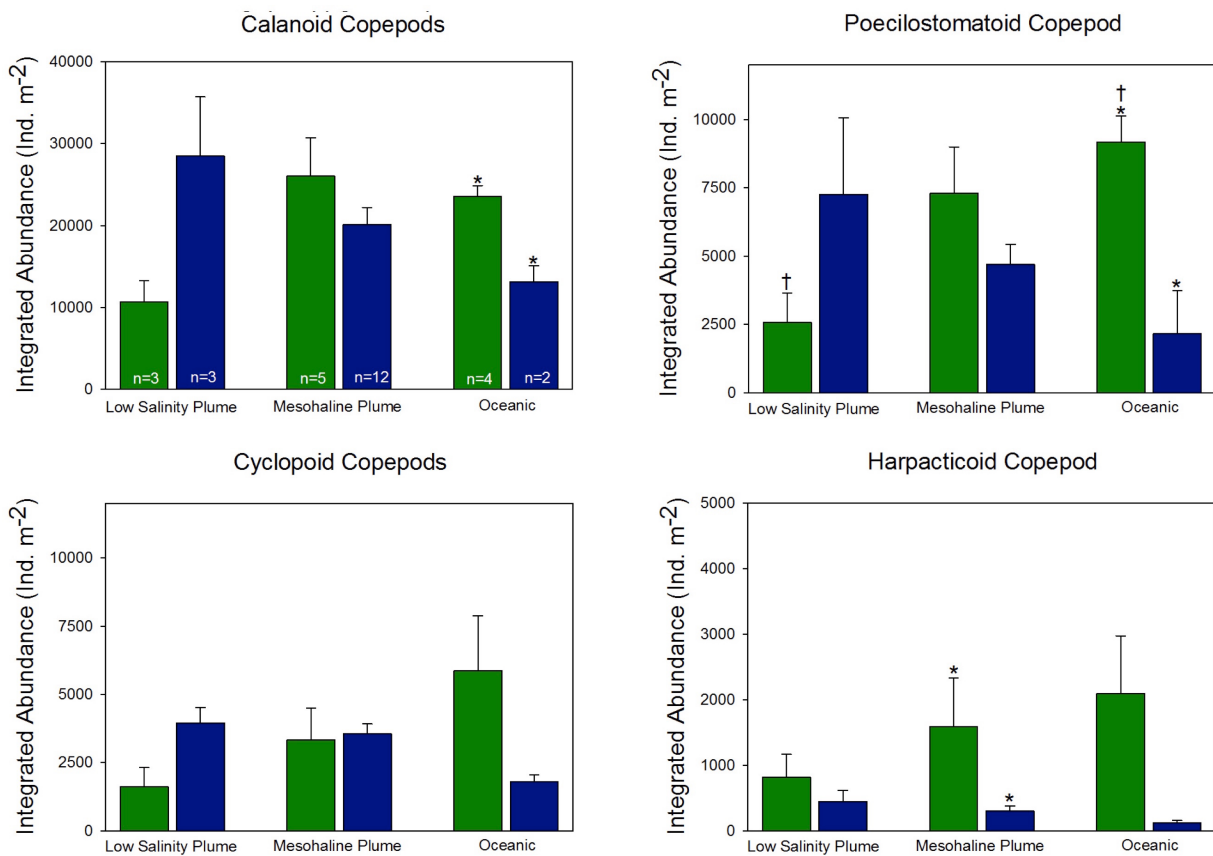


Fig. 3. Copepod abundance compared between salinity categories and season. Average \pm SE daytime 150 m depth-integrated abundance of four major copepod orders for spring (green) and fall (blue) across station salinity categories. Sample size (n) is the same across all copepod orders for each season and station salinity category, and is shown in top left graph. * indicates a significant difference between seasons for a particular station category, while † indicates a significant difference between station salinity categories within the same season. Note different y-axes scales.

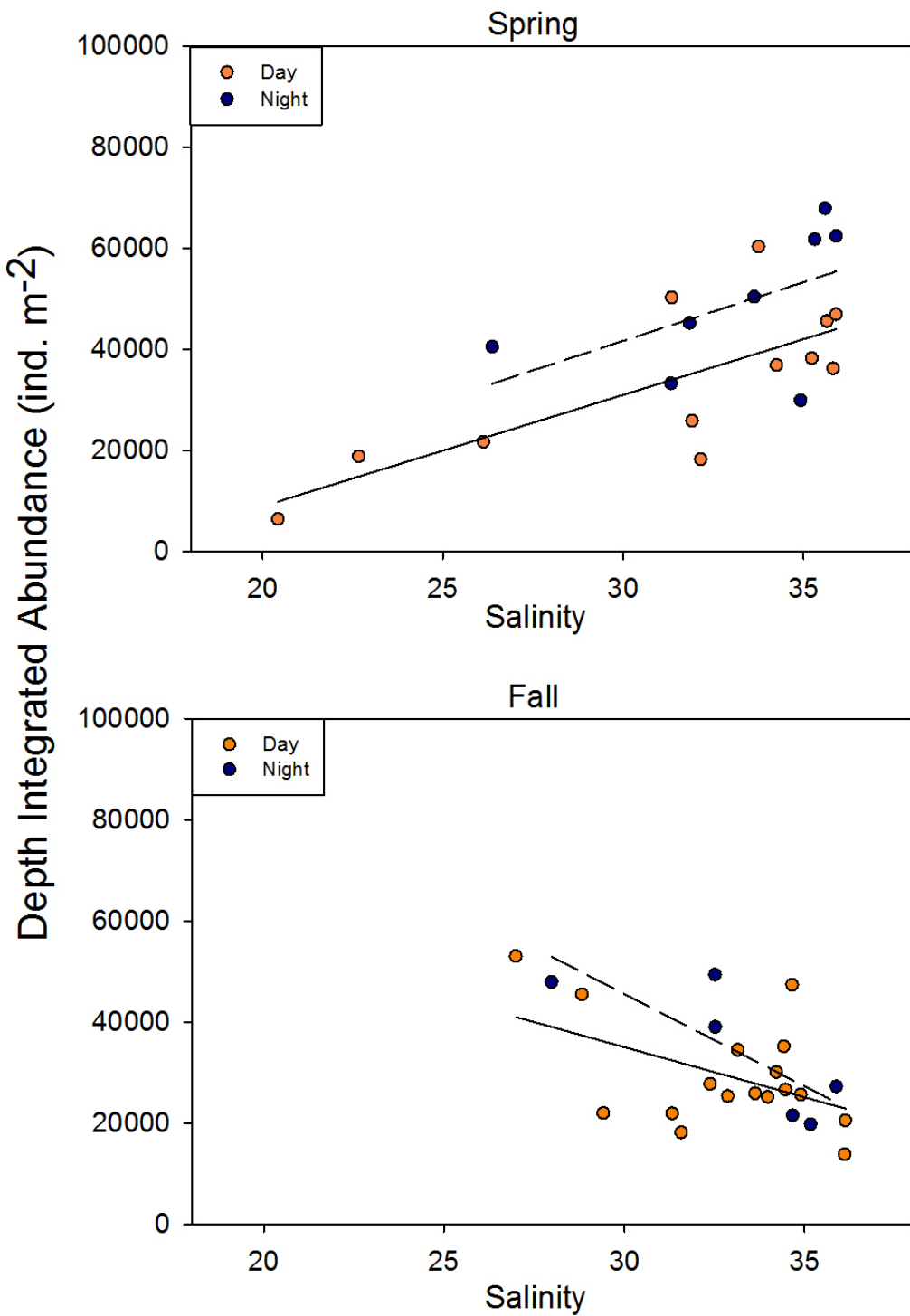


Fig. 4. Sea surface salinity vs. total copepod abundance (0-150m integrated) for spring (May-June; top) 2010 and fall (September-October) 2011. Daytime (orange; solid line) and nighttime (blue; dashed) regressions are reported for both seasons. Regression statistics and equations are as follows: spring daytime p=0.006, r²=0.55, y=2202x-35049; spring nighttime p=0.177, r²=0.28, y=2323x-27995; fall daytime p=0.055, r²=0.224, y=-1983x+94541; fall nighttime p=0.056, r²=0.64, y=-3649x+155018.

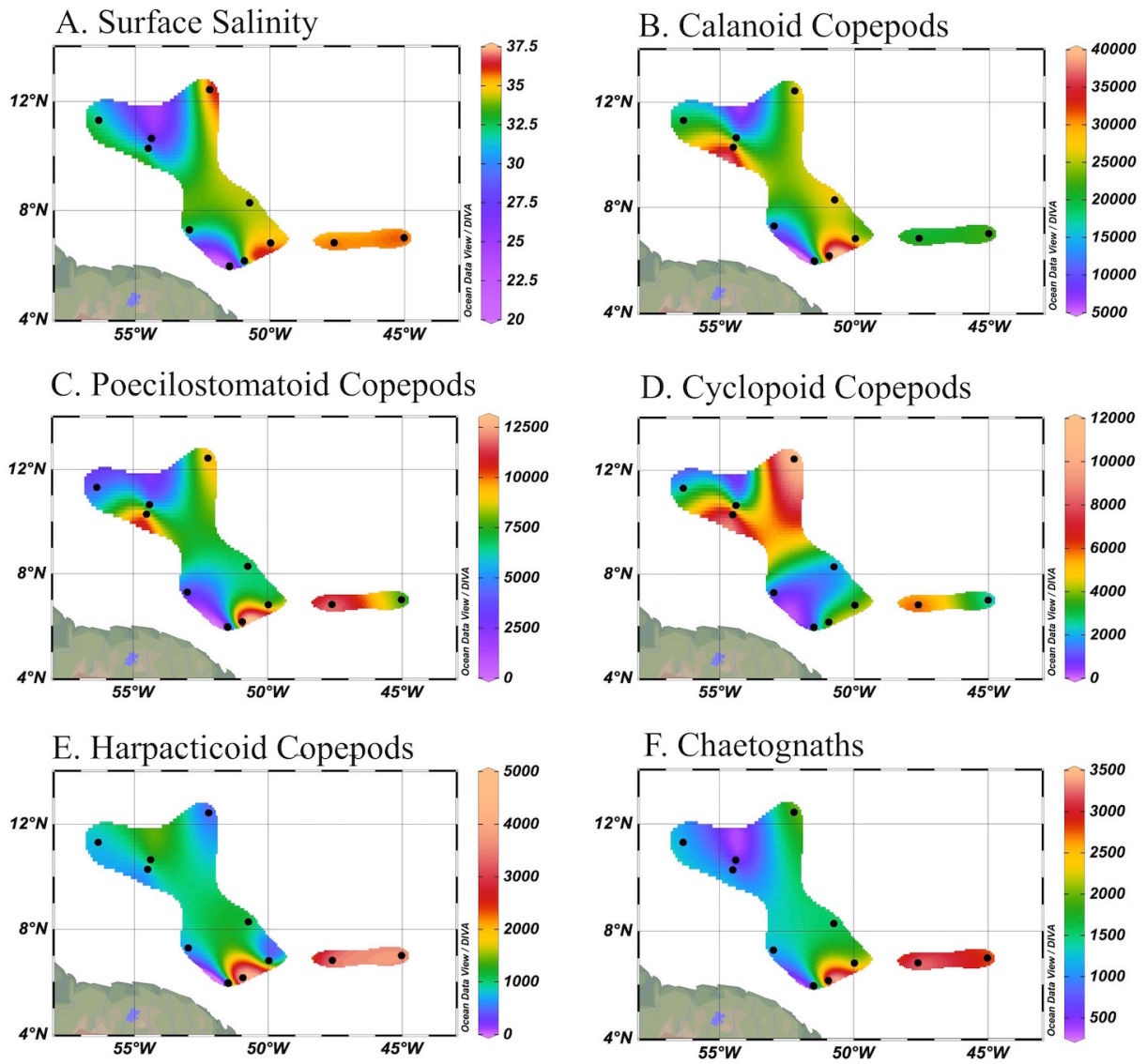


Fig. 5. Daytime areal distribution of sea surface salinity (A) and 150 m depth-integrated abundances (individuals m^{-2}) for copepod orders (B-E) and chaetognaths (F) in spring (May-June) 2010.

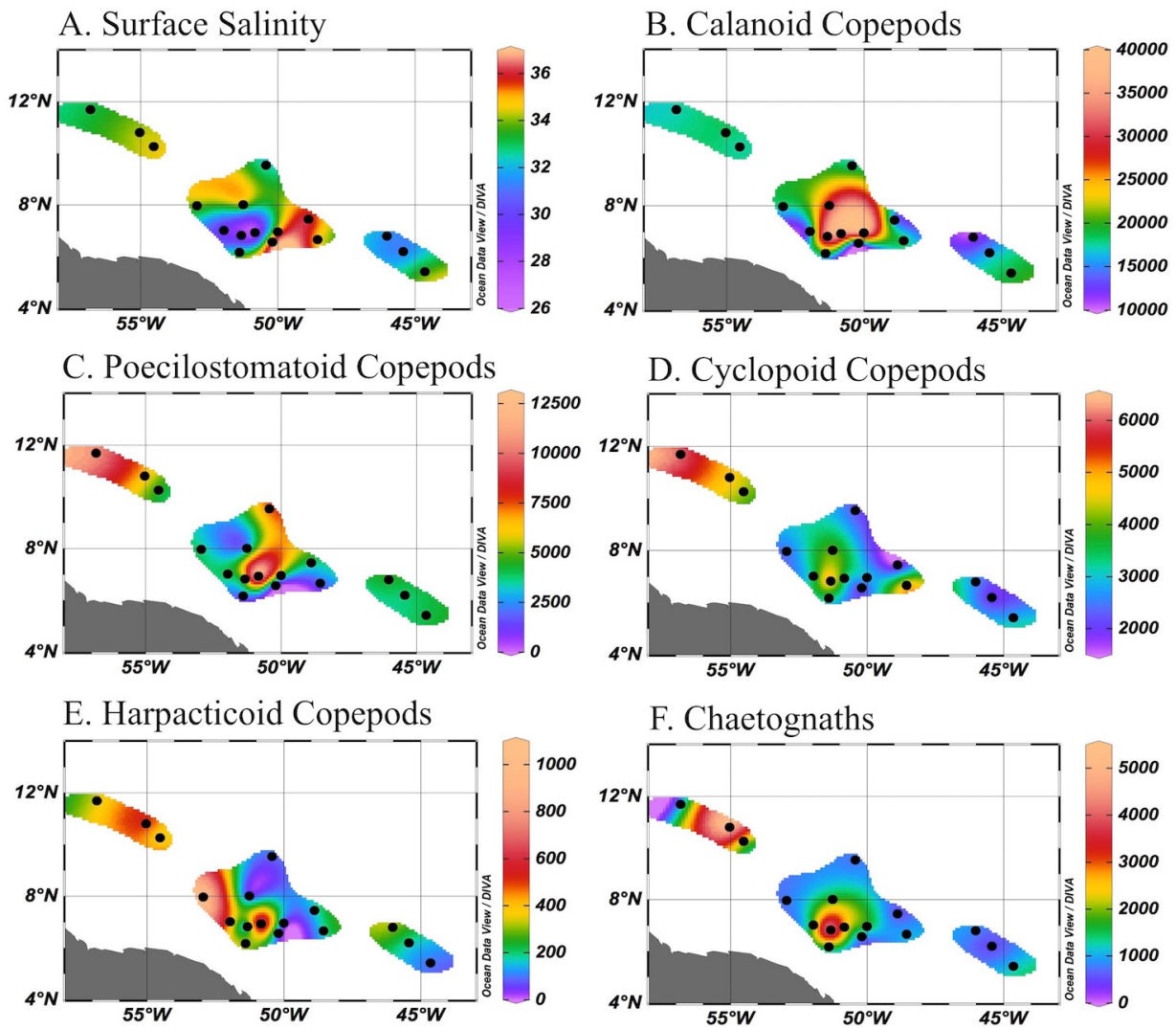


Fig. 6. Daytime areal distribution of sea surface salinity (A) and 150 m depth-integrated abundances (individuals m^{-2}) for chaetognaths (B) and copepod orders (C-F) in fall (September–October) 2011.

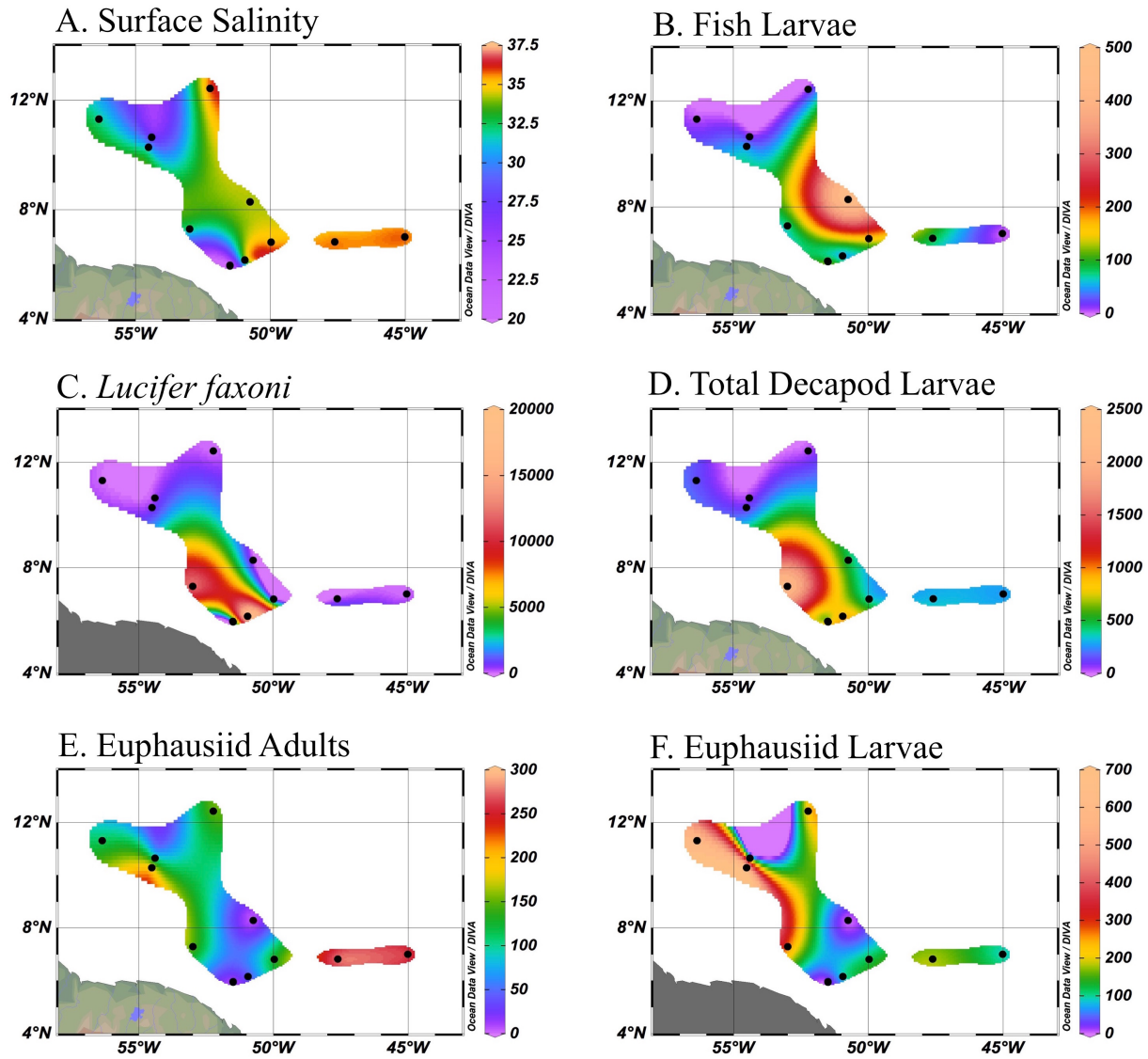


Fig. 7. Daytime areal distribution of sea surface salinity (A) and 150 m depth-integrated abundances (individuals m^{-2}) for fish larvae (B) decapods (C-D) and euphausiids (E-F) in spring (May-June) 2010.

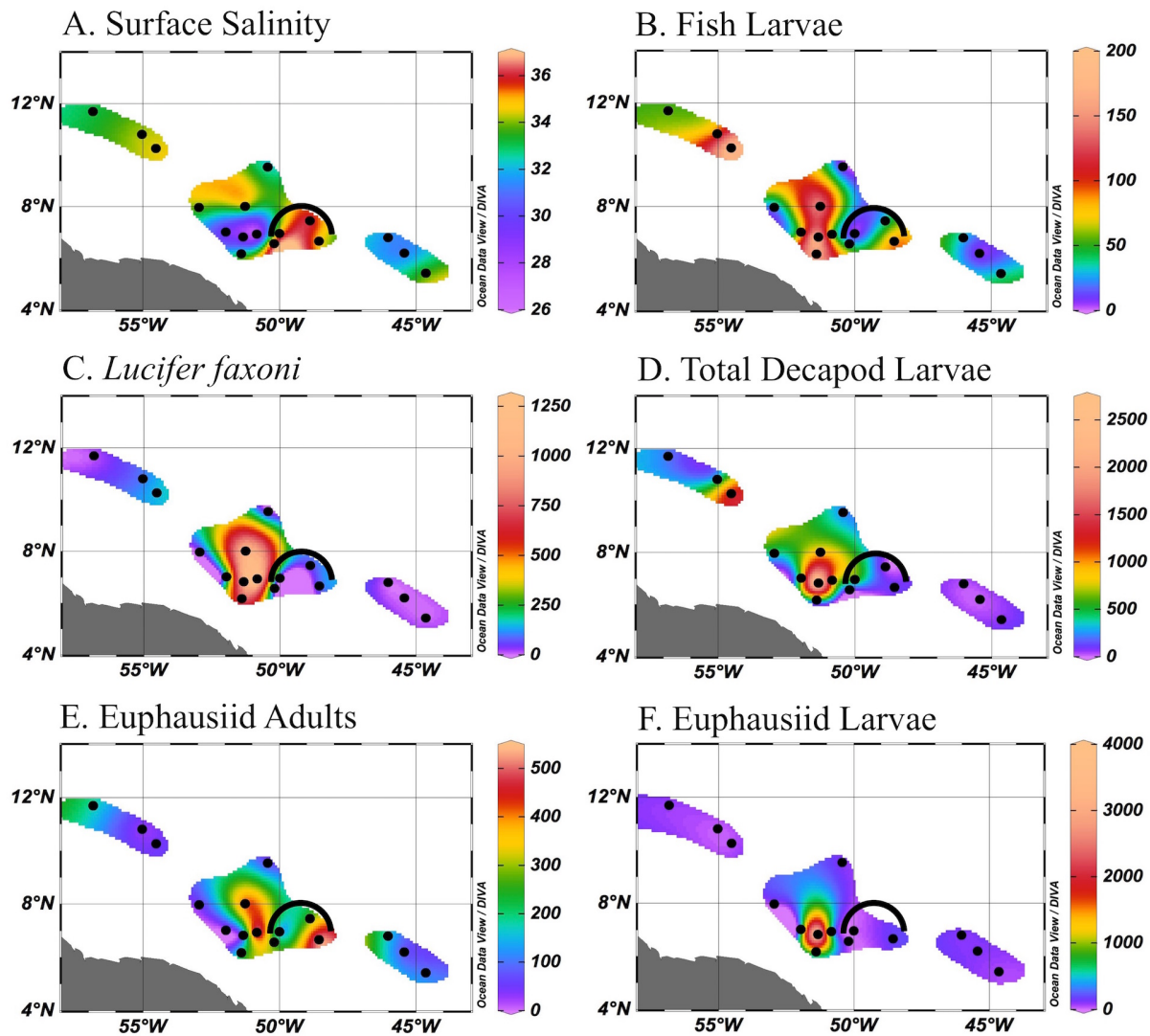


Fig. 8. Daytime areal distribution of sea surface salinity (A) and 150 m depth-integrated abundances (individuals m^{-2}) for fish larvae (B) decapods (C-D) and euphausiids (E-F) in fall (September-October) 2011. Black arc indicates frontal region associated with the mean current direction of the North Equatorial Counter Current as shown in Fig. 1 of Coles et al. 2013.

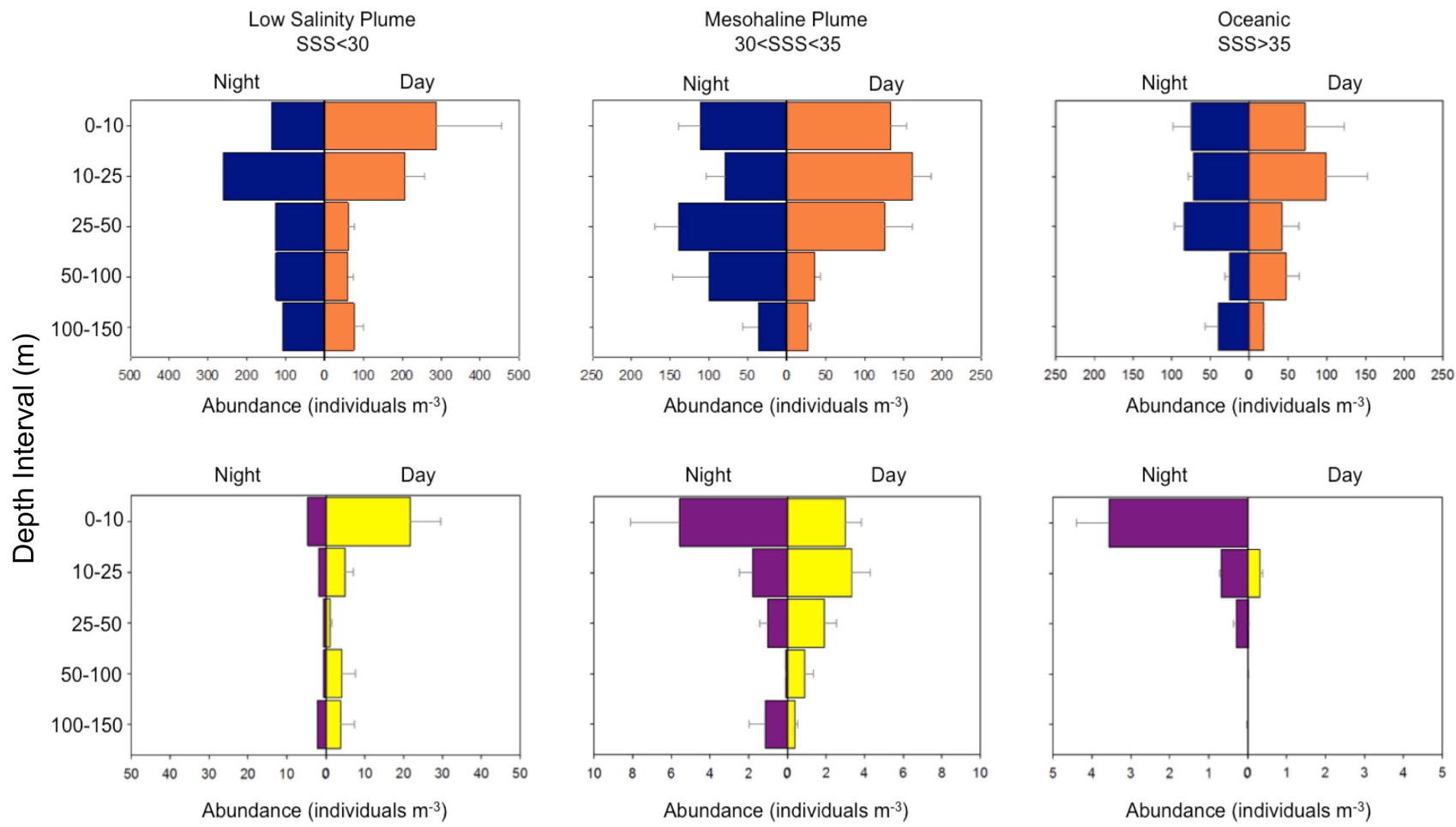
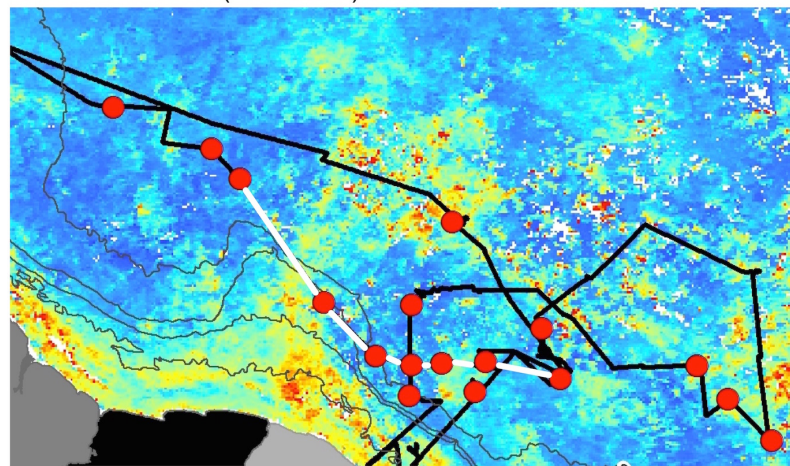
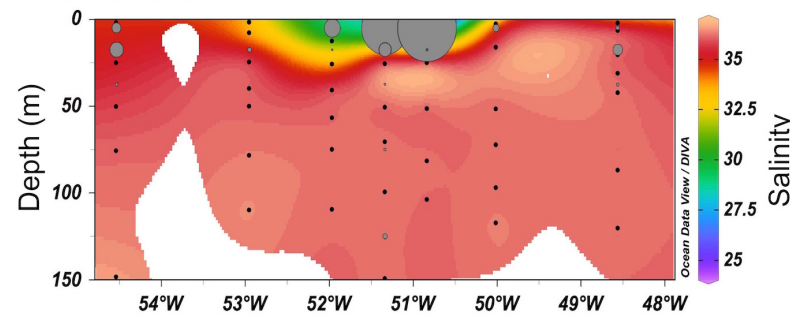


Fig. 9. Depth profiles for each station salinity category of calanoid copepods (top) and total decapod larvae (bottom) in night and day. Values are average \pm SE, n for the each depth strata ranges from 1-12. Note different x-axes scales.

A. Fall Transect (white line)



B. *Lucifer faxoni*



C. Chaetognaths

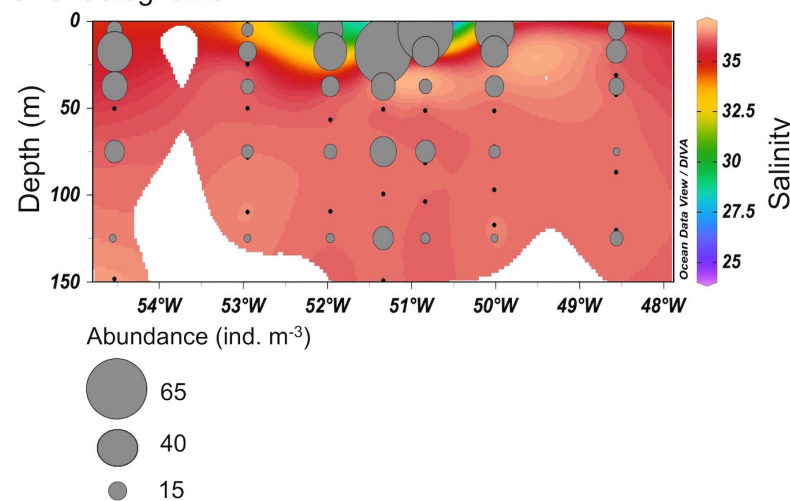


Fig. 10. Plume transect from fall (September-October) 2011 showing vertical distribution of taxa. Plume transect (A; white line) and depth profiles of salinity overlaid with abundance of (B) *Lucifer faxoni* and (C) chaetognaths (grey circles). Transect is overlaid on monthly average chromophoric dissolved organic matter (CDOM) concentration using Aqua-MODIS satellite data (oceancolor.gsfc.nasa.gov). *L. faxoni* and chaetognath abundances are plotted at the midpoint of the MOCNESS interval (e.g., 0-10 m is plotted at 5 m).

Table S1. Spring (May-June) 2010 150 m depth-integrated abundances for zooplankton taxa enumerated. Values are averages \pm standard error. Samples are arranged by station category and time of collection. Dashes indicate taxon was not present in any sample in given category.

Taxonomic Group	Low Salinity Plume		Mesohaline Plume		Oceanic	
	Day	Night	Day	Night	Day	Night
Amphipoda						
Hyperiidea	34.1 \pm 22.7	12.1	42.7 \pm 29.7	30.9 \pm 10.9	44.1 \pm 18.2	95.1 \pm 0.6
Gammaridea	38.7 \pm 38.2	-	0.5	0.9	-	-
Barnacles						
Cyprid	481.7 \pm 466.3	-	616.6 \pm 314.5	23.6	-	-
Nauplii	159.9	-	302.8	-	-	-
Chaetognatha						
Total	683.6 \pm 202.5	327.2	1,617 \pm 422.1	2,052 \pm 587.3	2,545 \pm 302.9	3,058 \pm 425.6
Cladocera						
Total	59.4	-	429.9	-	-	-
Copepoda						
Calanoida	10,638 \pm 2,653	29,326	26,016 \pm 4,710	25,002 \pm 2,880	23,547 \pm 1,290	39,404 \pm 1,401
Cyclopoida						
Oithonidae	1,224 \pm 546.0	3,643	3,284 \pm 1,171	3,585 \pm 1,116	5,243 \pm 2,144	6,080 \pm 2,403
Other	1,166.10	-	129.1 \pm 45.4	-	619.2 \pm 307.5	-
Harpactacoida						
<i>Macrosetella gracillis</i>	466.9 \pm 291	106.8	1,463 \pm 775.3	1,037 \pm 296.2	1,932 \pm 802.7	3,305 \pm 2311
<i>Miracia</i> spp.	346.9 \pm 330.1	84.3	200.6 \pm 52.1	138.4 \pm 36	79.1 \pm 37.4	309.9 \pm 122.5
Other	-	-	-	-	163.6 \pm 137.5	-
Poecilostomatoida						
Corycaeidae	937.9 \pm 355.9	2,486.7	3,586.2 \pm 962.1	2,279 \pm 244.2	4,110 \pm 965.8	3,960 \pm 488.0
Oncaeidae	1,610 \pm 851.5	4,868	3,700 \pm 743.0	6,732 \pm 2106	4,999 \pm 1,538	10,809 \pm 2,865
Saphirinidae	17.9 \pm 9.4	-	17.4 \pm 7.8	2.6 \pm 0.8	75.7 \pm 28.4	52.9 \pm 8.3

Unidentified Nauplii	85.5 ± 9.5	-	211.3 ± 99.6	$1,225 \pm 1,098$	254.2 ± 119.6	235
Ctenophora						
Total	0.4	-	0.5	-	-	-
Decapoda						
<i>Lucifer faxoni</i>	971.4 ± 441.3	1,167	$6,197 \pm 3,842$	760.6 ± 742.6	138.5 ± 95.4	471.8 ± 276.0
<i>Lucifer typus</i>	34.5 ± 34.1	-	2.1 ± 0.9	1.3	66.3 ± 62.9	4.3 ± 0.4
Adult (Other)	-	0.7	-	0.9 ± 0.1	-	0.3
Larvae						
Solenoceridae	10.2 ± 8.2	-	191.2 ± 186.4	27.2	17.4 ± 10.6	15.8
Thalassinidae	26.5 ± 22.6	6.2	39.8 ± 20.3	49.3 ± 37.8	51.6 ± 31	9.6 ± 5.2
Paguroidea	7.8 ± 7.5	2.6	37.3 ± 16.1	30.5 ± 25.9	2.4 ± 1.9	16.7 ± 13.0
Phyllosoma Larvae	0.2 ± 0.1	0.7	0.5 ± 0.4	1.1	1 ± 0.3	1.4 ± 0.6
Unidentified Larvae	443.3 ± 405.9	2.1	234.2 ± 86.1	291.7 ± 195.9	159.9 ± 55	44.4 ± 15
Unidentified Megalopae	8.3 ± 8.0	-	388.7 ± 388.4	85.5 ± 84.5	38.4 ± 22.8	50.1 ± 49.5
Unidentified Zoeae	6.8	-	206.3 ± 198.5	41 ± 31.1	0.9 ± 0.6	10.6
Euphausiacea						
Adult	31.7 ± 21.0	60.6	99.2 ± 34.6	774.3 ± 410.6	203.6 ± 38.2	$1,376 \pm 521.2$
Larvae	9.8	126.4	414.7 ± 138.8	413.8 ± 312.5	151.2 ± 28.6	663.5 ± 238.6
Teleost Fishes						
Larval fishes	68.9 ± 51.3	2.6	129.7 ± 86.4	30.1 ± 13.9	63.1 ± 38.2	347.3 ± 130.7
Leptocephali	0.2	1.0	0.6 ± 0.3	1.9 ± 1.3	1.4 ± 1.2	4.1 ± 3.0
<i>Cyclothona</i> spp.	-	-	0.2	-	-	-
<i>Chauliodus</i> spp.	-	-	-	0.3	-	-
Myctophidae	-	-	-	2.3 ± 1.1	-	2.1 ± 0.8
Foraminefera						
Total	106.6 ± 94.5	-	680.3 ± 18.9	-	608.3 ± 164.9	314.9 ± 102.2
Isopoda						
Total	-	-	-	-	-	-

Lancelets						
Total	-	-	5 ± 4.4	0.5	0.8	1.5
Hydrozoan						
Medusa	-	-	65 ± 64.5	82.5	4.1	0.6
Unidentified	-	-	-	0.2	0.4	0.6 ± 0.3
Mollusca						
Cephalopoda						
Octopoda	0.2	-	0.1	-	-	-
Teuthida	0.9 ± 0.6	-	7.4 ± 7.0	1.1 ± 0.2	0.5 ± 0.2	1.8 ± 0.4
Unidentified	-	0.5	-	-	-	-
Gastropoda						
Heteropoda	-	-	0.5	-	-	0.7
Unidentified	-	-	-	-	-	-
Bivalvia (total)	-	-	1.3	-	-	-
Mysidacea						
Total	84 ± 83.6	-	38.3 ± 28.3	0.6	0.9 ± 0.5	2.7 ± 1.2
Ostracoda						
Total	930.6 ± 515.9	359.5	701.6 ± 178.6	941.1 ± 146.7	728.9 ± 229.4	$1,506 \pm 230.5$
Polychaeta						
<i>Tomopteris</i> spp.	-	-	0.4	36.5 ± 36.3	-	31.6
Unidentified Adult	51.1 ± 5.5	11.7	42.2 ± 27	117.9 ± 65	111.3 ± 39.7	123 ± 60
Unidentified Larvae	82.7	-	68.4 ± 5.5	50.6 ± 30.2	57.8 ± 30.7	-
Pteropoda						
Thecosomata						
Clio spp.	-	0.3	0.2	0.2	-	15.9 ± 15.2
Creseis spp.	33.8 ± 12.8	-	5.6 ± 1.3	-	26.0	29.4
Limacina spp.	0.3	-	163.6 ± 121.7	93.2 ± 34.1	80.2	524.1 ± 413.7
Unidentified	17.5 ± 11.1	186.9	3.2 ± 1.6	98.2 ± 48.7	1.6 ± 0.7	19.9 ± 17.5

Gymnosomata (total)	0.6 ± 0.5	-	0.8 ± 0.4	2.4	0.4 ± 0.1	-
Radiolaria						
Total	36.4	-	-	104.6	-	-
Siphonophores						
Calycophorae						
Abylidae	20.5 ± 1.4	9.0	9.7 ± 2.7	23.2 ± 5.8	13.0 ± 10.1	12.3 ± 3.5
Diphyidae	104.5 ± 42.1	146.4	123.1 ± 66.3	233.1 ± 61.5	122 ± 52.4	285 ± 64.4
Hippopodiidae	1.4 ± 0.5	2.5	1.2	6.8 ± 4.5	-	3.1 ± 2.1
Unidentified	7.7	-	-	-	33.4 ± 6.3	-
Physonectae (total)	-	-	43.7	-	-	3.8
Stomatopoda						
Total	14.1 ± 9.8	7.6	10.4 ± 4.7	12.5 ± 5.5	50.3 ± 48.2	7.3 ± 4.0
Tunicata						
Appendicularians	34.0 ± 33.6	-	902.7 ± 710.6	173.4 ± 71.1	455.1 ± 108.2	$1,079 \pm 844.4$
Doliolids	172.4 ± 68.3	-	225.9 ± 75.4	67.5 ± 34.9	451.2 ± 262.1	337.9 ± 239.7
Salps	-	1.3	-	1.1 ± 0.7	1.7 ± 0.5	196.7 ± 83.5

Table S2. Fall (September-October) 2011 150 m depth-integrated abundances for zooplankton taxa enumerated. Numbers are averages \pm standard error. Samples are presented by station category and time of collection. Dashes indicate the associated taxa were not present in any samples from the respective category.

Taxonomic Group	Low Salinity Plume		Mesohaline Plume		Oceanic	
	Day	Night	Day	Night	Day	Night
Amphipoda						
Hyperiidea	74.4 \pm 46.5	80.4	20.3 \pm 4.1	57 \pm 19.4	84.9 \pm 8.7	62.1 \pm 5.0
Gammaridea	-	-	0.3	-	-	-
Barnacles						
Cyprid	886.3 \pm 613.9	2,045.0	229 \pm 92.5	385.9 \pm 154.3	26.6 \pm 15.9	84.7 \pm 60.7
Nauplii	80.4 \pm 58.4	-	65.9	-	-	4.3
Chaetognatha						
Total	2,980 \pm 855.2	2,422	1,555 \pm 376.4	1,949 \pm 756.0	709.2 \pm 130.2	942.6 \pm 34.6
Cladocera						
Total	-	-	72.2 \pm 23.6	180.7 \pm 136.3	-	-
Copepoda						
Calanoida	28,494 \pm 7,201	40,022	20,099 \pm 2,100	25,145 \pm 5,894	13,103 \pm 2,001	14,324 \pm 2,234
Cyclopoida						
Oithonidae	3,951 \pm 567.3	4,162	3,549 \pm 360.9	3,819 \pm 942.8	1,793 \pm 257.5	4,131 \pm 2,241
Other	-	-	15.3 \pm 11.6	17.4 \pm 16.3	-	-
Harpactacoida						
<i>Macrosetella gracillis</i>	406.9 \pm 145.6	271.2	288.4 \pm 80.7	430.7 \pm 87.9	123.1 \pm 33.9	36.9 \pm 18.5
<i>Miracia</i> spp.	60 \pm 36.8	-	26.2 \pm 8.8	7.1	-	6.7
Other	-	-	15.8	-	-	-
Poecilostomatoida						
Corycaeidae	2,253 \pm 846.2	1,242	1,914 \pm 267.5	1,776 \pm 160.0	655.4 \pm 392.5	1,957 \pm 1,054
Oncaeidae	4,994 \pm 1,956	2,178	2,719 \pm 611.7	5,362 \pm 1,501	1,499 \pm 1,195	3,068 \pm 329.6
Saphirinidae	19.7 \pm 17.1	48.5	63.1 \pm 23.2	107.5 \pm 38.7	0.9 \pm 0.3	11.6 \pm 7.2

Unidentified Nauplii	-	-	-	-	27.1	-
Ctenophora						
Total	0.2	-	0.3	-	-	-
Decapoda						
<i>Lucifer faxoni</i>	794.5 ± 356.4	3,821.3	181.4 ± 100.0	383.5 ± 200.4	54.6 ± 3.8	58.5 ± 13.5
<i>Lucifer typus</i>	-	-	2.6 ± 0.7	5.4 ± 3.5	0.6	0.2
Adult (Other)	-	41.6	-	0.6 ± 0.2	-	0.3
Larvae						
Solenoceridae	160 ± 38.9	128.1	121.7 ± 86.8	108.8 ± 37.0	-	3.1
Thalassinidae	53.3 ± 7.3	99.6	77.9 ± 33.7	40.8 ± 10.7	9.9 ± 1.0	66.6 ± 20.1
Paguroidea	21 ± 12.1	1.5	14.3 ± 6.9	2.5 ± 0.8	-	0.3
Phyllosoma Larvae	0.4	-	0.5 ± 0.1	-	0.1	1.2 ± 0.3
Unidentified Larvae	370.4 ± 180.4	150.9	120.2 ± 32.2	166.7 ± 113.5	1.7 ± 0.7	22.1 ± 9.7
Unidentified Megalopae	775.2 ± 595.5	29.6	60.2 ± 36.1	31.6 ± 16.2	-	12 ± 10.7
Unidentified Zoeae	35.8 ± 35.6	35.3	51.3 ± 14.5	22.7 ± 17.2	-	3.3 ± 2.9
Euphausiacea						
Adult	190.1 ± 168.8	120.7	166.3 ± 44.6	486.2 ± 152.6	270.6 ± 2.0	855.6 ± 327.3
Larvae	1,470 ± 1,148	1,264	158.2 ± 81.8	150.4 ± 47.2	32.6	132.2 ± 41.3
Teleost Fishes						
Larval fishes	99.1 ± 39.6	279.2	68.8 ± 18.6	228.1 ± 66.7	35.1 ± 0.9	60.9 ± 0.5
Leptocephali	2.3 ± 0.3	1.2	2.5 ± 1.8	4.2 ± 2.2	-	0.3
<i>Cyclothona</i> spp.	-	-	-	-	-	-
<i>Chauliodus</i> spp.	-	-	-	-	-	-
Myctophidae	-	0.3	-	1.1 ± 0.3	-	0.4
Foraminefera						
Total	260.1 ± 36.7	-	323.6 ± 286.1	-	10.7	-
Isopoda						
Total	-	-	-	-	-	12.0

Lancelet						
Total	-	16.0	1.9 ± 1.3	0.7 ± 0.2	-	5.2
Hydrozoan						
Medusa	73.3 ± 28.9	59.8	145.4 ± 132.2	19.9 ± 10.4	-	0.6 ± 0.4
Unidentified	-	-	-	0.3	-	-
Mollusca						
Cephalopoda						
Octopoda	-	-	0.2	-	-	-
Teuthida	0.8 ± 0.2	0.5	3.6 ± 2.1	0.2 ± 0.1	0.1	0.3
Unidentified	-	2.6	-	-	0.1	0.6
Gastropoda						
Heteropoda	-	-	0.3	3.9 ± 3.7	5.8	0.6
Unidentified	-	198.4	131.4 ± 47.8	88.9 ± 44.3	-	157.8 ± 112.3
Bivalvia (total)	-	238.3	15.3 ± 3.7	9.3	-	-
Mysidacea						
Total	1.5 ± 0.3	2.6	8.3 ± 4.1	31.6 ± 30.6	-	1.5
Ostracoda						
Total	628.0 ± 143.2	1,073	529.7 ± 71.7	805.8 ± 106.5	100.3 ± 46.8	360.2 ± 57.9
Polychaeta						
<i>Tomopteris</i> spp.	83.3	0.8	3.6 ± 3.4	-	0.3	-
Unidentified Adult	122.2 ± 36.8	538.0	119.1 ± 60.6	159.8 ± 124.3	17.7 ± 17.4	51.9 ± 25.4
Unidentified Larvae	242.2 ± 20.4	-	6.6 ± 4.1	16.9 ± 9.9	-	-
Pteropoda						
Thecosomata						
Clio spp.	-	-	0.1	3.2	-	-
Creseis spp.	2.4	1.8	19.1 ± 18.9	30.1	-	-
Limicina spp.	-	-	10.0	35.7	-	17.9
Unidentified	6.0 ± 4.3	0.3	5.9 ± 2.3	29.9 ± 10.4	14.1	12.9 ± 8.4

Gymnosomata (total)	0.5	-	0.2 ± 0.1	-	0.2 ± 0.1	3.1 ± 2.2
Radiolaria						
Total	-	-	245.2 ± 173.9	-	-	-
Siphonophores						
Calycophorae						
Abylidae	41.9 ± 17.8	35.5	24.4 ± 7.5	14.2 ± 5.8	37.7 ± 15.9	35.1 ± 20.3
Diphyidae	391.5 ± 235.6	347.1	116.4 ± 32	196.2 ± 10.4	139.5 ± 80.9	57.9 ± 23.8
Hippopodiidae	-	0.8	-	1.0	-	-
Unidentified	-	-	0.4 ± 0.1	-	-	-
Physonectae (total)	-	-	1.4 ± 0.5	0.5	0.6	1.1 ± 0.6
Stomatopoda						
Total	9.0 ± 6.1	5.8	27.7 ± 13.5	31.9 ± 25.9	1.9 ± 1.4	2.0 ± 0.1
Tunicata						
Appendicularians	17.9	316.2	436.4 ± 68.9	344.4 ± 334.0	599.6	103.9 ± 0.5
Doliolids	391.0 ± 77.4	745.7	311.6 ± 93.0	213.3 ± 54.7	-	33.6 ± 15.2
Salps	14.0 ± 12.4	9.6	78.8 ± 33.3	96.2 ± 68.5	-	6.1 ± 3.7

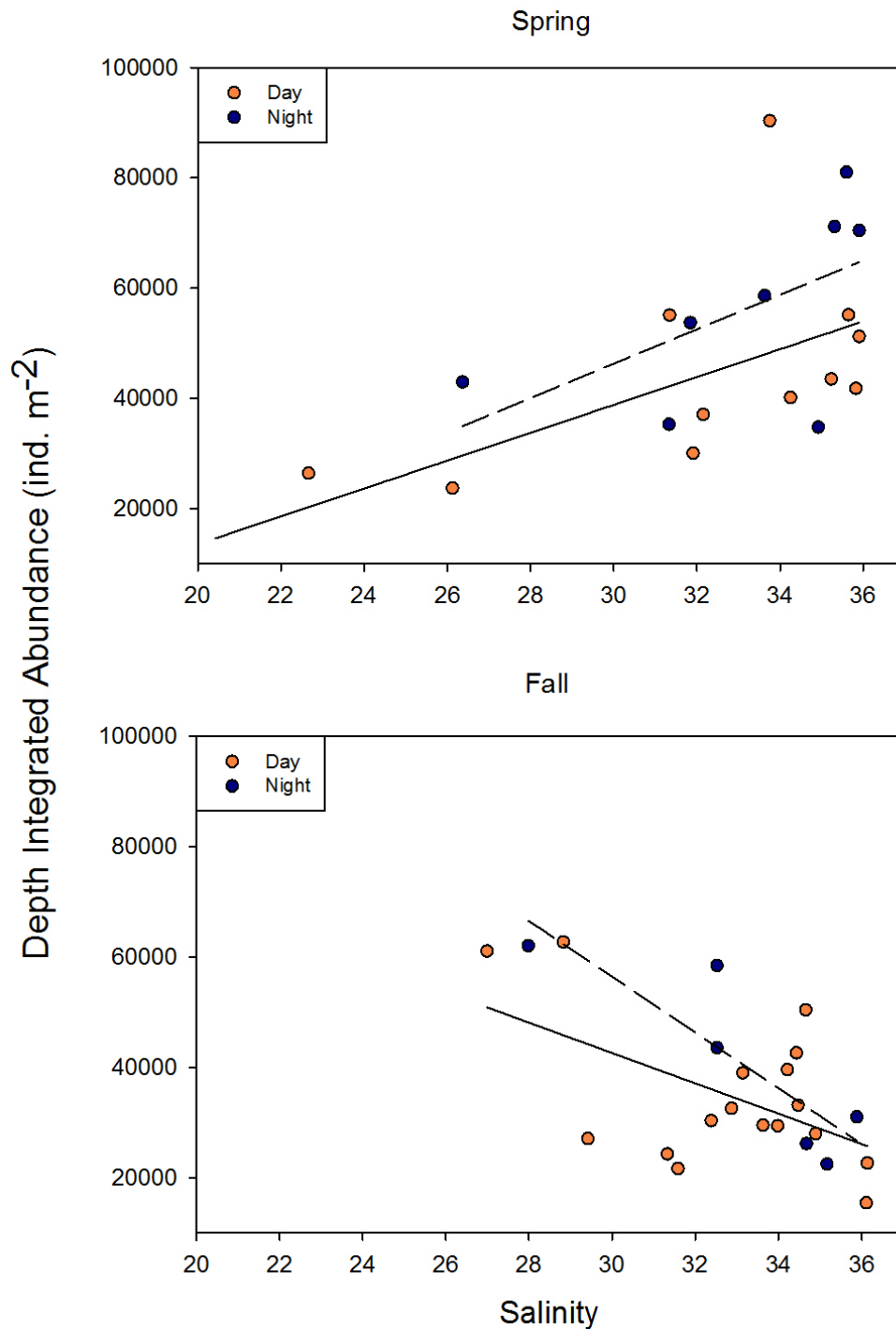


Fig. S1. Surface salinity vs. mesozooplankton abundance (integrated 0-150 m) for spring (May-June; top) 2010 and fall (September-October) 2011. Daytime (orange; solid line) and nighttime (blue; dashed) regressions are reported for both seasons. Regressions statistics and equations are as follows: spring daytime $p=0.019$, $r^2=0.44$, $y=2527x-37004$; spring nighttime $p=0.134$, $r^2=.33$, $y=3122x-47375$; fall daytime $p=.029$, $r^2=.28$, $y=-2752x+125134$; fall nighttime $p=.027$, $r^2=.74$, $y=-5056x+208056$.

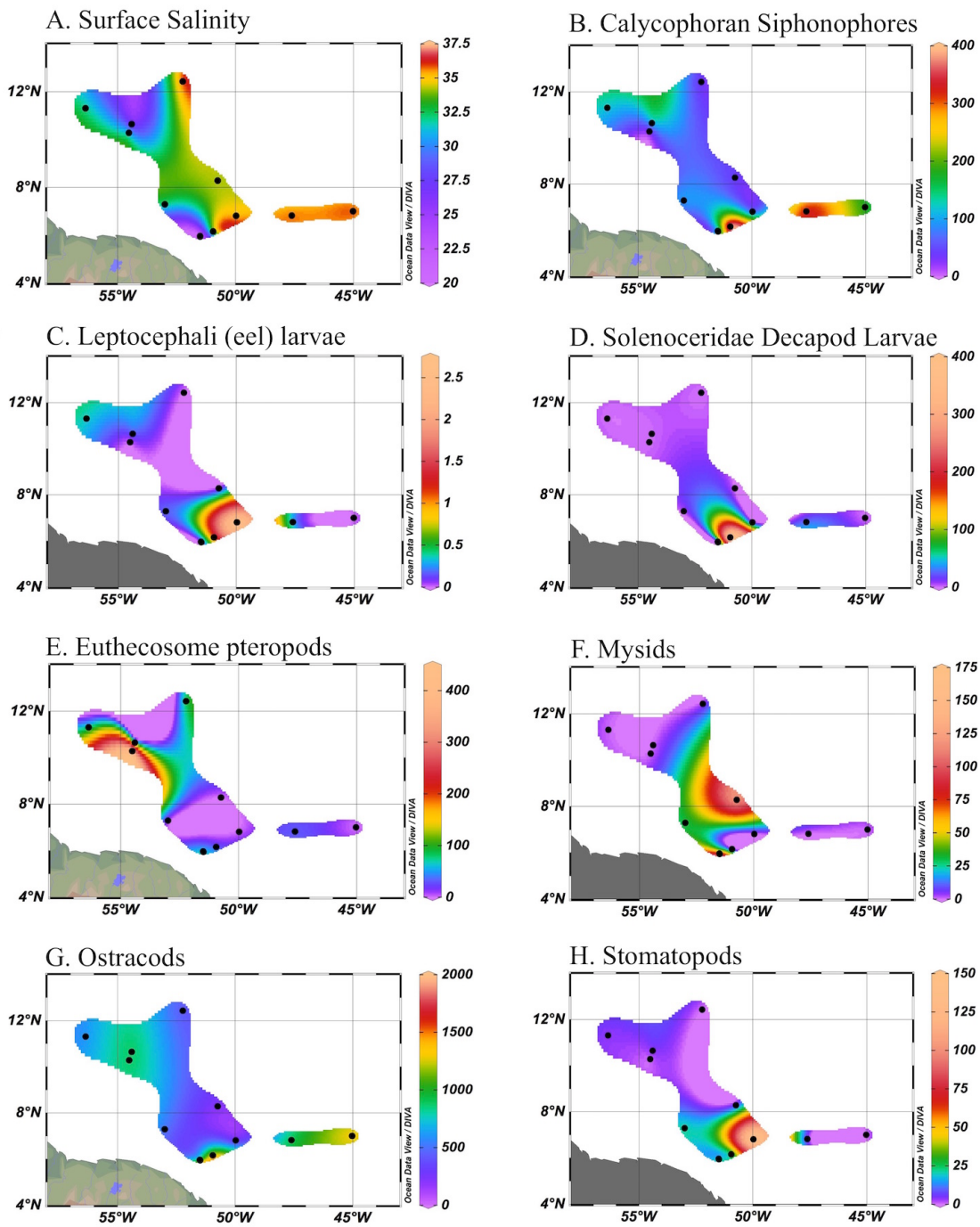


Fig. S2. Daytime areal distribution of surface salinity (A) and 150 m depth-integrated abundances (individuals m⁻²) for selected non-copepod taxa (B-H) from spring (May-June) 2010.

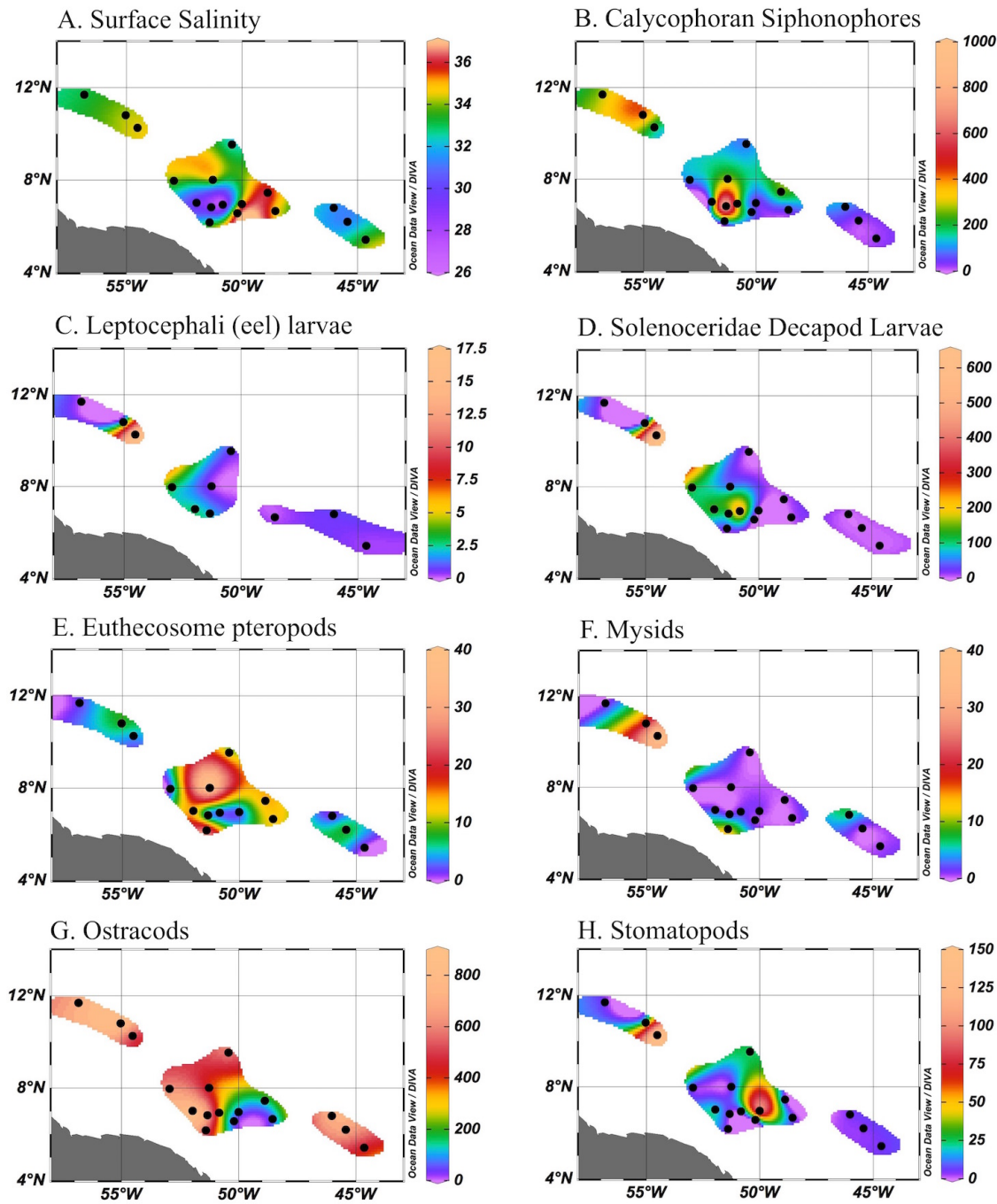


Fig. S3. Daytime areal distribution of surface salinity (A) and 150 m depth-integrated abundances (individuals m^{-2}) for selected non-copepod taxa (B-L) from fall (September–October) 2011.

CHAPTER 3

Meso- and microzooplankton grazing in the Amazon River plume and western tropical North Atlantic Ocean

This chapter published in the journal *Limnology and Oceanography* as:

Conroy, B. J., D. K. Steinberg, M. R. Stukel, J. I. Goes, and V. J. Coles. 2016. Meso- and microzooplankton grazing in the Amazon River plume and western tropical North Atlantic. *Limnology and Oceanography* **61**: 825–840. doi:10.1002/lno.10261

ABSTRACT

Largely due to size differences, mesozooplankton are important exporters of carbon and prey for larger organisms, while microzooplankton are important recyclers of nutrients, dominant grazers of phytoplankton, and a key link in the microbial loop. We investigated the relative importance of meso- and microzooplankton grazing in the western tropical North Atlantic Ocean (WTNA) and Amazon River plume. Sampling as part of the ANACONDAS project occurred in spring (May-June) 2010 during the peak outflow of the Amazon River and in fall (September-October) 2011 during the plume seasonal retroflection. Mesozooplankton grazing rates decreased with increasing salinity in both seasons, but during the fall both day and nighttime grazing rates were significantly negatively correlated with salinity. Mesozooplankton grazing was highest in plume-influenced surface waters (0-25m), and usually dominated by smaller size classes (0.2-0.5mm and 0.5-1.0mm). Microzooplankton grazing accounted for approximately 68% of bulk phytoplankton growth across all stations. Comparison of meso- and microzooplankton grazing suggests a transition in food web dynamics from a mesozooplankton dominated “export” structure in the plume transitioning to a microzooplankton dominated “retention” structure at mesohaline and oceanic stations above sea surface salinity of 33. Comparison between the seasons suggests a seasonal planktonic succession of low mesozooplankton grazing during the spring peak discharge followed by higher grazing rates and impact by this group during the fall retroflection. These results provide important baseline information required for examining effects of climate change on the planktonic food web of the WTNA and for use in biogeochemical models of the region.

1. INTRODUCTION

The role that zooplankton play in determining the structure and efficiency of pelagic food webs varies with a multitude of factors, including region, season, depth, and phytoplankton and zooplankton size. Retention food webs are considered characteristic of open ocean, oligotrophic environments, where microzooplankton efficiently graze small phytoplankton, and nutrients and organic material is retained and recycled in surface waters (Wassmann 1997). Export food webs on the other hand, common to upwelling or coastal regions, are characterized by large phytoplankton and shorter food webs, with phytoplankton sinking out in aggregates or grazed by large zooplankton producing rapidly sinking fecal pellets (Michaels and Silver 1988; Wassmann 1997; Stukel et al. 2013b). This study investigates meso- and microzooplankton grazing in a region where these two food web paradigms potentially overlap, due to the mingling of the nutrient rich outflow of the Amazon River with the oligotrophic western tropical North Atlantic Ocean (WTNA).

In the WTNA, the Amazon River flows onto the shelf, forming a thin, low salinity and high nutrient plume with very strong vertical stratification. The plume creates a unique environment for enhanced primary production driven primarily by diazotrophy (N_2 -fixation) from diatom-diazotroph associations (DDAs) (Subramaniam et al. 2008). The plume covers up to $1.5 \times 10^6 \text{ km}^2$ of the WTNA in July and August during the period of retroflection when the North Equatorial Countercurrent surfaces and advects fresh water eastward across the basin (Moller et al. 2010; Coles et al. 2013). Earlier in the spring, in May and June, the plume is primarily flowing northwestward, though the retroflection may initiate towards the end of this period. The plume ranges from 5 to 25m

thick (Coles et al. 2013) and supplies allochthonous silicon (Si) and phosphorus (P) to offshore regions of the WTNA. This input of plume Si and P into the nitrogen-limited open ocean at Si:N and P:N ratios in excess of that typically needed by phytoplankton creates a distinct niche for N₂ fixation by DDAs, leading to enhanced primary production in this region (Subramaniam et al. 2008). Carbon drawdown associated with this primary production challenges the previous view of the tropical ocean as a source of carbon to the atmosphere (Takahashi et al. 2002; Mikaloff Fletcher et al. 2007) and instead affirms that the region is a biologically-mediated carbon sink (Cooley and Yager 2006; Cooley et al. 2007; Subramaniam et al. 2008).

The fate of this enhanced production in the WTNA, however, is unknown. Aside from a historical study in this region that quantified copepods and cladocerans in the surface 200m (Calef and Grice 1967), characterization of zooplankton community composition has been restricted to the Amazon River coastal estuaries (Costa et al. 2009; Magalhães et al. 2009). Furthermore, there are no previous studies describing zooplankton grazing in the plume-influenced WTNA. Most studies of mesozooplankton grazing in the tropical open ocean have been limited to the Pacific Ocean, i.e., the Joint Global Ocean Flux Study (JGOFS) Equatorial Pacific study (EqPac) (Dam et al. 1995; Zhang et al. 1995; Roman and Gauzens 1997; Roman et al. 2002), and more recently the Equatorial Biocomplexity project (Décima et al. 2011; Landry et al. 2011). In the Atlantic Ocean, tropical mesozooplankton grazing is limited to the eastern portion of the basin, where results from the Atlantic Meridional Transect project indicate mesozooplankton grazing impact averaged 2.3% of Chl *a* (Isla et al. 2004) in the eastern tropical North

Atlantic and an average of 6% of Chl α in the subtropics near the Azores (Huskin et al. 2001).

Likewise, little is known about the impacts of microzooplankton grazing in the WTNA. Small protozoa are considered to be the dominant grazers globally, accounting for removal of 70-133% of primary production per day (Sherr and Sherr 2002) and 75% overall in the tropical and subtropical regions as determined by metadata analysis (Calbet and Landry 2004). A further metadata analysis of microzooplankton grazing, using Longhurst's classic biogeographic domains and an expanded dataset (nearly double the data points of the 2004 study), indicates that within the "Trades Atlantic" region, microzooplankton grazing accounts for approximately 70% of primary production grazed per day (Schmoker et al. 2013). However, this biogeographic region, which includes the WTNA, was specifically recommended for further study of microzooplankton grazing, as the only open ocean study was located near the Azores, with the remaining coming from subtropical or tropical estuaries (Schmoker et al. 2013).

Here we attempt to quantify meso- and microzooplankton grazing in the Amazon-influenced WTNA to address a distinct gap in our understanding of the fate of the enhanced primary production in this region. We also provide an important baseline of removal of primary production in the different water types of the WTNA under current climate conditions. Observed changes to the hydrological cycle in the Amazon basin (Gloor et al. 2013) and increasing temperature predicted with climate change (Doney et al. 2012) could directly impact the Amazon River discharge—which is linked with both the El Niño Southern Oscillation (ENSO) and sea surface temperature in the tropical north Atlantic (Richey et al. 1989; Espinoza et al. 2011). Furthermore, these measurements will

improve existing empirical and biogeochemical models of this dynamic region (Cooley et al. 2007; Stukel et al. 2014), as well as provide important comparisons with other major rivers discharging into the oceans (e.g., the Mississippi, Mekong, and Congo).

2. METHODS

2.1 Study area

Sampling in the Amazon River plume-influenced region of the WTNA (between 0-13° N and 44-57°W) was conducted as part of the Amazon Influence on the Atlantic: CarbOn export from Nitrogen fixation by DiAtom Symbioses (ANACONDAS) project. We report data from two cruises which occurred May 22-June 24, 2010 aboard the *R/V Knorr* and September 3-October 8, 2011 aboard the *R/V Melville*. The cruise in 2010, hereafter referred to as “spring”, focused on the plume during the season of peak discharge (Fig. 1A), and in 2011, referred to as “fall”, during the seasonal maximum reach and plume retroflection that advects the plume southeastward (Fig. 1B). Sampling design included stations in and out of the plume to capture variation in biogeochemistry with respect to plume influence. Station selection was based largely on sea surface salinity (SSS) and Chl *a* and phycobilipigment fluorescence measured underway (Goes et al. 2014), and other plume indicators (e.g., chromophoric dissolved organic matter-CDOM concentration) seen from satellite imagery. For the purposes of this analysis, we separate sampling stations into the following categories: stations with SSS < 30 were identified as “low salinity” plume, stations with SSS between 30 and 35 “mesohaline” plume, and stations with SSS > 35 “oceanic” non-plume.

2.2 Mesozooplankton collection

Mesozooplankton (i.e., zooplankton >0.2 mm) were collected in both years with a 1-m Multiple Opening and Closing Net and Environment Sensing System (MOCNESS; Wiebe et al. 1976) fitted with ten 202 µm mesh nets. Tows were performed to 150m or 500m. Only the 0-150 m depth intervals were processed for determination of gut

fluorescence to avoid problems with gut evacuation and pigment degradation during the tow, and were always sampled last in the tow. Discrete depth intervals within the top 150m were 0-25 m, 25-50 m, 50-100 m, and 100-150 m during the spring. In the fall, in order to better characterize the surface plume influence, we sampled the top 25 m at higher resolution (0-10 m and 10-25 m; deeper intervals remained the same as in spring). Occasionally, at shallow depth stations, a double oblique tow using a rectangular frame (0.8 x 1.2 m) single net with 202 μm mesh was performed in surface waters (within top 25 m). When possible, both day and night tows were performed. Daytime tows were performed between 1000 and 1400 h local time and nighttime tows between 2200 and 0200 h. Once the nets were onboard, zooplankton in the cod ends used for pigment analysis were immediately anesthetized with carbonated water to prevent gut evacuation (Gannon and Gannon 1975). Samples were then split into either $\frac{1}{4}$ or $\frac{1}{2}$ of the total sample using a Folsom plankton splitter, then size fractionated using nested sieves into the following size classes: 0.2-0.5 mm, 0.5-1.0 mm, 1.0-2.0 mm, 2.0-5.0 mm, and >5.0 mm. These size fractions were then concentrated onto pre-weighed, 0.2 mm Nitex mesh filters and rinsed with Milli-Q to remove salt. When large phytoplankton were caught in the nets, filters were first inspected and picked clean of phytoplankton, then the filters were placed in petri dishes and frozen and stored at -80 °C until they were processed on shore.

2.3 Gut fluorescence analysis and mesozooplankton grazing calculation

Gut fluorescence for each size fraction was determined fluorometrically similar to that described in (Décima et al. 2011). For the 0.2-0.5 mm, 0.5-1.0 mm, 1.0-2.0 mm, and 2.0-5.0 mm size fractions, replicate 1/8 or 1/4 sections of the frozen filter were processed.

Filters were sectioned in equal divisions using a sectioning template. On occasions when the 2.0-5.0 mm size fraction contained very low biomass, and always for the >5mm size fraction, the entire filter was processed. The samples were sonicated in 90% acetone and extracted for two hours. Samples were then centrifuged to settle particulates, and concentrations of chlorophyll *a* (Chl *a*) and phaeopigments (Phaeo) in the supernatant were measured in either a Turner TD-700 or Trilogy fluorometer pre-calibrated using standing Chl *a* (Parsons et al. 1984; Båmstedt et al. 2000). As suggested by Conover et al. (1986), we did not multiply the Phaeo values by a factor of 1.51, because standard fluorometric procedures express the values as chlorophyll weight equivalents already.

For each discrete depth interval the total pigment concentration was calculated as:

$$GPC = \frac{pig * \left(\frac{1}{split}\right) * \left(\frac{1}{f}\right)}{vol} \quad (\text{Eq. 1})$$

1)

where GPC is gut pigment content (mg m^{-3}), *pig* is the sum of the Chl *a* and Phaeo values (mg), *split* is the fraction of total tow, *f* is the fraction of filter analyzed and *vol* is the volume of water filtered through the net (m^3).

Ingestion (grazing) rates ($\text{mg Chl-}a \text{ equiv. m}^{-3} \text{ d}^{-1}$) were calculated as:

$$I = GPC * k$$

(Eq. 2)

where GPC is gut pigment content (mg m^{-3}) and *k* is the daily gut evacuation rate (day^{-1}). We estimated a *k* value for all nets using the temperature dependent function $k (\text{day}^{-1}) = (0.0124 e^{0.0765T(\text{ }^\circ\text{C})}) * 1440 \text{ minutes day}^{-1}$ from (Dam and Peterson 1988). For tows using

the MOCNESS the average temperature of each depth interval was used to calculate k . For occasional oblique tows with a single net in the surface 25m, surface temperature was used to calculate k . We chose a temperature-dependent formula to determine k in order to reflect grazing rate changes with decreasing temperature and increasing depth, rather than apply an average k determined from equatorial waters that shows somewhat lower k at higher temperature than would be predicted by Eq. 2 (Zhang et al. 1995). Following the recommendation of Durbin and Campbell (2007), and the procedure used in recent studies (Landry et al. 2009; Décima et al. 2011; Bernard et al. 2012), we calculated grazing rates without the gut pigment degradation value previously included in grazing rate equations (Båmstedt et al. 2000).

Mesozooplankton grazing impact (%) was calculated for Chl a in the top 150m of the water column. Chl a was measured following the standard fluorometric methods outlined by the JGOFS program (Knap et al. 1996) and trapezoidally integrated to 150m. Briefly, 0.5-1.0 L of seawater from the CTD rosette was vacuum filtered onto a 25mm GF/F filter. Filters were then placed in 90% acetone and allowed to extract for 4 hours. They were then measured onboard using a Turner Trilogy fluorometer with before and after acidification with 2 drops of 1.2M HCl. Grazing rates were also depth-integrated by multiplying I ($\text{mg m}^{-3} \text{ day}^{-1}$) by the appropriate depth interval for each MOCNESS net then summing the nets from each tow. For oblique tows, grazing rates were multiplied by the maximum depth of the net.

We note several potential sources of error in the gut fluorescence method. As in our analysis, many previous studies assume that pigment degradation is accounted for in experimental determination of k (Durbin and Campbell 2007; Landry et al. 2009; Gleiber

et al. 2015). However, the study of Karaköylü and Franks (2012) using *in vivo* gut fluorescence in copepods found traditional gut evacuation rate experiments may underestimate grazing by 15-70%, which they attributed largely to differences between copepod feeding state (i.e., they measured gut fluorescence during active feeding). Furthermore, sampling bias from using a 202 μm net may have occurred between our mesozooplankton and microzooplankton collection creating a “grey zone” in our data potentially excluding organisms from roughly 100-450 μm (Hopcroft et al. 2001). These sources of error lead to potential underestimation of grazing rates and our estimates should therefore be considered conservative.

2.4 Microzooplankton grazing

In the fall we conducted two types of experiments to measure phytoplankton growth and protozoan grazing rates: full serial dilution series (Landry and Hassett 1982) at surface depths and two-point “mini” dilutions (Landry et al. 1984, 2008) to determine depth profiles of grazing. All samples were taken from a Niskin rosette and incubated in 2.2 or 1-L polycarbonate bottles. All incubations were carried out for 24 hours in deck-board incubators maintained at surface temperatures by a flow-through seawater system. Bottles were screened with black mesh to hold them at *in situ* light levels.

Serial dilutions – Serial dilutions were carried out at surface depths to confirm that grazing pressure decreased linearly with dilution. Duplicate treatments were set up at dilution levels of 24%, 37%, 61%, and 73% whole seawater, and amended with 200 μl of 100mM NH₄⁺ and 50 mM PO₄³⁻ (final concentrations were 8.5 μM and 4.3 μM respectively). Nutrients were added to ensure that a reduction in nutrient cycling in treatment bottles would not alter phytoplankton growth rates. Four control bottles were

also set up (100% whole seawater), including two nutrient-amended replicates and two natural replicates. All treatment bottles were prepared by first filtering water with a peristaltic pump directly from the Niskin bottle through a $0.1\mu\text{m}$ Acropak filter cartridge and into a known volume bottle of appropriate size for the respective dilution. Filtered water was then poured into a 2.2-L clear polycarbonate incubation bottle. The incubation bottle was then gently filled the rest of the way with whole seawater from the Niskin using silicon tubing. Net growth rates for each bottle were calculated from initial and final chl *a* concentrations as: $k_{\text{net}} = \ln(\text{chl}_{\text{final}}/\text{chl}_{\text{init}})$. Net growth rates of all nutrient-amended treatments were then regressed on dilution factor and the slope (equal to grazing rate) and y-intercept (equal to nutrient-amended gross growth rate) were calculated using a type I linear regression. Ambient phytoplankton gross growth rates were then calculated as the sum of grazing rate (i.e., slope) and the net growth rate of non-nutrient amended whole seawater samples.

Two-point dilutions – Two point dilutions were set up similarly to the serial dilutions described above, except that only two bottles were used (37% treatment level and whole seawater) and were not nutrient amended. Two-point dilutions were not nutrient-amended so that we could determine natural phytoplankton growth rates. Typically we conducted four sets of two-point dilutions at light levels of 33%, 11%, 4%, and 1% surface irradiance. Grazing rate was calculated as $(k_{\text{dilute}} - k_{\text{whole}})/0.63$ and gross growth rate was calculated as $k_{\text{whole}} + \text{grazing rate}$.

2.5 Microzooplankton and mesozooplankton instantaneous grazing rate comparisons

In order to compare the daily impact of micro-and mesozooplankton grazing on phytoplankton, mesozooplankton grazing rates were converted to instantaneous grazing rates (day^{-1}) by the equation:

$$\ln \left(\frac{\text{Chl}_D - I_D}{\text{Chl}_D} \right)$$

(Eq. 3)

where Chl_D and I_D are depth-integrated chlorophyll ($\text{mg Chl-}a \text{ m}^{-2}$) and grazing ($\text{mg Chl-}a \text{ equiv. m}^{-2} \text{ day}^{-1}$) respectively. When night and day values of grazing were available, values were reported as total mesozooplankton impact ($M_{\text{TOT}} \text{ day}^{-1}$) and I_D was calculated

$$\text{as: } \frac{\Sigma(I_{\text{DAY}} + I_{\text{NIGHT}})}{2}$$

(Eq. 4)

so that equation 2 was corrected for twelve hours of daytime grazing and 12 hours of nighttime grazing. If only day tows were available, values are reported as daytime mesozooplankton impact ($M_{\text{DAY}}, \text{ day}^{-1}$) and only I_{DAY} (i.e., for 24-hr. period) was used to calculate I_D . Mesozooplankton grazing was integrated to the nearest possible depth interval to the corresponding 2-point microzooplankton depth profiles (i.e., to depth of 1% light level; average of 70m for all experiments but ranged from 25-120m, depending on station).

2.6 Statistical analyses

Data were analyzed using SigmaPlot 11.0. Integrated grazing rates were regressed against salinity for both night and day tows. Comparisons between seasons were made with unpaired t-tests while comparisons between station categories for the same seasons were analyzed using one-way ANOVA. When data did not meet expectations of equal

variance and normality, they were ranked and analyzed using non-parametric tests. These included the Mann-Whitney rank sum test for between season comparisons, and the Kruskal-Wallis ANOVA on ranks for comparison between station categories.

Statistical significance of serial microzooplankton dilution experiments was determined using a Type I linear regression. To determine the uncertainties for two-point “mini” dilutions, we made the assumption that the full serial dilutions yielded accurate growth and grazing rates, then calculated the apparent growth and grazing rates that would have been determined from using only a single pair of 37% and 100% whole seawater treatments from the full dilutions. The mean differences between the full dilution and two-point dilution growth and grazing measurements were -0.02 ± 0.11 and $0.001 \pm 0.13 \text{ d}^{-1}$, respectively (mean \pm standard error), suggesting that the two-point dilutions do not bias either growth or grazing rate measurements. We calculated the root mean square errors to estimate the uncertainty of any particular two-point growth or grazing rate measurement to be 0.21 and 0.24 d^{-1} , respectively. These uncertainty estimates were then propagated through future calculations to determine the measurement uncertainty associated with using the two-point dilution technique.

3. RESULTS

3.1 Seasonal and regional depth-integrated mesozooplankton grazing patterns

Mean mesozooplankton grazing rates (integrated from 0-150 m) for all salinities combined were ~2 to 2.4-fold higher in fall than spring during the day (2.49 vs. 1.15 mg Chl-*a* equiv. m⁻² day⁻¹, fall vs. spring, respectively) and night (2.39 vs. 0.99 mg Chl-*a* equiv. m⁻² day⁻¹ fall vs. spring) (Table 1). Mean values for comparison between seasons of all salinities did not meet assumptions of normality but median grazing rates for both night and day were significantly different and higher in the fall (*p* = 0.03 for daytime rates and *p* = 0.04 for nighttime).

During both years mesozooplankton grazing generally decreased as salinity increased (Fig. 2). In spring, daytime grazing rates ranged from 0.24 to 4.02 mg Chl-*a* equiv. m⁻² day⁻¹ and nighttime rates ranged from 0.27 to 2.70 mg Chl-*a* equiv. m⁻² day⁻¹; neither nighttime nor daytime grazing rates were significantly different across the salinity range (Fig. 2A). In fall, daytime grazing rates ranged from 0.31 to 11.34 mg Chl-*a* equiv. m⁻² day⁻¹, and nighttime rates ranged from 0.33 to 8.99 mg Chl-*a* equiv. m⁻² day⁻¹; both daytime and nighttime grazing significantly decreased with increasing surface salinity (Fig. 2B).

Spatial patterns in mesozooplankton grazing were evident when the expanse of the plume was examined. During spring the plume extended northwestward and was sampled to approximately 14°N, with the highest grazing at low salinity plume stations on the continental shelf or on the slope (Fig. 3A,B). Grazing rates were low outside of the core plume region with two exceptions: a station located northwest in the outer plume (daytime and nighttime grazing rates were 0.71 and 2.7 mg Chl-*a* equiv. m⁻² day⁻¹,

respectively), and a deep, open ocean station (daytime grazing rate of 1.6 mg Chl-*a* equiv. m⁻² day⁻¹). During fall we observed a similar pattern of grazing, although rates were two to three times higher and more strongly correlated with surface salinity compared to spring. Grazing was highest in the same low salinity shelf and slope region as in spring but was also elevated within the outer plume retroflection (Fig. 3C,D). In the outer most portion of the retroflection, grazing rates ranged from 1.9 to 4.0 mg Chl-*a* equiv. m⁻² day⁻¹ during the daytime, and reached 3.7 mg Chl-*a* equiv. m⁻² day⁻¹ at night. The other region of elevated grazing was in the farthest northwest station with respective day and night grazing rates of 2.9 and 3.6 mg Chl-*a* equiv. m⁻² day⁻¹ (Fig. 3C,D).

3.2 Mesozooplankton grazing depth profiles

Patterns of grazing with depth were similar between seasons, and are illustrated for the fall in Fig. 4. Highest grazing occurred in surface waters at low salinity, plume stations, with higher grazing rates shifting to deeper in the water column as surface salinity increased (Fig. 4). At plume stations, the highest grazing rates were concentrated in the top 25m meters where plume influence was strongest (Fig. 4A,D); at mesohaline stations grazing rates followed a similar pattern although rates were not as high. Open ocean stations were characterized by lower grazing rates throughout the water column (an order of magnitude lower than at plume stations) with a slight peak at depth corresponding to a deep chlorophyll max (Fig. 4C,F). This pattern is also apparent in a transect through the plume during the fall cruise which starts on the periphery of the plume and ends in the open ocean (Fig. 5).

Across all stations and nearly all depth intervals the highest grazing rates were in the smallest size fractions of mesozooplankton (0.2-0.5mm and 0.5-1.0mm) (Fig. 4). A

notable exception occurred whereby daytime grazing rates for the 1.0-2.0mm size fraction at oceanic stations exceeded the smaller size fractions at depths of 50-100m and 100-150m (Fig.4C), near the depth of the Chl-*a* maximum (Fig. 4F). Calanoid copepods dominated mesozooplankton abundance in nearly all depths, size fractions, and salinities, with cyclopoid and poecilostomatoid copepods only occasionally exceeding abundance of calanoids. Rare exceptions to copepod dominance occurred in larger size fractions (usually >2.0mm) where decapod larvae and shrimp (e.g., families Sergestidae and Luciferidae, respectively) were prevalent in the surface plume layers.

3.3 Mesozooplankton grazing impact

In spring average mesozooplankton grazing impact across all salinities on phytoplankton standing stock was 2.3 % during the day and 1.9 % at night, compared to 7.1 and 6.0% for day and night, respectively, in the fall (Table 2). Mean values across all salinities were non-normal but the median was significantly higher in 2011 ($p = <0.001$). Mean values of both mesohaline day ($p = 0.038$) and night ($p = 0.003$) grazing impact were significantly higher in fall than spring.

To further explore grazing within the plume we also determined mesozooplankton grazing impact in the top 25m only (Table 2). The average daytime grazing impact in fall was almost ten-fold that in spring, while nighttime grazing impact was ~ 3 times higher. Mean values were non-normal but median values were significantly higher across all stations ($p < 0.001$), for daytime mesohaline ($p = 0.004$) and plume ($p = 0.029$) stations in fall compared to spring.

3.4 Microzooplankton grazing rates

In the fall we conducted a total of 7 serial dilutions and 55 two-point, “mini” dilutions. We compared the full dilutions and mini dilutions to confirm linearity of both phytoplankton growth and microzooplankton grazing between the two methods. Both were linear, although grazing was more variable, and we report mini dilution results below.

From the mini-dilutions, microzooplankton grazing was strongly positively correlated with bulk phytoplankton growth (Fig. 6). Across the range of conditions sampled, protozoan grazing averaged 68% of phytoplankton growth. Neither phytoplankton growth nor microzooplankton grazing was significantly correlated to sea surface salinity. There was no statistically significant trend of phytoplankton growth or microzooplankton grazing with level of photosynthetically active radiation (PAR), although generally phytoplankton growth was suppressed in surface waters where PAR was highest and then increased and peaked at light levels approximately 10% of surface irradiance (Fig. 7A). Microzooplankton grazing was not inhibited at high PAR but did decrease as light levels decreased in the same way as phytoplankton growth (Fig. 7B). We note that samples collected at depth were incubated at temperatures higher than ambient for their respective depth due to variation in the thermocline. This likely did not lead to significant overestimation of grazing rates, which at depth were consistently the lowest observed.

3.5 Comparison of mesozooplankton and microzooplankton grazing impact

A total of nine stations were available to compare the relative importance of microzooplankton and mesozooplankton grazing on phytoplankton growth (μ) across the plume (Fig. 8). Of the four lowest salinity stations (12, 25, 19, and 20) the net calculated

change (k') was negative for all except station 25. At all four of these stations μ did not exceed 0.6 day⁻¹. Of these low salinity stations, mesozooplankton grazing impact exceeded that of microzooplankton at all but station 25. For the remaining mesohaline and oceanic stations (13, 8, 26, 9, and 10) that pattern was reversed, with a positive k' and only one value for μ below 0.6 day⁻¹. At the highest salinity, oceanic stations, microzooplankton grazing impact was 2-13 times higher than that of mesozooplankton.

4. DISCUSSION

4.1 Grazing patterns

Plume Stations— The highest mesozooplankton grazing rates in spring were concentrated in the low salinity plume, a region characterized by an ‘estuarine type’ phytoplankton assemblage consisting of a high abundance of diatoms, cryptophytes, and green-water *Synechococcus* spp. (Goes et al. 2014). This was also the only region with detectable nitrate and nitrite, and contained the highest concentrations of silicate (Goes et al. 2014). During the fall plume retroflection, the highest grazing rates at the low salinity plume stations occurred in nearly the same geographic region although the rates were double to triple those in spring (Fig. 3). A similar diatom-dominant phytoplankton assemblage with *Chaetoceros* spp., *Hemiaulus hauckii* without the endosymbiont, and *Pseudonitzchia* spp. were found in the region (A. Kalmbach & E. Carpenter, personal communication). Other preliminary pigment results also support that this low-salinity plume region was dominated by coastal diatoms, although in lower abundance than during spring. In the plume station in the fall where microzooplankton and mesozooplankton grazing rates were both measured, the relative importance of mesozooplankton grazing was approximately 4 times higher than microzooplankton grazing (station 12 in Fig. 8).

From the patterns in grazing and phytoplankton assemblage, the inshore, coastal region of the plume can likely be characterized as a shorter, ‘export food web’, with diatoms and mesozooplankton grazers prevalent (Michaels and Silver 1988; Legendre and Michaud 1998). Further support comes from previous reports of a similar pattern of phytoplankton distribution in the plume (Carpenter et al. 1999; Shipe et al. 2006;

Subramaniam et al. 2008), as well as seasonal accumulation of calanoid copepods on the Amazon shelf corresponding to peak river discharge (Aller and Todorov 1997) which leads to a high biomass of coastal mesozooplankton grazers. The relatively lower importance of microzooplankton grazing rate compared to mesozooplankton in the inshore plume region (albeit measured from just one station) support this food web structure as well.

Mesohaline Stations— During spring a large DDA bloom occurred between 9-14°N and 53-56°W throughout the mesohaline region. Goes et al. (2014) characterized the assemblage there as dominated by DDAs, but also with some dinoflagellates, cryptophytes, and *Trichodesmium*. However, mesozooplankton grazing rates in the same region were lower compared to the plume stations (Figures 2A and 3B). In the fall the mesohaline stations were predominantly located in the outer arm of the plume during its seasonal retroflection (area of low salinity between 45-50°W in Figure 3C) and characterized by diatoms, dinoflagellates, abundant *Synechococcus* spp., and very few DDAs. Given the largely different geographic regions of mesohaline stations, differences in grazing rates and phytoplankton assemblages may be unrelated or may be indicative of a seasonal succession (discussed below).

Comparison of the mesozooplankton and microzooplankton grazing impact in the mesohaline region suggests a transition from an export food web to a retention food web (Figure 8). Compared to lower salinities, between a SSS of 32-33 phytoplankton growth rates increase, as does the importance of microzooplankton grazing on the net change of phytoplankton biomass. At stations below 32 SSS, except for station 25, mesozooplankton grazing was higher than microzooplankton grazing (stations 12, 19, and

20), resulting in a negative net calculated change in phytoplankton (k'). At stations above 33 SSS, k' became positive and microzooplankton grazing impact dominated. Further sampling is required to determine if this transition consistently occurs over such a small salinity range.

In the mesohaline region in both seasons, mesozooplankton grazing rates in the furthest northwest station were elevated relative to adjacent mesohaline stations. In spring the plume was distributed northwest towards the Caribbean, which may explain the observed elevated grazing there, but in fall the seasonal retroflection had occurred and adjacent stations were not Amazon plume-influenced. A potential explanation for enhanced grazing in this region during fall is influence from the Orinoco River plume, which has maximum discharge in August-November and flows north westward into the Caribbean and WTNA (Hellweger and Gordon 2002; Chérubin and Richardson 2007). Furthermore, a previous study in this region suggested a combination of the Amazon and Orinoco plumes supporting DDA blooms in this region (Carpenter et al. 1999).

Oceanic Stations— On both cruises, mesozooplankton grazing rates were lowest in open ocean stations without plume influence. Higher mesozooplankton grazing impact on Chl a in the top 25m at oceanic stations compared to lower salinity stations (Table 2) is best explained by low surface chlorophyll, rather than elevated grazing (Figure 8C, F) at these stations. Higher rates of microzooplankton grazing compared to mesozooplankton occurred at oceanic stations with a phytoplankton assemblage comprised of *Trichodesmium*, *Synechococcus*, as well as some dinoflagellate species (Goes et al., in prep.) supporting a “retention” food web. The average phytoplankton growth and microzooplankton grazing rates at oceanic stations ($\mu=0.80 \text{ day}^{-1}$ and $m=0.49 \text{ day}^{-1}$,

respectively, n=3) as well as the higher salinity (SSS>33) mesohaline stations ($\mu=0.83$ day $^{-1}$ and $m=0.35$ day $^{-1}$, n=2), compare well with the median value reported in the large meta-analysis of Schmoker et al. (2013) for the “Trades Atlantic” biogeographical subset ($\mu= 0.83$ day $^{-1}$ and $m= 0.49$ day $^{-1}$; from Table II Schmoker et al., 2013), although the measurements for that region were restricted to the eastern Atlantic. Furthermore, $\delta^{13}\text{C}$ data from the 2010 cruise showed an average 2.9 ‰ difference between particles and mesozooplankton at oceanic stations (Loicke-Wilde et al., in press), indicative of a complex microbial loop in the food web (Rau et al. 1990), but no significant difference at mesohaline or plume stations.

There was one exception in the spring where higher depth-integrated grazing occurred at an open ocean station compared to other oceanic stations and some mesohaline stations (Figure 3B). Goes et al. (2014) characterized phytoplankton at that station as an oceanic assemblage comprised almost entirely of *Trichodesmium* and *Synechococcus* spp., although abundances of these cyanobacteria were not exceptionally high compared to other stations (see Figure 6E-F from Goes et al. 2014). Based on this phytoplankton assemblage, elevated mesozooplankton grazing at this station is surprising as *Trichodesmium* is considered unpalatable to most mesozooplankton, with the exception of some harpacticoid copepods (Hawser et al. 1992; O’Neil and Roman 1994; O’Neil 1998). Mesozooplankton grazing on *Synechococcus* individuals has been documented (Gorsky et al. 1999; Stukel et al. 2013a), or mesozooplankton may consume *Synechococcus* via feeding on aggregates (Wilson and Steinberg 2010). Analysis of zooplankton gut contents for phycoerythrin, a diagnostic pigment for *Synechococcus*, and cyanobacteria molecular markers will help determine direct consumption by zooplankton

(Conroy et al., in prep.). Aside from this exception in 2010, the grazing patterns of meso- and microzooplankton at oceanic stations support a “retention” style food web dominated by microzooplankton rather than mesozooplankton.

Vertical Patterns– To our knowledge this is the first grazing study to utilize a depth-stratified sampling design using the MOCNESS, which enabled us to investigate how the strong salinity gradient in the upper water column created by the plume influenced grazing with depth. Depth profiles of grazing at plume and mesohaline stations indicated highest grazing in the surface 25m in plume-influenced waters, while at oceanic stations grazing was higher at depth. This pattern largely followed chlorophyll a profiles, with deeper grazing in oceanic stations in particular reflecting the deep Chl *a* maximum. Slightly reduced grazing rates for some size fractions in the surface 10m (compared to 10-25 m) at all stations may reflect feeding avoidance in surface waters with more intense solar radiation (Alonso et al. 2004). Finally, depth-stratified sampling is a useful approach for grazing studies in a region with pronounced vertical physical structure, and our integrated grazing rates fall within the range of similar grazing studies using non-stratified sampling (e.g., Huskin et al. 2001; Isla et al. 2004; Décima et al. 2011).

Diel Patterns– We expected higher nighttime grazing impact due to additional feeding in surface waters by diel vertical migrators at night, but interestingly, nighttime grazing impact across all salinities was similar to daytime. Vertical migrators thus may have been preying on small invertebrates rather than primary producers, a pattern observed in the Sargasso Sea (Schnetzer and Steinberg 2002). Alternatively, at least in the plume, PAR profiles indicated that incident light was rapidly attenuated to 15% of

surface irradiance within the top 2-8m, rendering day light conditions more similar to night in plume waters, resulting in a lack of a diel pattern in grazing impact.

4.2 Seasonal Comparison

ANACONDAS was designed to provide seasonal snapshots of the Amazon Plume region with a focus on the fate of DDAs. While the seasons were sampled in two different years, the overall patterns provide some insight into planktonic succession and functioning of the food web in the region. In the lowest salinity plume stations in both spring and fall, phytoplankton assemblages are consistent with previous reports in low salinity, inshore regions of the plume. After initial low biomass at the mouth of the Amazon River due to light limitation (Smith Jr and Demaster 1996), biomass increases further offshore and comprises mostly coastal diatoms (Smith Jr and Demaster 1996; Subramaniam et al. 2008; Goes et al. 2014). Despite similar coastal phytoplankton assemblages at plume stations in both years, mesozooplankton grazing rates and impact on Chl-*a* were higher in the fall than spring. We view this as a seasonal rather than an interannual signal, and a reflection of a lag in the increase in mesozooplankton grazing and biomass following peak discharge. A similar explanation was used to describe the initial lag in copepod grazing on the phytoplankton bloom associated with the Mississippi River plume entering the Gulf of Mexico (Dagg 1995). They reported copepod grazing of 4-5% of daily production in the late spring during the onset of the phytoplankton bloom compared to 14-62% when the Mississippi plume was sampled in the late summer. This pattern is similar in our study (See Table 2). This is also supported by overall higher mesozooplankton biomass observed in fall compared to spring (Steinberg et al., in prep). While a seasonal bloom is counter to the steady year-round productivity in the plume

seen by Demaster and Pope (1996) discussed above, it is important to note the differences in distance from the mouth of the Amazon. Almost all of their stations were in shallow water (majority were <100m with max ~200m bottom depth) while ANACONDAS was further north of the mouth and focused on the slope and offshore regions of the plume-influenced WTNA. Therefore, a seasonal bloom progression may be important in the offshore plume waters as the Amazon progresses through peak discharge in the late spring, while inshore and closer to the mouth primary productivity is steady year round as observed by Demaster and Pope (1996). Loick-Wilde et al. (in press) suggest that the inshore phytoplankton assemblage acts as a seed population for blooms in the outer plume, especially of DDAs in the mesohaline region, which would support a seasonal progression of increasing phytoplankton biomass followed by zooplankton in the outer plume.

Furthermore, higher grazing rates and grazing impact occurred later in the season (higher in fall than spring) at plume and mesohaline stations (see Tables 1 & 2), supporting an initial lag in mesozooplankton growth and grazing before they are able to catch up to the pulse of primary production. However, in contrast to the plume region where phytoplankton assemblages were similar between seasons, in spring a DDA bloom appeared to have just initiated, based on cell condition (E. Carpenter and R. Foster, personal communication), and DDAs were prevalent throughout the mesohaline, while in the fall DDAs were scarce. Lower grazing in the spring may thus alternatively be due to intense grazing by zooplankton on DDAs later in the fall; stable isotope analysis indicated diazotrophic nitrogen was incorporated into mesozooplankton during our and a previous study in the region (Montoya et al. 2002) as well as in the subtropical Atlantic

(Landrum et al. 2011), although direct grazing on DDAs is not distinguishable using this method.

An alternative explanation for lower grazing in spring is that mesozooplankton avoid grazing on DDAs, and the high abundances of DDAs suppressed grazing. The DDA bloom observed in spring was dominated by the diatom *Hemiaulus hauckii* with the endosymbiont *Richelia intracellularis*, although *Rhizosolenia clevei* with *R. intracellularis* was present as well (Goes et al. 2014). Chain-formation in diatoms such as *Hemiaulus* and *Rhizosolenia* may decrease the risk of being grazed (Bergkvist et al. 2012), however, similar sized chain-forming diatoms are actively grazed by copepods (Bochdansky and Bollens 2004) and stable isotope analysis of mesozooplankton sampled in spring and fall indicates diazotrophic nitrogen in both years (Loicke-Wilde et al., in press). These observations suggest mesozooplankton don't avoid DDAs, but instead relate to a pattern of seasonal planktonic progression in the plume, especially in the mesohaline region where DDA blooms are more prevalent (Subramaniam et al. 2008; Goes et al. 2014).

5. CONCLUSION

We present the first analysis of zooplankton grazing in the Amazon Plume-influenced WTNA. Results from both years indicate that the Amazon Plume enhances grazing in the WTNA compared to areas with no plume influence. A shift in food web structure occurs along the plume salinity gradient, with mesozooplankton dominating grazing in plume and low salinity mesohaline stations, suggestive of an export food web, transitioning to microzooplankton dominating grazing at higher salinity mesohaline (>33 SSS) and oceanic stations, and a retention food web. Comparison between the two seasons/years indicated lower mesozooplankton grazing during peak spring discharge compared to the fall retroflection phase of the plume. This pattern represents a seasonal phytoplankton-zooplankton progression in the outer plume through peak discharge into the retroflection period. During the onset of a bloom in mesohaline waters, mesozooplankton grazing appears to lag phytoplankton growth, before catching up and grazing down the bloom, by the fall retroflection phase.

This study also provides an important baseline of zooplankton grazing impact in the WTNA with regards to a changing climate. Elevated precipitation and evaporation rates, driven by warming atmospheric and ocean temperatures, (Doney et al. 2012) would directly affect the expanse of the plume into the WTNA, potentially altering the food web dynamics highlighted in this study. Some changes have already been observed in the hydrological cycle of the Amazon basin over the last two decades, with an increased wetting trend driving an increase in annual river discharge (Gloor et al. 2013). A warming ocean will increase stratification, decreasing nutrient flux from depth (Doney et al. 2012); under these conditions N₂-fixation may increase in importance, making

diazotrophy important in fueling secondary production. Furthermore, our estimates of grazing can be incorporated into existing biogeochemical models for this region (Cooley et al. 2007; Stukel et al. 2014) to understand how changes in precipitation, temperature, or other factors may impact biogeochemical cycling, and to predict energy transfer in future ocean food webs.

REFERENCES

- Aller, J. Y., and J. R. Todorov. 1997. Seasonal and spatial patterns of deeply buried calanoid copepods on the Amazon Shelf: Evidence for periodic erosional/depositional cycles. *Estuar. Coast. Shelf Sci.* **44**: 57–66.
doi:10.1006/ecss.1996.0111
- Alonso, C., V. Rocco, J. P. Barriga, M. A. Battini, and H. Zagarese. 2004. Surface avoidance by freshwater zooplankton: Field evidence on the role of ultraviolet radiation. *Limnol. Oceanogr.* **49**: 225–232.
- Båmstedt, U., D. J. Gifford, X. Irigoien, A. Atkinson, and M. Roman. 2000. Feeding, p. 297–399. *In* R.P. Harris, P.H. Wiebe, J. Lenz, H.R. Skjodal, and M. Huntley [eds.], ICES Zooplankton Methodology Manual. Elsevier Academic Press.
- Bergkvist, J., P. Thor, H. Henrik Jakobsen, S.-Å. Wängberg, and E. Selander. 2012. Grazer-induced chain length plasticity reduces grazing risk in a marine diatom. *Limnol. Oceanogr.* **57**: 318. doi:10.4319/lo.2012.57.1.0318
- Bernard, K. S., D. K. Steinberg, and O. M. E. Schofield. 2012. Summertime grazing impact of the dominant macrozooplankton off the Western Antarctic Peninsula. *Deep Sea Res. Part Oceanogr. Res. Pap.* **62**: 111–122.
doi:10.1016/j.dsr.2011.12.015
- Bochdansky, A. B., and S. M. Bollens. 2004. Relevant scales in zooplankton ecology: Distribution, feeding, and reproduction of the copepod *Acartia hudsonica* in response to thin layers of the diatom *Skeletonema costatum*. *Limnol. Oceanogr.* **49**: 625–636. doi:10.4319/lo.2004.49.3.0625
- Calbet, A., and M. R. Landry. 2004. Phytoplankton Growth, microzooplankton grazing,

- and carbon cycling in marine systems. *Limnol. Oceanogr.* **49**: 51–57.
- Calef, G. F., and G. D. Grice. 1967. Influence of the Amazon River Outflow on the Ecology of the Western Tropical Atlantic II. Zooplankton Abundance, Copepod Distribution, with Remarks on the Fauna of Low-Salinity Areas. *J. Mar. Res.* **25**: 84–92.
- Carpenter, E. J., J. P. Montoya, J. Burns, M. R. Mulholland, A. Subramaniam, and D. G. Capone. 1999. Extensive bloom of a N₂-fixing diatom/cyanobacterial association in the tropical Atlantic Ocean. *Mar. Ecol. Prog. Ser.* **185**: 273–283.
- Chérubin, L. M., and P. L. Richardson. 2007. Caribbean current variability and the influence of the Amazon and Orinoco freshwater plumes. *Deep Sea Res. Part Oceanogr. Res. Pap.* **54**: 1451–1473. doi:10.1016/j.dsr.2007.04.021
- Coles, V. J., M. T. Brooks, J. Hopkins, M. R. Stukel, P. L. Yager, and R. R. Hood. 2013. The pathways and properties of the Amazon River Plume in the tropical North Atlantic Ocean: AMAZON RIVER PLUME. *J. Geophys. Res. Oceans* **118**: 6894–6913. doi:10.1002/2013JC008981
- Conover, R. J., R. Durvasula, S. Roy, and R. Wang. 1986. Probable Loss of Chlorophyll-Derived Pigments During Passage Through the Gut of Zooplankton, and Some of the Consequences. *Limnol. Oceanogr.* **31**: 878–887.
- Cooley, S. R., V. J. Coles, A. Subramaniam, and P. L. Yager. 2007. Seasonal variations in the Amazon plume-related atmospheric carbon sink: SEASONALITY OF CO₂ IN AMAZON PLUME. *Glob. Biogeochem. Cycles* **21**: GB3014 doi:10.1029/2006GB002831
- Cooley, S. R., and P. L. Yager. 2006. Physical and biological contributions to the western

- tropical North Atlantic Ocean carbon sink formed by the Amazon River plume. *J. Geophys. Res.* **111**. doi:10.1029/2005JC002954
- Costa, R. M., N. R. Leite, and L. C. C. Pereira. 2009. Mesozooplankton of the Curuçá Estuary (Amazon Coast, Brazil). *J. Coast. Res.* 400–404.
- Dagg, M. J. 1995. Copepod grazing and the fate of phytoplankton in the northern Gulf of Mexico. *Cont. Shelf Res.* **15**: 1303–1317. doi:10.1016/0278-4343(94)00086-3
- Dam, H. G., and W. T. Peterson. 1988. The effect of temperature on the gut clearance rate constant of planktonic copepods. *J. Exp. Mar. Biol. Ecol.* **123**: 1–14. doi:10.1016/0022-0981(88)90105-0
- Dam, H. G., X. Zhang, M. Butler, and M. R. Roman. 1995. Mesozooplankton grazing and metabolism at the equator in the central Pacific: Implications for carbon and nitrogen fluxes. *Deep Sea Res. Part II Top. Stud. Oceanogr.* **42**: 735–756. doi:10.1016/0967-0645(95)00036-P
- Décima, M., M. R. Landry, and R. R. Rykaczewski. 2011. Broad scale patterns in mesozooplankton biomass and grazing in the eastern equatorial Pacific. *Deep Sea Res. Part II Top. Stud. Oceanogr.* **58**: 387–399. doi:10.1016/j.dsr2.2010.08.006
- Demaster, D. J., and R. H. Pope. 1996. Nutrient dynamics in Amazon shelf waters: results from AMASSEDS. *Cont. Shelf Res.* **16**: 263–289.
- Doney, S. C., M. Ruckelshaus, J. Emmett Duffy, and others. 2012. Climate Change Impacts on Marine Ecosystems. *Annu. Rev. Mar. Sci.* **4**: 11–37. doi:10.1146/annurev-marine-041911-111611
- Durbin, E. G., and R. G. Campbell. 2007. Reassessment of the gut pigment method for estimating *in situ* zooplankton ingestion. *Mar. Ecol. Prog. Ser.* **331**: 305–307.

- Espinoza, J. C., J. Ronchail, J. L. Guyot, C. Junquas, P. Vauchel, W. Lavado, G. Drapeau, and R. Pombosa. 2011. Climate variability and extreme drought in the upper Solimões River (western Amazon Basin): Understanding the exceptional 2010 drought. *Geophys. Res. Lett.* **38**: L13406. doi:10.1029/2011GL047862
- Gannon, J. E., and S. A. Gannon. 1975. Observations on the Narcotization of Crustacean Zooplankton. *Crustaceana* **28**: 220–224.
- Gleiber, M. R., D. K. Steinberg, and O. M. E. Schofield. 2015. Copepod summer grazing and fecal pellet production along the Western Antarctic Peninsula. *J. Plankton Res.* fbv070. doi:10.1093/plankt/fbv070
- Gloor, M., R. J. W. Brienen, D. Galbraith, and others. 2013. Intensification of the Amazon hydrological cycle over the last two decades: AMAZON HYDROLOGIC CYCLE INTENSIFICATION. *Geophys. Res. Lett.* **40**: 1729–1733. doi:10.1002/grl.50377
- Goes, J. I., H. do R. Gomes, A. M. Chekalyuk, and others. 2014. Influence of the Amazon River discharge on the biogeography of phytoplankton communities in the western tropical north Atlantic. *Prog. Oceanogr.* **120**: 29–40. doi:10.1016/j.pocean.2013.07.010
- Gorsky, G., M. J. Chrétiennot-Dinet, J. Blanchot, and I. Palazzoli. 1999. Picoplankton and nanoplankton aggregation by appendicularians: Fecal pellet contents of *Megalocercus huxleyi* in the equatorial Pacific. *J. Geophys. Res. Oceans* **104**: 3381–3390. doi:10.1029/98JC01850
- Hawser, S. P., J. M. O’Neil, M. R. Roman, and G. A. Codd. 1992. Toxicity of blooms of the cyanobacterium *Trichodesmium* to zooplankton. *J. Appl. Phycol.* **4**: 79–86.

- Hellweger, F. L., and A. L. Gordon. 2002. Tracing Amazon River water into the Caribbean Sea. *J. Mar. Res.* **60**: 537–549. doi:10.1357/002224002762324202
- Hopcroft, R. R., J. C. Roff, and F. P. Chavez. 2001. Size paradigms in copepod communities: a re-examination. *Hydrobiologia* **453**: 133–141.
- Huskin, I., R. Anadón, G. Medina, R. N. Head, and R. P. Harris. 2001. Mesozooplankton Distribution and Copepod Grazing in the Subtropical Atlantic Near the Azores: Influence of Mesoscale Structures. *J. Plankton Res.* **23**: 671–691. doi:10.1093/plankt/23.7.671
- Isla, J. A., M. Llope, and R. Anadón. 2004. Size-fractionated mesozooplankton biomass, metabolism and grazing along a 50°N–30°S transect of the Atlantic Ocean. *J. Plankton Res.* **26**: 1301–1313. doi:10.1093/plankt/fbh121
- Karaköylü, E. M., and P. J. S. Franks. 2012. Reassessment of copepod grazing impact based on continuous time series of in vivo gut fluorescence from individual copepods. *J. Plankton Res.* **34**: 55–71. doi:10.1093/plankt/fbr086
- Knap, A. H., A. Michaels, A. R. Close, H. Ducklow, and A. G. Dickson. 1996. Protocols for the joint global ocean flux study (JGOFS) core measurements. *JGOFS Repr. IOC Man. Guid. No 29 UNESCO* **19**.
- Landrum, J. P., M. A. Altabet, and J. P. Montoya. 2011. Basin-scale distributions of stable nitrogen isotopes in the subtropical North Atlantic Ocean: Contribution of diazotroph nitrogen to particulate organic matter and mesozooplankton. *Deep Sea Res. Part Oceanogr. Res. Pap.* **58**: 615–625. doi:10.1016/j.dsr.2011.01.012
- Landry, M., L. Haas, and V. Fagerness. 1984. Dynamics of microbial plankton communities. *Mar. Ecol. Prog. Ser.* **16**: 127–133.

- Landry, M. R., S. L. Brown, Y. M. Rii, K. E. Selph, R. R. Bidigare, E. J. Yang, and M. P. Simmons. 2008. Depth-stratified phytoplankton dynamics in Cyclone Opal, a subtropical mesoscale eddy. Deep Sea Res. Part II Top. Stud. Oceanogr. **55**: 1348–1359. doi:10.1016/j.dsr2.2008.02.001
- Landry, M. R., and R. P. Hassett. 1982. Estimating the grazing impact of marine microzooplankton. Mar. Biol. **67**: 283–288.
- Landry, M. R., M. D. Ohman, R. Goericke, M. R. Stukel, and K. Tsyrklevich. 2009. Lagrangian studies of phytoplankton growth and grazing relationships in a coastal upwelling ecosystem off Southern California. Prog. Oceanogr. **83**: 208–216. doi:10.1016/j.pocean.2009.07.026
- Landry, M. R., K. E. Selph, A. G. Taylor, M. Décima, W. M. Balch, and R. R. Bidigare. 2011. Phytoplankton growth, grazing and production balances in the HNLC equatorial Pacific. Deep Sea Res. Part II Top. Stud. Oceanogr. **58**: 524–535. doi:10.1016/j.dsr2.2010.08.011
- Legendre, L., and J. Michaud. 1998. Flux of biogenic carbon in oceans: size-dependent regulation by pelagic food webs. Mar. Ecol. Prog. Ser. **164**: 1–11.
- Loick-Wilde, N., S. C. Weber, B. J. Conroy, D. G. Capone, V. J. Coles, P. M. Medeiros, D. K. Steinberg, and J. P. Montoya. 2015. Nitrogen sources and net growth efficiency of zooplankton in three Amazon River Plume food webs. Limnol. Oceanogr. **in press**.
- Magalhães, A., N. da R. Leite, J. G. Silva, L. C. Pereira, and R. M. da Costa. 2009. Seasonal variation in the copepod community structure from a tropical Amazon estuary, Northern Brazil. An. Acad. Bras. Ciênc. **81**: 187–197.

- Michaels, A. F., and M. W. Silver. 1988. Primary production, sinking fluxes and the microbial food web. Deep Sea Res. Part Oceanogr. Res. Pap. **35**: 473–490.
- Mikaloff Fletcher, S. E., N. Gruber, A. R. Jacobson, and others. 2007. Inverse estimates of the oceanic sources and sinks of natural CO₂ and the implied oceanic carbon transport: NATURAL AIR-SEA FLUXES OF CO₂. Glob. Biogeochem. Cycles **21**: GB1010 doi:10.1029/2006GB002751
- Moller, G. S. F., E. M. L. d. M. Novo, and M. Kampel. 2010. Space-time variability of the Amazon River plume based on satellite ocean color. Cont. Shelf Res. **30**: 342–352. doi:10.1016/j.csr.2009.11.015
- Montoya, J. P., E. J. Carpenter, and D. G. Capone. 2002. Nitrogen fixation and nitrogen isotope abundances in zooplankton of the oligotrophic North Atlantic. Limnol. Oceanogr. **47**: 1617–1628.
- O’Neil, J. M. 1998. The colonial cyanobacterium *Trichodesmium* as a physical and nutritional substrate for the harpacticoid copepod *Macrosetella gracilis*. J. Plankton Res. **20**: 43–59. doi:10.1093/plankt/20.1.43
- O’Neil, J. M., and M. R. Roman. 1994. Ingestion of the cyanobacterium *Trichodesmium* spp. by pelagic harpacticoid copepods *Macrosetella*, *Miracia* and *Oculosetella*. Hydrobiologia **292**: 235–240. doi:10.1007/BF00229946
- Parsons, T. R., Y. Maita, and C. M. Lalli. 1984. A manual of chemical and biological methods for seawater analysis., Pergamon Press.
- Rau, G. H., J.-L. Teyssie, F. Rassoulzadegan, and S. W. Fowler. 1990. ¹³C/¹²C and ¹⁵N/¹⁴N variations among size-fractionated marine particles: implications for their origin and trophic relationships. Mar. Ecol. Prog. Ser. **59**: 33–38.

- Richey, J. E., C. Nobre, and C. Deser. 1989. Amazon River Discharge and Climate Variability. *Science* **246**: 101–103.
- Roman, M. R., H. G. Dam, R. Le Borgne, and X. Zhang. 2002. Latitudinal comparisons of equatorial Pacific zooplankton. *Deep Sea Res. Part II Top. Stud. Oceanogr.* **49**: 2695–2711.
- Roman, M. R., and A. L. Gauzens. 1997. Copepod grazing in the equatorial Pacific. *Limnol. Oceanogr.* **42**: 623–634.
- Schmoker, C., S. Hernández-León, and A. Calbet. 2013. Microzooplankton grazing in the oceans: impacts, data variability, knowledge gaps and future directions. *J. Plankton Res.* **35**: 691–706. doi:10.1093/plankt/fbt023
- Schnetzer, A., and D. Steinberg. 2002. Natural diets of vertically migrating zooplankton in the Sargasso Sea. *Mar. Biol.* **141**: 89–99. doi:10.1007/s00227-002-0815-8
- Sherr, E. B., and B. F. Sherr. 2002. Significance of predation by protists in aquatic microbial food webs. *Antonie Van Leeuwenhoek* **81**: 293–308.
- Shippe, R. F., J. Curtaz, A. Subramaniam, E. J. Carpenter, and D. G. Capone. 2006. Diatom biomass and productivity in oceanic and plume-influenced waters of the western tropical Atlantic ocean. *Deep Sea Res. Part Oceanogr. Res. Pap.* **53**: 1320–1334. doi:10.1016/j.dsr.2006.05.013
- Smith Jr, W. O., and D. J. Demaster. 1996. Phytoplankton biomass and productivity in the Amazon River plume: correlation with seasonal river discharge. *Cont. Shelf Res.* **16**: 291–319.
- Stukel, M. R., V. J. Coles, M. T. Brooks, and R. R. Hood. 2014. Top-down, bottom-up

- and physical controls on diatom-diazotroph assemblage growth in the Amazon River plume. *Biogeosciences* **11**: 3259–3278. doi:10.5194/bg-11-3259-2014
- Stukel, M. R., M. Décima, K. E. Selph, D. A. A. Taniguchi, and M. R. Landry. 2013a. The role of *Synechococcus* in vertical flux in the Costa Rica upwelling dome. *Prog. Oceanogr.* **112–113**: 49–59. doi:10.1016/j.pocean.2013.04.003
- Stukel, M. R., M. D. Ohman, C. R. BenitezNelson, and M. R. Landry. 2013b. Contributions of mesozooplankton to vertical carbon export in a coastal upwelling system. *Mar. Ecol. Prog. Ser.* **491**: 47–65. doi:10.3354/meps10453
- Subramaniam, A., P. L. Yager, E. J. Carpenter, and others. 2008. Amazon River enhances diazotrophy and carbon sequestration in the tropical North Atlantic Ocean. *Proc. Natl. Acad. Sci.* **105**: 10460–10465. doi:10.1073/pnas.0710279105
- Takahashi, T., S. C. Sutherland, C. Sweeney, and others. 2002. Global sea-air CO₂ flux based on climatological surface ocean pCO₂, and seasonal biological and temperature effects. *Deep Sea Res. Part II Top. Stud. Oceanogr.* **49**: 1601–1622. doi:10.1016/S0967-0645(02)00003-6
- Wassmann, P. 1997. Retention versus export food chains: processes controlling sinking loss from marine pelagic systems. *Hydrobiologia* **363**: 29–57. doi:10.1023/A:1003113403096
- Wiebe, P. H., K. H. Burt, S. H. Boyd, and A. W. Morton. 1976. A multiple opening/closing net and environmental sensing system for sampling zooplankton. *J. Mar. Res.* **34**: 313–326.
- Wilson, S., and D. Steinberg. 2010. Autotrophic picoplankton in mesozooplankton guts:

- evidence of aggregate feeding in the mesopelagic zone and export of small phytoplankton. *Mar. Ecol. Prog. Ser.* **412**: 11–27. doi:10.3354/meps08648
- Zhang, X., H. G. Dam, J. R. White, and M. R. Roman. 1995. Latitudinal variations in mesozooplankton grazing and metabolism in the central tropical Pacific during the U.S. JGOFS EqPac study. *Deep Sea Res. Part II Top. Stud. Oceanogr.* **42**: 695–714. doi:10.1016/0967-0645(95)00032-L

Table 1. Depth integrated (0–150 m) mesozooplankton grazing rates (mg Chl *a* equivalent m⁻² d⁻¹) in spring (May–June) 2010 and fall (September–October) 2011. Values are averages \pm 1 standard deviation for each year by station category and day or night tow.

Season	Station category	Day	Night
Spring	Low salinity plume	1.60 \pm 1.72 (<i>n</i> = 4)	1.08 (<i>n</i> = 1)
	Mesohaline plume	1.05 \pm 0.97 (<i>n</i> = 5)	1.08 \pm 1.00 (<i>n</i> = 5)
	Oceanic	0.82 \pm 0.55 (<i>n</i> = 4)	0.82 \pm 0.27 (<i>n</i> = 3)
	Total	1.15 \pm 0.31 (<i>n</i> = 13)	0.99 \pm 0.24 (<i>n</i> = 9)
Fall	Low salinity plume	5.34 \pm 4.13 (<i>n</i> = 4)	6.87 (<i>n</i> = 1)
	Mesohaline plume	1.96 \pm 1.46 (<i>n</i> = 14)	2.46 \pm 1.25 (<i>n</i> = 7)
	Oceanic	0.48 (<i>n</i> = 2)	0.76 \pm 0.53 (<i>n</i> = 3)
	Total	2.49 \pm 0.57 (<i>n</i> = 20)	2.39 \pm 0.59 (<i>n</i> = 11)

Table 2. Mesozooplankton grazing impact of all size fractions combined from 0–150 m and 0–25 m in spring (May–June) 2010 and fall (September–October) 2011. Values are average percentages \pm 1 standard deviation for each year by station category and day or night tow. *Indicates a significant difference ($p < 0.05$) between years while † indicates a significant difference between station categories within given year.

Season	Station category	150 m Chl α impact		25 m Chl α impact	
		Day	Night	Day	Night
Spring	Low salinity plume	3.33 \pm 5.47 ($n = 4$)	3.39 ($n = 1$)	2.08 \pm 2.51 ($n = 4$)	7.18 ($n = 1$)
	Mesohaline plume	1.65 \pm 1.89* ($n = 5$)	1.53 \pm 0.92* ($n = 5$)	1.40 \pm 1.76 ($n = 5$)	4.75 \pm 2.61 ($n = 3$)
	Oceanic	1.94 \pm 0.90 ($n = 4$)	2.08 \pm 0.99 ($n = 3$)	4.28 \pm 1.54 ($n = 4$)	4.94 \pm 1.39 ($n = 3$)
	Total	2.26 \pm 3.07 ($n = 13$)	1.92 \pm 1.02 ($n = 9$)	2.49 \pm 2.19 ($n = 13$)	5.18 \pm 1.92 ($n = 7$)
Fall	Low salinity plume	11.70 \pm 11.61 ($n = 4$)	9.37 ($n = 1$)	25.94 \pm 25.50 ($n = 4$)	17.26 ($n = 1$)
	Mesohaline plume	6.44 \pm 4.50* ($n = 13$)	7.19 \pm 3.06*† ($n = 7$)	21.69 \pm 23.80 ($n = 13$)	17.01 \pm 12.26 ($n = 7$)
	Oceanic	1.82 ($n = 2$)	2.16 \pm 1.36† ($n = 3$)	4.16 ($n = 2$)	6.86 \pm 3.76 ($n = 3$)
	Total	7.06 \pm 6.65 ($n = 19$)	6.02 \pm 3.54 ($n = 11$)	20.74 \pm 22.88 ($n = 19$)	14.26 \pm 10.75 ($n = 11$)

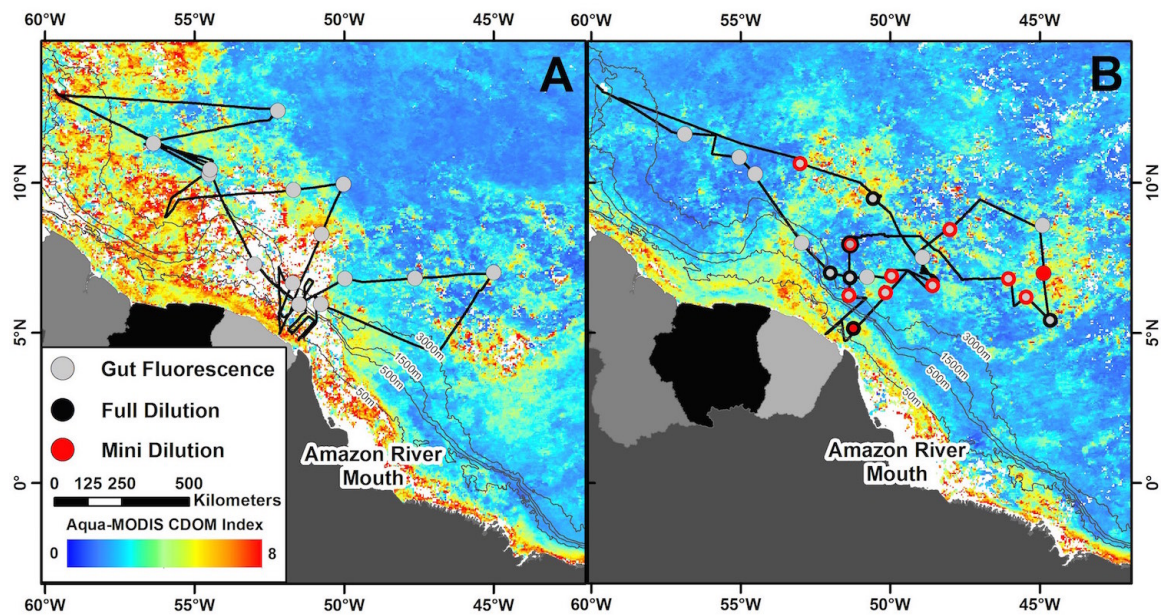


Fig. 1. Stations sampled for mesozooplankton gut fluorescence and microzooplankton grazing in the Amazon River plume-influenced waters and the western tropical North Atlantic. Stations with cruise track (black line) are overlaid on monthly averaged chromophoric dissolved organic matter (CDOM) concentration using Aqua-MODIS satellite data (oceancolor.gsfc.nasa.gov). (A) Stations sampled in spring (May–June) 2010 during the Amazon River peak discharge. (B) Stations sampled in fall (September–October) 2011 during the seasonal maximum areal reach of the plume. Station color or combination of colors indicates sampling protocol performed at that station. Bathymetry lines are shown in gray.

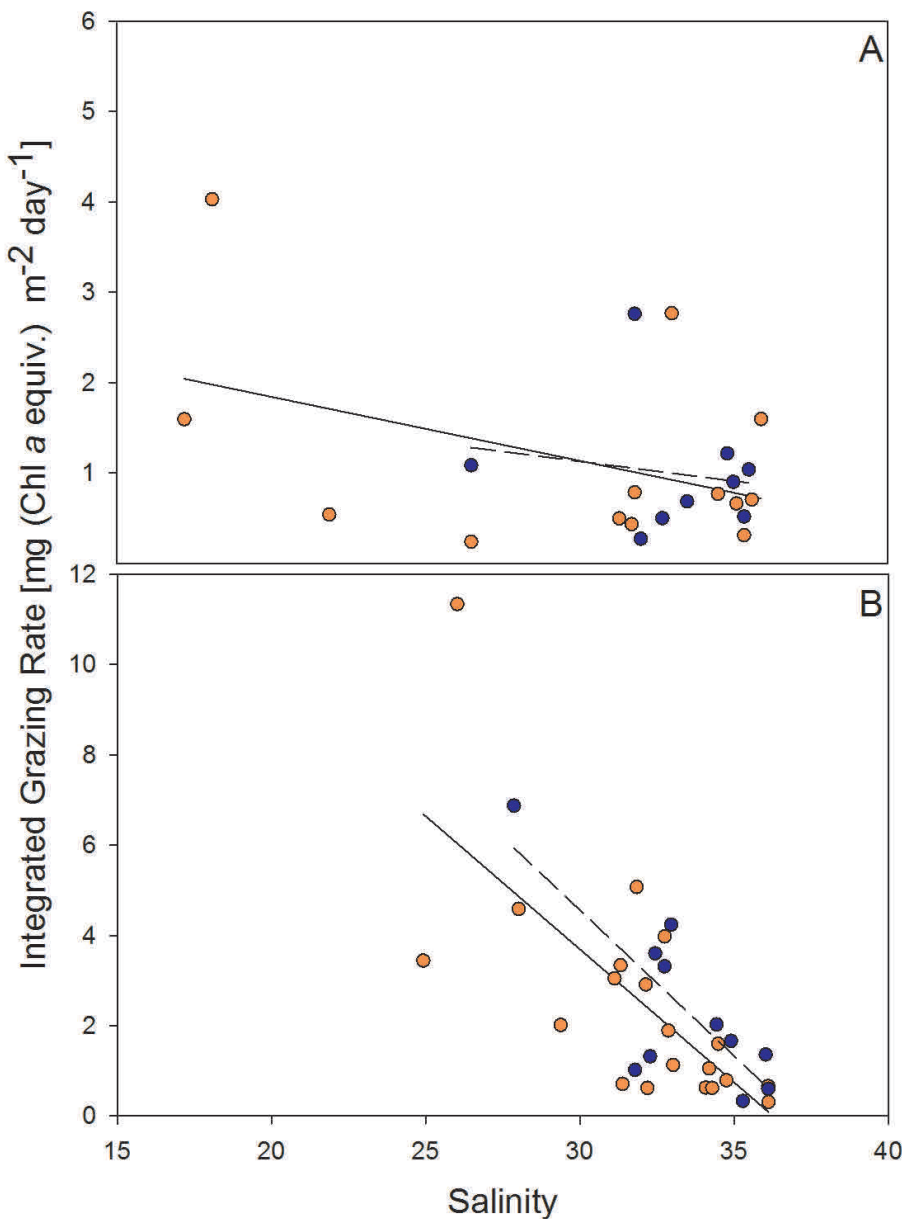


Fig. 2. Surface salinity vs. mesozooplankton grazing (0–150 m integrated) during day (orange) and night (blue) in (A) spring, and (B) fall. Regression lines are shown separately for day (solid) and night (dashed). Note that the y-axis (grazing) scale in B is double that in A. Regression equations and statistics are as follows: (A) day, $n=13$, $y=-0.0708x+3.258$, $p=0.146$, $R^2=0.182$; night, $n=9$, $y=-0.0436x + 2.4333$, $p=0.665$, $R^2=0.0283$; (B) day, $n=20$, $y=-0.590x + 21.382$, $p=<0.001$, $R^2=0.491$; night, $n=11$, $y=-0.646x + 23.937$, $p=0.004$, $R^2=0.627$.

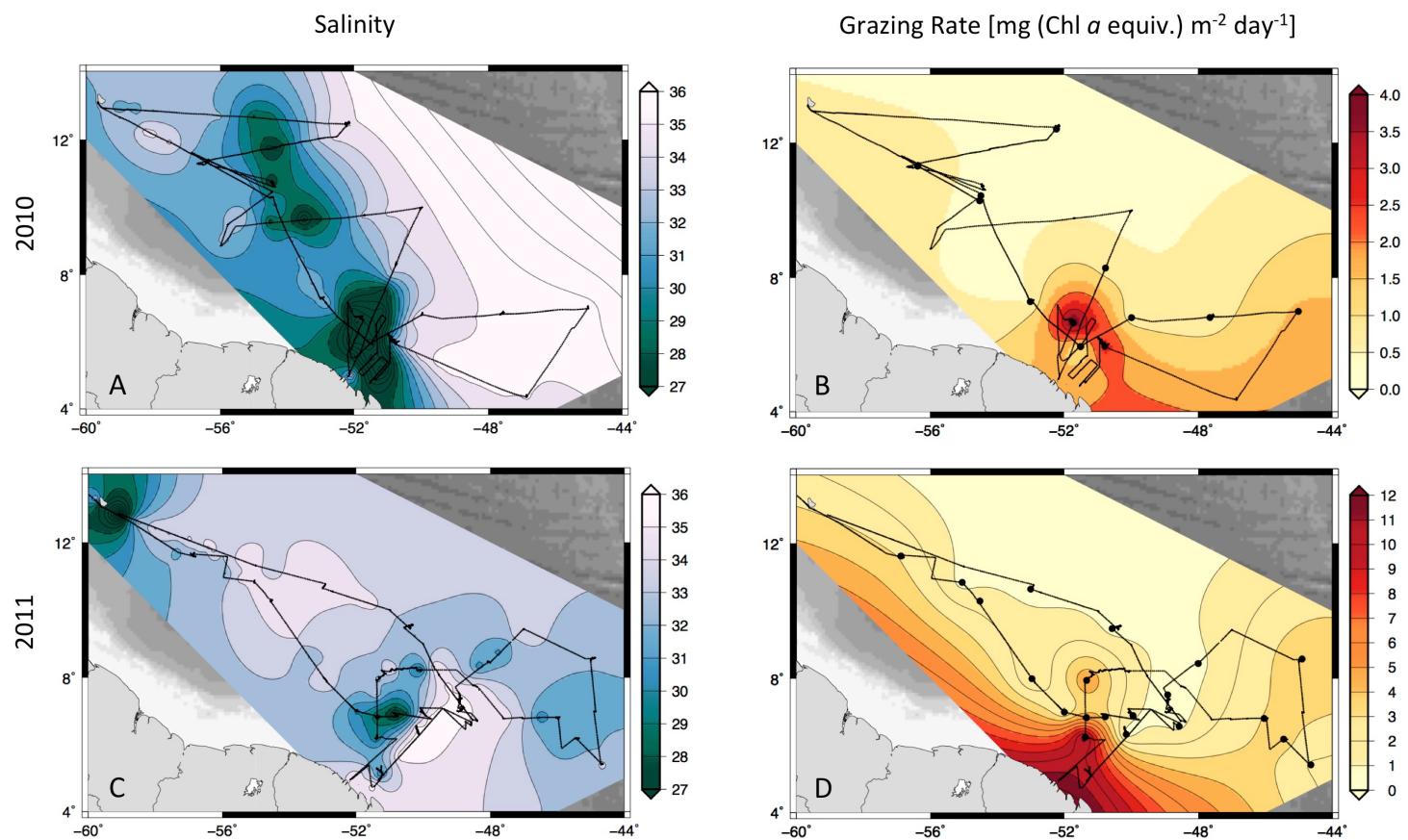


Fig. 3. Surface salinity and daytime mesozooplankton grazing (0–150 m integrated) in spring (A and B, respectively) and fall (C and D, respectively) in the Amazon River plume region. Note the scale in D is triple that in B.

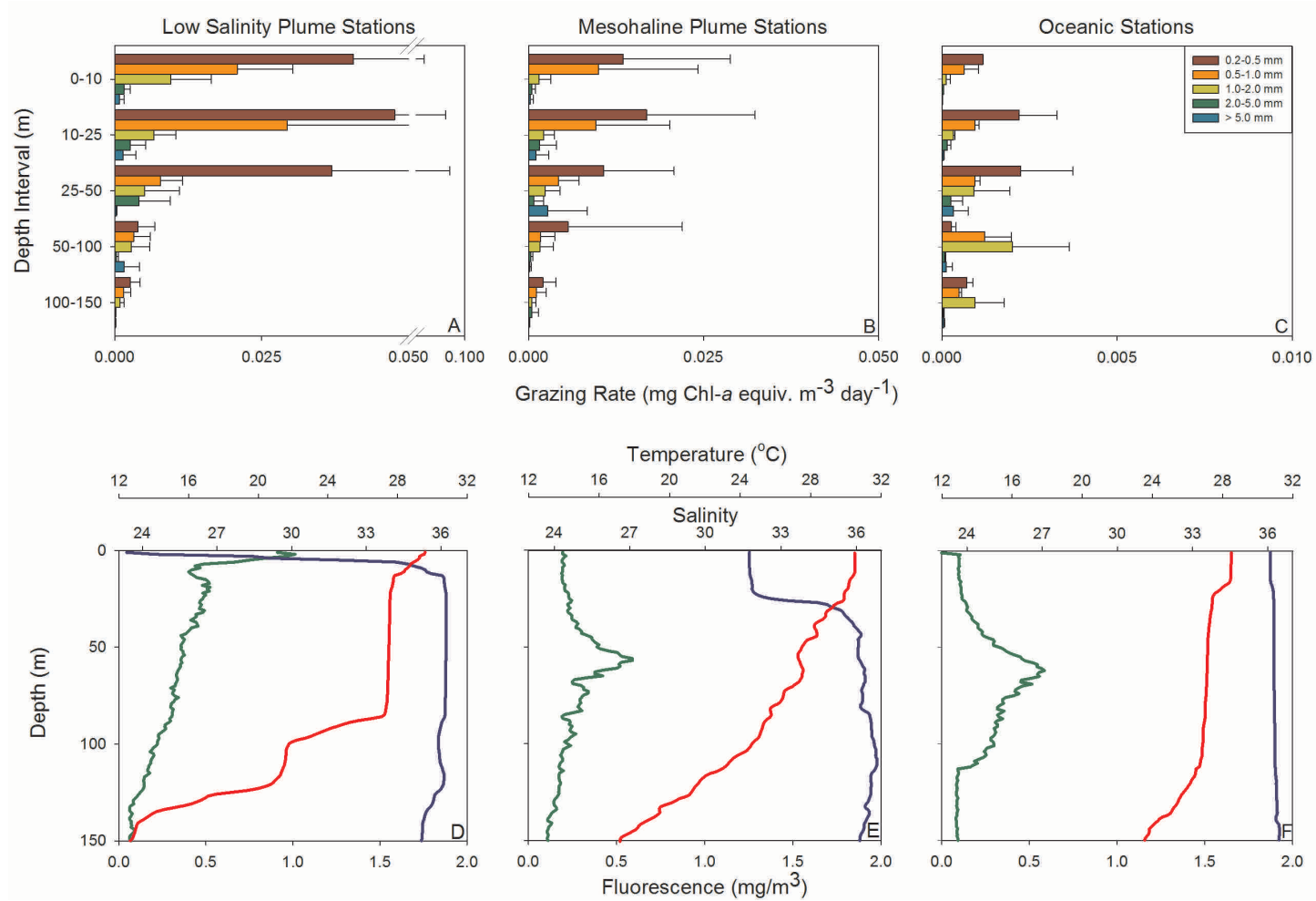


Fig. 4. Size-fractionated mesozooplankton daytime grazing (A–C) depth profiles in fall averaged by salinity category, size class, and depth interval. Error bars are standard deviation. Note different x-axis scales. D–F are depth profiles of salinity (blue), fluorescence (green), and temperature (red) characteristic of each salinity category.

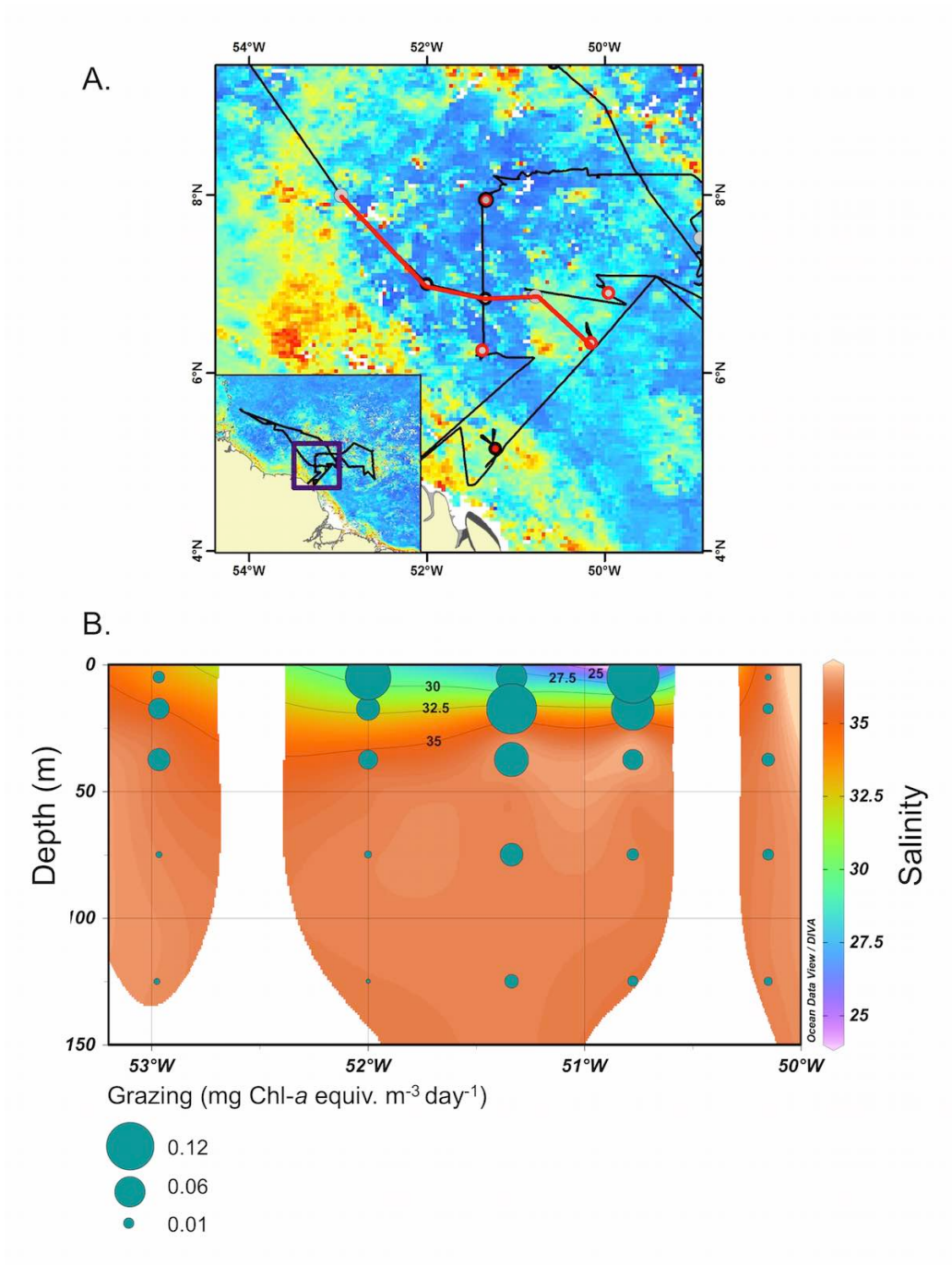


Fig. 5. Plume transect from the fall cruise (A; red line) and (B) depth profiles of salinity and mesozooplankton community grazing (green circles). Transect is overlaid on monthly averaged chromophoric dissolved organic matter (CDOM) concentration using Aqua-MODIS satellite data (oceancolor.gsfc.nasa.gov). The grazing depth profiles are plotted at the midpoint of the MOCNESS depth interval (i.e., 0–10 m is plotted at 5 m).

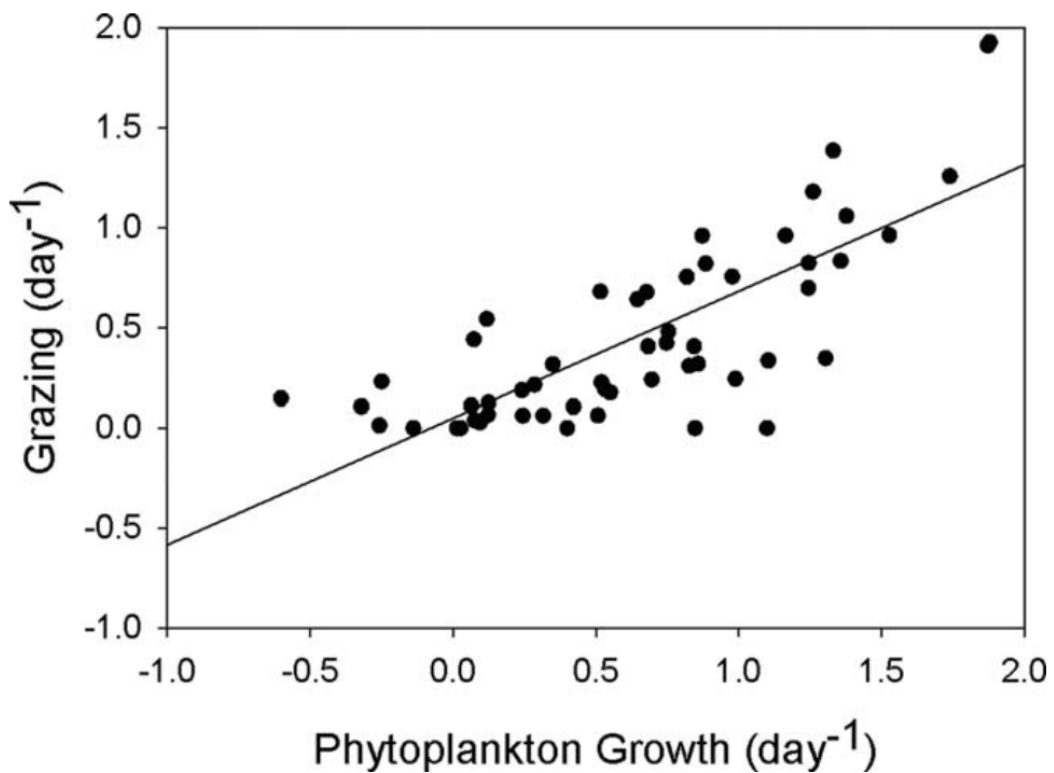


Fig. 6. Bulk phytoplankton growth vs. microzooplankton grazing rate across all salinity ranges. Microzooplankton grazing is significantly correlated with bulk phytoplankton growth rate ($R^2 = 0.602$, $p < 0.001$). Data are from two-point “mini” dilution experiments in fall.

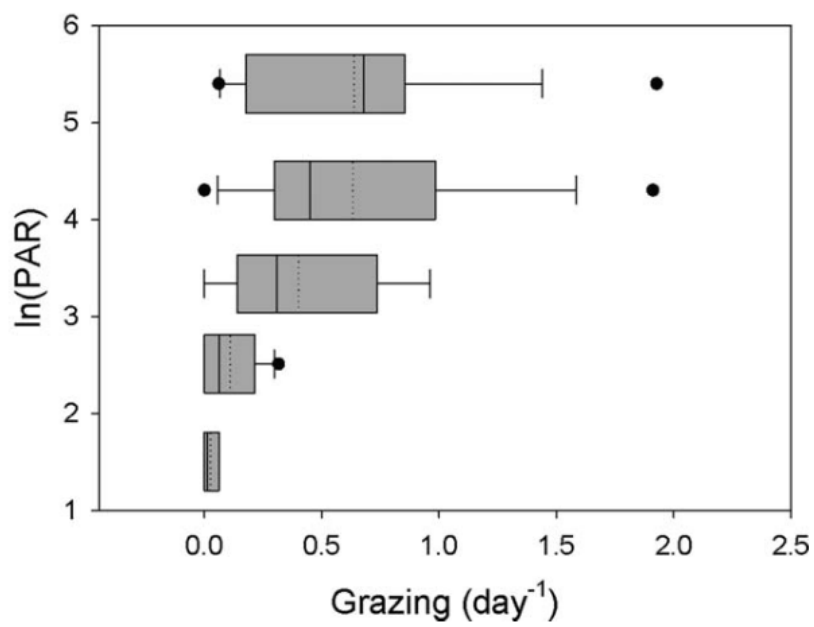
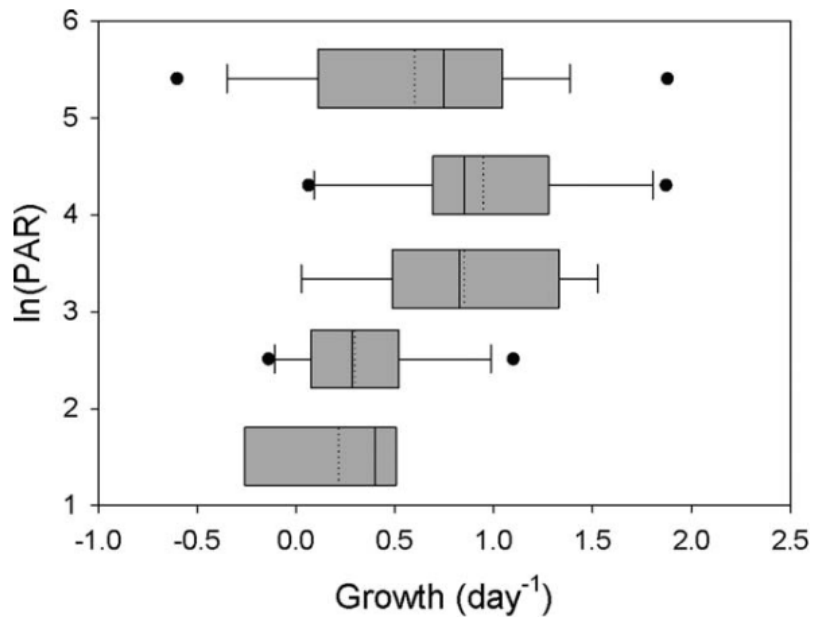


Fig. 7. Natural logarithm of photosynthetically active radiation (PAR) vs. bulk phytoplankton growth (A) and microzooplankton grazing (B) in fall. Box boundaries represent the 25th and 75th percentiles. The solid line is the median while the dashed is the mean. Whiskers represent the 10th and 90th percentiles. Maximum phytoplankton growth rates occur at intermediate PAR levels corresponding to irradiances of roughly 10% surface irradiance.

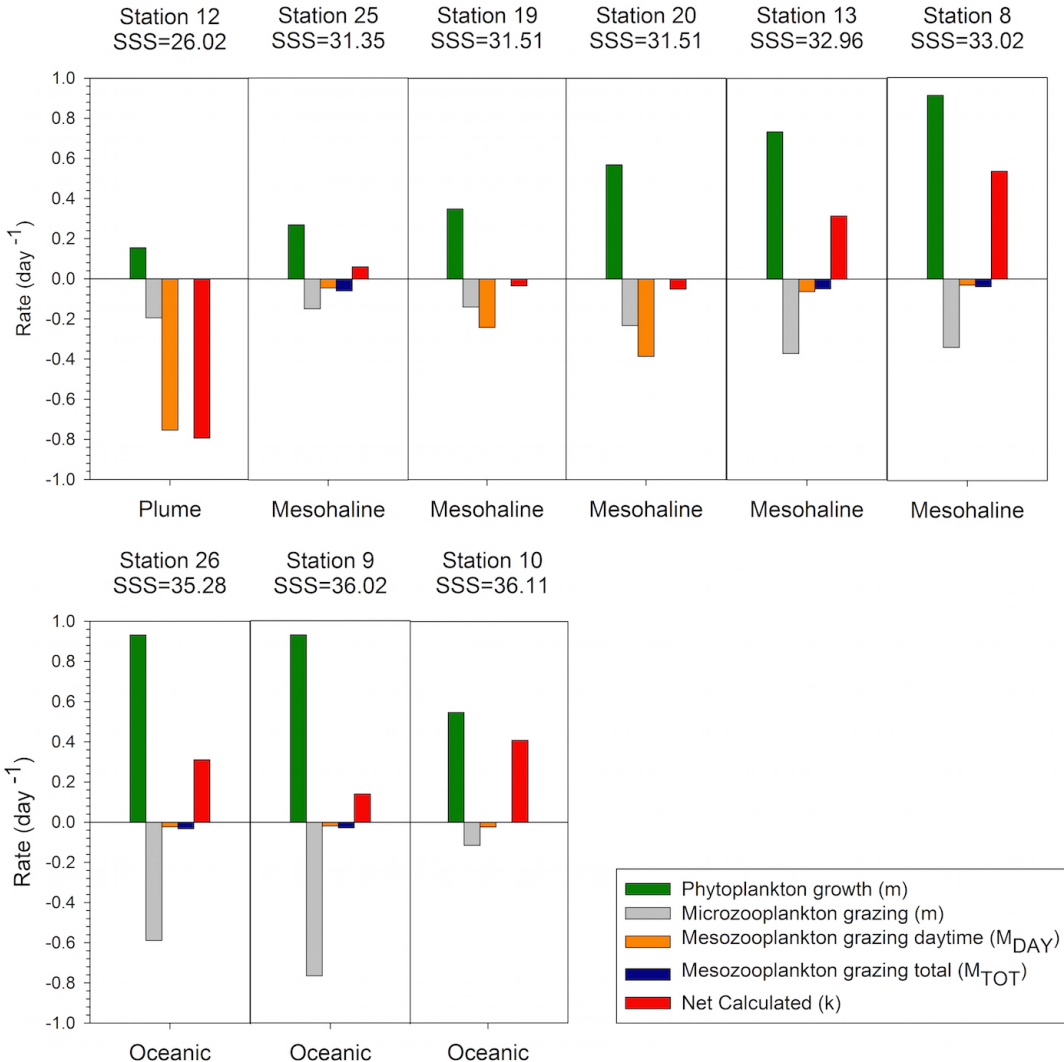


Fig. 8. Instantaneous rates of change for phytoplankton growth (μ), microzooplankton grazing (m), and mesozooplankton total grazing (M_{TOT}) or daytime mesozooplankton (M_{DAY}) in fall. The net calculated change k' is equal to $\mu - m - M_{\text{TOT}}$ (or M_{DAY} for Sts. 10, 12, 19, and 20 where no night tow was performed).

CHAPTER 4

**Mesozooplankton grazing of cyanobacteria in the Amazon River plume and western
tropical North Atlantic Ocean**

ABSTRACT

Diazotrophic cyanobacteria, those capable of fixing nitrogen, are considered the major source of new nitrogen (N) in the oligotrophic tropical ocean. In the Amazon River-influenced western tropical North Atlantic (WTNA), diatom diazotroph associations (DDAs) and *Trichodesmium* have seasonally high abundances. We sampled epipelagic mesozooplankton in the Amazon River plume and WTNA in May-June 2010. We investigated direct grazing by mesozooplankton on two DDA populations: *Richelia* associated with *Rhizosolenia* diatoms (het-1) and *Richelia* associated with *Hemiaulus* diatoms (het-2), and on *Trichodesmium* using a highly specific qPCR approach. In parallel, we used 16S next generation sequencing (NGS) to investigate the cyanobacterial diversity associated with gut contents of mesozooplankton. Both DDAs and *Trichodesmium* occurred in zooplankton gut contents, with higher detection of het-2 predominantly in calanoid copepods and detection of grazing on *Trichodesmium* by calanoid copepods at high salinity (>35) stations. Cyanobacterial diversity from 16S NGS was dominated by the non-diazotrophic unicellular phylotypes *Synechococcus* and *Prochlorococcus*, although sequences from the globally significant unicellular diazotroph UCYN-A *Candidatus Atelocyanobacterium thalassa* were present as well. This study is the first evidence of consumption of DDAs, *Trichodesmium*, and UCYN-A by zooplankton, and in addition, provides for a direct pathway of diazotrophic N into the food web. These results have important implications for biogeochemical cycles, particularly oligotrophic regions where N₂ fixation is the main source of new nitrogen.

1. INTRODUCTION

A number of factors influence primary production in the marine environment with one of the most significant being the availability of nitrogen (Gruber 2008). In the open ocean dissolved inorganic nitrogen (DIN) is rare, while di-nitrogen (N_2) is abundant. However, few organisms can utilize N_2 . In oligotrophic environments, diazotrophic organisms, those able to utilize N_2 through the process of biological N_2 fixation, play a significant role as drivers of primary production by provision of new nitrogen (N) (Dugdale and Goering 1967). The most abundant and best investigated of these diazotrophs are cyanobacteria. The non-heterocyst forming, filamentous cyanobacterium *Trichodesmium* has been the focus of most of the research and is especially well studied throughout the tropical and subtropical oceans. Estimations of N_2 fixation by *Trichodesmium* vary, but globally it is a significant source of new nitrogen to the open ocean (Capone et al. 1997; Capone 2001; Sohm et al. 2011) through varied pathways including exudation (Glibert and Bronk 1994; Bronk and Steinberg 2008), program cell death (Berman-Frank et al. 2004) and viral lysis (Hewson et al. 2004).

More recently other diazotrophs including several lineages of unicellular cyanobacteria have been identified as important N_2 fixers in the open ocean where these lineages have broader distributions, and thus the range of N_2 fixation now includes areas of the worlds ocean outside the tropical and subtropical latitudes (e.g. cooler temperate regions, inverse estuary) (Zehr et al. 2001; Moisander et al. 2010; Thompson et al. 2012). High N_2 -fixation rates from unicellular cyanobacteria in both the Pacific and Atlantic Oceans are observed, with those in the tropical North Atlantic comparable to *Trichodesmium* (Falcon et al. 2004; Montoya et al. 2004) Although N_2 -fixation rates are

not reported in all studies, unicellular cyanobacteria are observed throughout tropical and subtropical oceans (Moisander et al. 2010); suggesting they play an important role as a new nitrogen source. DDAs are of considerable interest because they are capable of expansive blooms and high rates of N₂ fixation (Carpenter et al. 1999; Foster et al. 2007; Subramaniam et al. 2008; Villareal et al. 2012). High densities, including blooms, have been observed in many tropical river plumes including the Amazon (Foster et al. 2007; Subramaniam et al. 2008), Congo (Foster et al. 2009a), and Mekong (Grosse et al. 2010; Bombar et al. 2011), and at least in the western tropical North Atlantic Ocean (WTNA), DDA blooms enhance carbon export from surface waters (Cooley and Yager 2006; Subramaniam et al. 2008; Yeung et al. 2012).

However, little is understood about the impacts of N₂-fixers on secondary production. For example, compared to other dominant primary producers, grazing by zooplankton is not considered a major pathway for new N from *Trichodesmium* to enter the food web. Toxicity and unpalatability are thought to be the major deterrents for grazing (O'Neil and Roman 1994; O'Neil 1998; Carpenter and Capone 2008), although harpacticoid copepods are known to feed on *Trichodesmium* (O'Neil and Roman 1994; O'Neil et al. 1996; O'Neil 1998). Moreover, the harpacticoid, *Macrosetella gracilis* relies on *Trichodesmium*, using the colonies as a habitat and a substrate for juvenile development (O'Neil & Roman 1992; Sheridan et al. 2002). The calanoid copepod *Acartia tonsa* was also observed to graze on *Trichodesmium* during a bloom along the coast of North Carolina (Guo and Tester 1994). As the bloom aged, *A. tonsa* exhibited physiological responses such as a distended gut, and mortality of *A. tonsa* was attributed to toxin production by senescing *Trichodesmium* colonies (Guo and Tester 1994). A

recent review by Turner (2014) highlights the varied responses of zooplankton to toxic algae (including a number of cyanobacteria) with grazing impact varying considerably according to predator and prey species and their environment.

Low $\delta^{15}\text{N}$ ratios of both suspended particles and mesozooplankton in the tropical and subtropical North Atlantic (Montoya et al. 2002, Landrum et al. 2011) indicate diazotrophic nitrogen (N_D) incorporation into zooplankton and the food web. However, this methodology does not delineate which zooplankton actively consume diazotrophs or the source of N_D incorporated into the zooplankton (e.g., DDAs or *Trichodesmium*). Likewise, unicellular cyanobacteria-zooplankton interactions are not well understood. Several studies have found at least one non-diazotrophic unicellular cyanobacterium, *Synechococcus*, is grazed by zooplankton either individually or as a component of aggregates (Pfannkuche and Lochte 1993; Gorsky et al. 1999; Wilson and Steinberg 2010; Stukel et al. 2013). More recently, Hunt et al. (2016) showed the diazotrophic unicellular cyanobacteria UCYN-C was grazed by zooplankton and contributed significantly to N_D entering the food web in the southwest Pacific Ocean.

In contrast to the paucity of studies on zooplankton-diazotroph grazing in the marine environment, freshwater literature provides many examples of these interactions. The number of toxic cyanobacteria blooms in freshwater and estuarine systems have increased due to eutrophication and climate change (Paerl and Otten 2013). Subsequently, considerable effort has focused on cyanobacteria bloom successional patterns and fate (Ger et al. 2014; Gerphagnon et al. 2015). Similar to the results of O’Neil and Roman (1994) and O’Neil (1998) in the marine environment, many freshwater studies have suggested morphology, toxicity, and unpalatability of cyanobacteria as deterrents to

zooplankton grazing (von Elert et al. 2003; Ger et al. 2014). Yet size-selective herbivorous copepods target cyanobacteria (Bouvy et al. 2001), and Kâ et al. (2011) observed that copepods, cladocerans, and rotifers actively graze and fragment larger filamentous cyanobacteria. While there are differences between freshwater and marine planktonic food webs, it seems improbable that dominant freshwater grazers (e.g., copepods and cladocerans) are able to adapt to utilizing large-scale cyanobacterial blooms as a food source (Kâ et al. 2011; Gerphagnon et al. 2015) while their marine counterparts almost entirely avoid feeding on diazotrophs.

The goal of this study is to investigate whether mesozooplankton grazers in the Amazon River plume-influenced WTNA directly graze upon diazotrophic organisms. In concert with this study, we recently reported elevated mesozooplankton grazing in the Amazon River plume relative to non-plume influenced waters (Conroy et al. 2016), although we used a community-based approach and as such could not distinguish the exact prey items. Here, we apply a molecular based approach that utilizes the *nifH* gene, which encodes for the nitrogenase enzyme for N₂ fixation, and highly specific qPCR assays targeting the *nifH* gene of two DDA populations and *Trichodesmium* to probe gut contents of zooplankton in the WTNA. We also used 16S next generation sequencing (NGS) to investigate the whole cyanobacterial community diversity in the gut contents.

2. Methods

2.1 Study area

Samples were collected from 9 stations in the Amazon River plume-influenced region of the WTNA (between 0-13° N and 44-57°W) as part of the Amazon INfluence on the Atlantic: CarbOn export from Nitrogen fixation by DiAtom Symbioses (ANACONDAS) project. Data presented here are from a cruise aboard the *R/V Knorr* May 22-June 24, 2010, during the period of peak plume discharge (Figure 1) and a large scale DDA bloom of *Hemiaulus-Richeliea* (Goes et al. 2014). Underway monitoring of sea surface salinity (SSS) and photosynthetic pigments as well as satellite monitoring of plume indicators such as chromophoric dissolved organic matter (CDOM) were the major factors used to determine station location. Station categorizations were determined by SSS at time of the respective tow for each sample. We sampled from 1 plume station (23) with SSS < 30; 4 mesohaline stations (2, 3, 19, 21) with SSS between 30 and 35; and 4 oceanic stations (5, 6, 20, 27) with SSS > 35.

2.2 Mesozooplankton collection

Mesozooplankton were collected with a 1-m Multiple Opening and Closing Net and Environment Sensing System (MOCNESS; Wiebe et al. 1976) fitted with ten 202 µm mesh nets. Daytime tows were performed between 1000 and 1400 h while nighttime tows were collected between 2200 and 0200 h (local time). Four depth intervals within the top 150 m were sampled with the MOCNESS, although molecular analysis was performed on animals collected from the two shallowest depth intervals (0-25 and 25-50 m) since shipboard observations and cell abundances detected the highest number of microscopically identified diazotrophs (e.g. *Trichodesmium*, DDAs) in the upper 50 m.

Once the nets were onboard, zooplankton were immediately anesthetized with carbonated water to prevent gut evacuation (Gannon and Gannon 1975). Samples were subsequently split into either $\frac{1}{4}$ or $\frac{1}{2}$ of the total sample volume using a Folsom plankton splitter, then size fractionated using nested sieves into the following size fractions: 0.2-0.5 mm, 0.5-1.0 mm, 1.0-2.0 mm, 2.0-5.0 mm, and >5.0 mm. Each size fraction was then concentrated onto a pre-weighed, 0.2 mm Nitex mesh filter, rinsed with Milli-Q to remove salt, and frozen at -80°C until processed in the laboratory.

2.3 DNA Extraction and quantitative PCR (qPCR) assays

Animals from the 0.5-1.0 mm and 1.0-2.0 mm size fractions were selected after visual inspection under a stereomicroscope to insure they were intact. Harpacticoid copepods (*Macrosetella gracilis* and *Miracia spp.*) and the decapod shrimp *Lucifer faxoni* were identified to species or genus level, while calanoid copepods, fish larvae, and decapod larvae from the family Thalassinidae were not (Table S1). These targets were chosen based on mesozooplankton community composition of each station, onboard microscopic counts from the cruise, pigment concentrations (Goes et al. 2014), and stable isotope analysis (Loick-Wilde et al. 2015) for the same cruise. Calanoid copepods were selected as they were present in high abundance across all samples, while the harpacticoid copepods were selected because of known associations with *Trichodesmium*. The *L. faxoni*, fish, and decapod larvae were included given their periodic high abundance. Animals were sorted and placed in autoclaved artificial seawater and inspected for exterior contamination with phytodetritus in appendages and mouthparts. Animals were picked clean of any obvious large particles using a needle and forceps, and following the procedure of Boling et al. (2012) subsequently rinsed five times with

autoclaved artificial seawater. Animals were inspected again for contaminating phytoplankton and cyanobacteria using blue (450-490 nm) and green (510-560 nm) excitation filters on an epifluorescent compound microscope at 200-450x magnifications. This procedure ensured animals chosen for molecular analysis were phytoplankton-free on their exterior. Between 25-50 animals were pooled per DNA extraction (Table S1); the number of individuals varied depending on size and availability of target and the results from preliminary PCR assays which determined the lowest number of pooled individuals needed for consistent amplification (see below). Samples were extracted using a modification to the Qiagen DNeasy® Blood and Tissue Kit Animal Tissue (Spin-Column) protocol. For example, a 12-hr lysis step was performed and all recommended reagent volumes were halved during the extraction. The final elution volume was 35 µl in the provided AE buffer.

We performed qPCR assays for three of the major diazotrophs in the WTNA, two DDAs (het-1, *Richelia* associated with *Rhizosolenia* diatoms and het-2, *Richelia* associated with *Hemiaulus* diatoms), and *Trichodesmium* spp. using the previously described oligonucleotides (Church et al. 2005a; Foster et al. 2007; Table S2) and a modified TaqMAN assay (see below). A total of 72 samples were analyzed for all three targets (het-1, het-2, *Trichodesmium*) with the exception of two calanoid copepod samples collected from St. 2 that were not run with the het-1 assay, and six samples from St. 3 were not run with the *Trichodesmium* due to low template (Table S2). In preliminary attempts (data not shown) to optimize the extraction and detection by qPCR, we identified a minimum number of individuals for replicable amplification. From those

results we used a minimum of 25 pooled individuals per extraction but, unless limited by abundance of the taxa in a sample, we pooled 50 individuals per extraction.

For all TaqMan PCR, the 12 μL reactions contained 6.25 μL TaqMan 2X Master Mix (Applied Biosystems), 0.5 μL forward and reverse 0.5 μM primers, 0.25 μL fluorogenic 0.5 μM probe, 2.5 μL of nuclease free water, and 2 μL of DNA template. All reactions were run in triplicate, and for the no-template controls, 2 mL of 5-kD filtered nuclease free water was added to each reaction. All qPCR assays were performed on an ABI 7500 Fast machine (Applied Biosystems) with the following thermal cycling conditions: 50°C for 2 minutes, 95°C for 10 minutes, and 45 cycles of 95°C for 15 seconds, followed by 60°C for 1 minute. Gene copy abundances were calculated from the mean cycle threshold (C_t) value of three replicates and the standard curve for the appropriate primer and probe set. For each primer and probe set, triplicate standard curves were made from 10-fold dilution series ranging from 10^8 to 1 gene copies per reaction. The standard curves were made from linearized plasmids of the target *nifH*. Regression analyses of the results (number of cycles = C_t) of the duplicate standard curves were analyzed in Excel. In some samples only one of the three replicates produced an amplification signal; these were noted as detectable, but not quantifiable (dnq). For samples where two or three of the replicates amplified the values were averaged and reported as *nifH*-gene copies/organism. We note that while we report gene copies per individual as is convention with qPCR, we do not scale our numbers to an estimation of feeding rate. Instead we consider amplification of our targets as confirmation of grazing on either DDAs or *Trichodesmium* (see detailed explanation in Discussion).

2.4 16S rRNA gene sequencing of zooplankton

Sequencing of zooplankton (containing their gut contents) followed a modified barcode protocol (Arfken et al. 2015) using the Ion Torrent PGM sequencer (Life Technologies). DNA concentrations from the extractions were measured on a NanoDrop 2000 (Thermo Scientific) and PCR was performed on samples normalized to $5 \text{ ng } \mu\text{l}^{-1}$ per reaction, except for fish larvae, which were normalized to $20 \text{ ng } \mu\text{l}^{-1}$ (see Table 2 for samples included in sequencing). The V4 hypervariable region of 16S rRNA genes was targeted with 515F and 805R primers for PCR reactions using GoTaq Green Master Mix (Promega). The 805R primers have barcodes with fusion sequences while the 515F contains fusion sequences only. PCR reactions were performed as follows: an initial denaturing step for 3 min at 95°C , then 30 cycles of 30s at 95°C , 1 min at 55°C , 1 min at 72°C , and finally at 72°C for 5 min. PCR products for each sample were then combined and sequencing was conducted. Barcoded samples were sequenced using the Ion Torrent 400 bp sequencing protocol with samples pooled onto a 316 chip. We note that for the 16S analysis we consider our results representative of the zooplankton “microbiome”, similar to other studies (Shoemaker and Moisander 2015; Scavotto et al. 2015), however we focus our results on the cyanobacteria and are confident that the cleaning methods adapted from Boling et al. (2012) allow us to focus on targets consumed by mesozooplankton.

2.5 Statistical analyses and bioinformatics pipeline

Sequencing output was downloaded from the Torrent Server using Torrent Suite v3.0 to obtain the FastQ file. A total of 33 libraries were created using the barcoded sequences. The open-source bioinformatics program Mothur (Schloss et al. 2009) was

used to trim and align the sequences. Chimeras were removed using UCHIME and remaining 16S sequences for each library were processed through the Greengenes database (<http://greengenes.lbl.gov/>) for taxonomic relative abundance. Cyanobacteria sequences identified through Greengenes were subsequently used for Blastn searches to identify sequences to genus level when possible. Principal coordinate analysis (PCO) was performed on square-root transformed relative abundance data in PRIMER 6.

3. RESULTS

3.1 Station phytoplankton assemblages and environmental conditions

Station selection was based on phytoplankton distribution from Goes et al. (2014) and physical and chemical properties described in Loick-Wilde et al. (2016). Detailed descriptions can be found in those reports but briefly we describe the station characteristics here. Station 23 was within the low salinity plume ($\text{SSS} < 30$) characterized by a DDA assemblage, high surface silicate and phosphate concentrations. Station 2, 3, and 19 were mesohaline plume stations ($30 > \text{SSS} > 35$) characterized by a DDA assemblage. Station 3 had high surface silicate and phosphate concentrations, while stations 2 and 19 had low surface silicate and phosphate levels. Station 21 was also a mesohaline plume station, but was characterized by a *Trichodesmium* and *Synechococcus* spp. phytoplankton assemblage rather than DDAs, and low surface silicate and phosphate levels. Stations 5, 6, 20, and 27, were all oceanic stations ($\text{SSS} > 35$) with a *Trichodesmium* and *Synechococcus* spp. phytoplankton assemblage and low surface silicate and phosphate concentrations. Surface nitrate and nitrite were not detectable at any of the stations.

3.2 quantitative PCR of gut contents

DDAs— Both the het-1 (*Richelia* associated with *Rhizosolenia* diatoms) and het-2 (*Richelia* associated with *Hemiaulus* diatoms), targets were successfully amplified from the gut content extractions (Table S1; Figure 2). Het-2 was the most common target amplified across all extractions, with a total of 25 samples amplified—24 from calanoid copepods and one from *Macrosetella gracilis*. Of those, 11 (10 calanoids and *M. gracilis*), were detectable not quantifiable (*dng*) (Figure 2). The remaining samples ranged from

1.6-16.8 het-2 *nifH*-copies/organism. All stations except for station 3, the furthest inshore mesohaline station, had samples that amplified the het-2 target. Comparatively, the other DDA primer, het-1, was found only in calanoid copepods collected at night at Station 19. Each of the two size fractions at this station had very low detection with the smaller calanoid copepods *dng* and larger calanoid copepods 0.10 *nifH* copies/copepod. No detectable pattern was observed between night (n=12) and day (n=13) het-2 amplifications, whereas both het-1 amplifications occurred in night samples (Table S1).

Trichodesmium— The *Trichodesmium* spp. target was also successfully amplified in the gut contents (Table S2; Figure 2). A total of 20 samples showed amplification, 14 in calanoid copepods (7 *dng*), 4 in *M. gracilis* (3 *dng*), and 2 in crab megalopae (1 *dng*) (Figure 2). All oceanic stations (St. 5, 6, 20, and 2; Figure 1), as well as one mesohaline station (St. 19), included in this analysis had zooplankton with amplification for *Trichodesmium*. Values ranged from 1.1-4.0 *Trichodesmium nifH* copies/organism with the highest value found in crab megalopae. No pattern was observed between day (n=11) and night (n=9) amplifications for *Trichodesmium*.

3.3 Characterization of cyanobacteria diversity in guts

Sample selection for 16S analysis was guided by our qPCR assays and resulted in the 33 samples selected for analysis. Not all samples with amplification from the qPCR were included due to template limitation, but a representative number of samples provided over 1.7 million sequences for analysis (see Table 2 for NGS samples).

Principle coordinates analysis of 16S sequences showed a tight clustering of two groups (Figure 3). Calanoid copepods (blue circle in Figure 3) and all harpacticoid

copepods (green circle in Figure 3) clustered by taxa. Other variables analyzed (salinity, size fraction, depth interval, time of day) resulted in no significant grouping.

Proteobacteria were the most abundant phyla represented in our samples, with 16 of the 33 samples having over 50 percent of sequences associated with proteobacteria (Figure 4). Cyanobacteria represented between 0-45% of bacterial composition across all samples and represented 11.3% of total sequences (Table 2). For non-calanoid copepod samples ($n=14$) only the decapod shrimp *Lucifer faxoni* had cyanobacterial sequences associated and represented >1% of total sequences. Harpacticoid copepods *M. gracilis* and *Miracia* spp. had cyanobacterial sequences present but were all <1% of total sequences, and the fish larvae sample analyzed was devoid of cyanobacterial sequences present (Table 2 and Figure 4).

When composition of cyanobacterial sequences ($n=197,298$) was analyzed, the most representative class was Synechococcophycideae (Figure 5). When investigated to genus level, the most abundant within this class was *Synechococcus* ($n=83,745$, representing 42.4% of all cyanobacterial sequences). *Prochlorococcus* was the next largest contributor at the genus level ($n=22,734$ representing 11.4% of all cyanobacterial sequences) although 21.2% of cyanobacterial sequences in Synechococcophycideae were unidentifiable to genus classification.

Blastn sequence results from the cyanobacterial sequences produced a number of significant alignments with *Synechococcus* sequences. Other cyanobacterial sequences resulting in significant alignments were from the unicellular groups UCYN-A as well as cyanobacterial endosymbionts. The former were present in over half of the NGS samples ($n=18$) whereas the latter were not sequences associated with either of the *Rhizosolenia*

or *Hemiaulus* DDAs. Lastly, a number of eukaryotic phytoplankton associated with chloroplast sequences were observed including: *Psuedo-nitzschia* spp., *Nitzschia* spp., *Chaetoceros* spp., *Phaeocystis* spp., *Nannochloropsis* spp., and *Imantonia* spp., as well as a number of Prasinophyte species.

4. DISCUSSION

Studying the pathway of diazotrophically derived production (N_D) in the marine food web is challenging; however, with several of the molecular-based approaches, new insights can be achieved. For example using *nifH* qPCR as a highly selective approach for determining direct grazing on DDAs and *Trichodesmium* combined with 16S NGS to determine cyanobacterial diversity in zooplankton guts, we found calanoid copepods were the most common grazer of DDAs and *Trichodesmium*. Templates derived from the harpacticoid copepod *M. gracilis*, commonly considered the major grazer of *Trichodesmium*, were often below detection. We also found evidence for crab megalopae consuming *Trichodesmium*. Finally, our NGS data concluded that mesozooplankton taxa frequently consume the non-diazotrophic cyanobacterium *Synechococcus* spp. These results provide insights on cyanobacteria-zooplankton dynamics with important implications for the pathways of N_D entering marine food webs and for nitrogen cycling in the WTNA.

4.1 Diazotroph Consumption by Mesozooplankton

DDAs—Stable isotope studies in the subtropical and tropical Atlantic Ocean (Montoya et al. 2002; Landrum et al. 2011; Loick-Wilde et al. 2015), including the region of our study, established that new nitrogen attributed to N_2 -fixation from diazotrophs is incorporated in the planktonic food web, but the pathway was unclear (i.e. through the microbial loop, exudation, grazing). The results of the gut content qPCR assays indicate diazotrophic nitrogen enters the food web via consumption of DDAs, as both DDA targets (het-1 and het-2) were present in the zooplankton gut contents. This is the first evidence for consumption of DDAs; moreover, of the various mesozooplankton sampled,

calanoid copepods grazed predominantly on het-2. Het-2 was the found consistently in calanoid copepods. These results are consistent with DDA distributions from qPCR assays of seawater, where het-2 was the most dominant of the two DDAs present during our study (Foster et al. in prep) as well as in a prior study of the Amazon-influenced WTNA (Foster et al. 2007). Our results also support the decreased $\delta^{15}\text{N}$ content of zooplankton reported by Loick-Wilde et al. (2016) from mesohaline stations, particularly at Stations 2 and 19 (their figure 9). At St. 19, the only station where het-1 was detected in the guts of mesozooplankton, qPCR assays from seawater are not available, but microscopic counts indicate both symbioses of *Hemiaulus* and *Rhizosolenia* diatoms were present at this station, although *Hemiaulus-Richeliea* symbiosis were 1-2 orders of magnitude more abundant than the *Rhizosolenia-Richeliea* symbiosis. (E.J. Carpenter, unpublished).

The pattern of DDA distribution in the WTNA largely follows the nutrient and salinity gradients outlined in Subramaniam et al. (2008), with DDAs occurring in the mesohaline region of the plume (Goes et al. 2014; Loick-Wilde et al. 2015). Hence, het-2 consumption at all four oceanic stations we sampled is unexpected, as phytoplankton at three of these four stations were characterized as an oceanic assemblage with abundant *Trichodesmium* and *Synechococcus*, (Goes et al. (2014) (note the remaining station 6 was not included in their study). The physical and chemical properties at these four stations also fit into the oceanic station categorization of Loick-Wilde et al. (2016). The presence of DDAs in zooplankton guts in oceanic stations suggests opportunistic and preferential grazing on het-2 when available, either in plume meanders or along the front between the mesohaline plume and oceanic waters.

These results, while novel, are not unexpected. Conroy et al. (2016) characterized the mesozooplankton food web in low salinity plume and mesohaline waters with SSS <33 as an export style food web. Export food webs are characterized by shorter diatom and mesozooplankton food webs (Michaels and Silver 1988; Legendre and Michaud 1998) and while both DDAs investigated form chains, often suggested as a grazing deterrent, copepods actively graze similar diatoms of similar size (Bergkvist et al. 2012), supporting a short export food web in mesohaline waters.

Trichodesmium were consumed by zooplankton at all four oceanic stations, as well as at two mesohaline stations. Calanoid copepods were again the primary consumers, although the highest *nifH* gene copies individual⁻¹ were amplified from crab megalopae. Despite the higher abundance of *M. gracilis* at oceanic stations relative to plume stations (Conroy et al. in prep.) and its known association with, and grazing on, *Trichodesmium* (O’Neil and Roman 1994; O’Neil et al. 1996; O’Neil 1998), this species only showed one amplification for *Trichodesmium* that was not *dng* (Table S2 and Figure 2). We do not suggest *M. gracilis* does not graze on *Trichodesmium*, but that this result is an artifact of our methodology, discussed in detail below.

Prior to our study there was little evidence of calanoid copepod grazing on *Trichodesmium*, and a general consensus emerged that it did not occur or was severely limited (Capone et al. 1997; Carpenter and Capone 2008). Our observation of calanoid copepod ingestion of *Trichodesmium* in the WTNA is novel and builds on other limited evidence for calanoid grazing on *Trichodesmium* globally (Hawser et al. 1992; Guo and Tester 1994). Calanoid copepods were typically the most abundant organism across all stations in the three smallest size fractions (0.2-0.5 mm, 0.5-1.0 mm, 1.0-2.0 mm)

(Conroy et al. in prep), as also found in zooplankton community composition studies in the subtropical North Atlantic (Steinberg et al. 2008; Eden et al. 2009). Thus, grazing by copepods on *Trichodesmium* in the oligotrophic tropical and subtropical ocean where *Trichodesmium* is abundant (Capone et al. 1997, 2005) has potential for a significant input of N_D into the food web. Furthermore, these results support that some fraction of the N_D incorporated into mesozooplankton, suggesting that the decline of δ¹⁵N at oceanic stations (Loick-Wilde et al. 2015) was due to direct grazing on *Trichodesmium*.

Previous work from stable isotope analysis suggests that decreases in δ¹⁵N in *Trichodesmium*-dominated waters is due to N_D exudation and incorporation into the food web via the microbial loop (Montoya et al. 2002; Mulholland 2007) rather than direct grazing, predominantly due to lack of grazing on *Trichodesmium* because of their potentially allelopathic toxins (Hawser et al. 1992). However, Hawser et al. (1992) showed that toxicity was species dependent and that not all *Trichodesmium* spp. are toxic to zooplankton. Furthermore, Guo and Tester (1994) investigated the effect of *Trichodesmium* sp. on the calanoid copepod *Acartia tonsa* after a meander from the Gulf Stream transported *Trichodesmium* inshore towards Albemarle Sound, North Carolina. They found no toxic effects of *Trichodesmium* on *A. tonsa* when fed healthy cells, but observed toxic effects, including distended guts and mortality, when fed aging or senescent cells or when treated with a filtered cell homogenate (Guo and Tester 1994). Given the ephemeral exposure *A. tonsa* has to *Trichodesmium* as a predominantly coastal copepod, it is reasonable that calanoid copepods exposed to *Trichodesmium* during development in the open ocean would have a similar ability to consume *Trichodesmium*. Furthermore, a study from the tropical North Atlantic between the Cape Verde Islands

and Barbados reports that $\delta^{15}\text{N}$ values for zooplankton and *Trichodesmium* are similar, so that direct consumption is the likeliest explanation (McClelland et al. 2003, see their Figure 6). Zooplankton grazing on *Trichodesmium* is further supported by evidence from freshwater habitats. Kâ et al. (2011) performed feeding experiments with calanoid copepods, cladocerans, and rotifers and found grazing could be a significant factor in controlling filamentous cyanobacteria. While we are unable to scale our numbers to estimate the grazing impact on *Trichodesmium* (see below), our results support that *Trichodesmium* is directly consumed by mesozooplankton.

4.2 Microbial and cyanobacterial diversity associated with zooplankton

Pairing the highly selective qPCR approach with a 16S NGS provides insight into the broader zooplankton-cyanobacterial dynamics in the WTNA. Our 16S sequences show abundant phyla that varied between samples, but proteobacteria, cyanobacteria, bacteroidetes and firmicutes were consistently a large percentage of all sample sequences. Similar to findings of Shoemaker and Moisander (2015) from the subtropical North Atlantic, our results indicate a distinct partitioning of microbes based on taxonomic groups rather than environmental factors (Figure 3). While an understanding of the complete microbiome of zooplankton is important (Shoemaker and Moisander 2015; Scavotto et al. 2015), particularly in the oligotrophic ocean where microenvironments (e.g., zooplankton) support unique bacterial assemblages (Azam & Malfatti, 2007), we limit the scope of our discussion to the cyanobacteria given their potential role in nitrogen fixation.

Predominance of *Synechococcus*- and to a lesser extent *Prochlorococcus*-associated sequences within the most abundant cyanobacteria class (Figure 5) is similar

to results from the same cruise investigating free-living and particle-associated cell genomes. Satinsky et al. (2014) compared protein sequences with reference genomes and found the prokaryotic assemblage was dominated by the Synechococcaceae family of cyanobacteria (Satinsky et al. 2014, See Figure S1 of that study). Those results are limited to one station, which we did not sample; however, it does provide insight into why our sequences were dominated by *Synechococcus* and *Prochlorococcus*.

Synechococcus and *Prochlorococcus* are considered too small to be directly consumed by most mesozooplankton, but may be consumed indirectly through feeding on marine snow aggregates or fecal pellets (Wilson and Steinberg 2010), or by ingesting microzooplankton which previously consumed small cells. Satinsky et al. (2014) showed a higher percentage of Synechococcaceae cyanobacteria in “particle-associated” sequences compared to “free-living”, while HPLC pigment data showed abundant *Synechococcus* throughout the plume and WTNA (Goes et al. 2014). We conclude that predominance of *Synechococcus* and *Prochlorococcus* sequences in the crustacean zooplankton are likely from consumption of cyanobacteria-containing aggregates or microzooplankton.

While less abundant than *Synechococcus* and *Prochlorococcus*, the presence of UCYN-A in a majority of samples indicates a pathway of diazotrophic nitrogen into the food web, as *Synechococcus* and *Prochlorococcus* are non-diazotrophic and UCYN-A is capable of fixing nitrogen (Zehr 2011; Thompson et al. 2012, 2014). To our knowledge this is the first observation of zooplankton consumption of UCYN-A. Comparable in size to *Synechococcus* and *Prochlorococcus*, it also seems likely that UCYN-A are consumed on aggregates. We do not have water column abundance data for UCYN-A; however,

results from prior studies in the tropical Atlantic suggest it is widely distributed, particularly in the eastern Atlantic and outer most regions of the plume-influenced WTNA (Foster et al. 2007; Goebel et al. 2010). Globally, UCYN-A is observed throughout the tropics and thus our results suggest a broad potential pathway for N_D from UCYN-A into planktonic food webs, particularly in areas such as the south Pacific where high UCYN-A concentrations are observed (Moisander et al. 2010).

4.3 Perspectives for scaling up to grazing

While molecular methods to quantify zooplankton grazing rates are becoming more common (Nejstgaard et al. 2008; Troedsson et al. 2009), we hesitate to extend our qPCR results beyond a qualitative assessment of grazing. The *nifH* qPCR assays are highly selective; thus the percentage of the total gut contents an amplified target represents is unknown, making it inappropriate to scale to a grazing rate. Other non-targeted organisms consumed, which our NGS methodology confirms, would not be detected by the assays we utilized and could affect qPCR amplification (Kanagawa 2003; Nejstgaard et al. 2008). This is likely why we did not observe DDA sequences in the NGS data. Using a 16S primer allowed for a wide taxonomic investigation but likely led to some exclusion of the highly selective *nifH* targets.

Furthermore, target DNA degradation in the gut is a significant factor in underestimating zooplankton grazing, particularly in copepods, with molecular methods (Troedsson et al. 2009; Simonelli et al. 2009). Conroy et al. (2016) observed elevated grazing in both the low salinity plume stations and in the intermediate mesohaline stations utilizing the gut pigment method, yet our qPCR assays all yielded low gene copies organism⁻¹ regardless of station category. Similarly, Nejstgaard et al. (2008) found

a pattern of underrepresentation of gut contents when comparing qPCR estimates to gut pigment estimates. Regardless of the low gene copies, we are confident our results are indicative of grazing on DDAs and Trichodesmium given the high selectivity of our qPCR assays and our sanitation techniques. In order to account for low gene copies due to gut degradation, we suggest future work include a culture of the targeted diazotroph for analyses so that a differential length amplification qPCR (dla-qPCR) method, similar to that utilized in Troedsson et al. (2009), could account for DNA degradation, and be used to estimate grazing rate on diazotrophs.

5. CONCLUSION

Diazotrophic nitrogen incorporation into the planktonic food web has long been observed through the use of nitrogen stable isotope analysis. While an extremely robust method, stable isotope analysis lacks the nuance to determine the exact pathways fixed nitrogen enters the planktonic food web. We provide direct evidence that two DDAs, *Hemiallus-Richeliea* and *Rhizosolenia-Richeliea*, are consumed by mesozooplankton. We further show that *Trichodesmium* is consumed by calanoid and harpacticoid copepods, as well as some decapod larvae. Lastly, we show that unicellular cyanobacteria, particularly non-diazotrophic *Synechococcus* and *Prochlorococcus*, as well as diazotrophic UCYN-A, are consumed by zooplankton, likely as components of aggregates. Grazing on UCYN-A provides an additional and previously undocumented pathway for diazotrophic nitrogen incorporation into the food web.

This study has important implications for our understanding of cyanobacterial-zooplankton dynamics in a changing ocean. Increased stratification, due to warming surface waters, is expected to elevate the importance of N₂-fixation in the oligotrophic open ocean (Doney et al. 2012), and our results suggest that mesozooplankton that consume diazotrophs would likely benefit. Our results are applicable beyond the WTNA, as in other areas with DDA blooms such as the Congo, Niger, and Mekong River plumes (Foster et al. 2009b; Grosse et al. 2010; Bombar et al. 2011), the South Pacific Ocean (Turk-Kubo et al. 2015), as well as globally where *Trichodesmium* (Capone et al. 1997, 2005) and unicellular cyanobacteria (Moisander et al. 2010; Goebel et al. 2010) are important diazotrophs. Questions do remain, however, concerning what other mesozooplankton taxa target diazotrophs, and what are the grazing rates and impacts on

DDAs and *Trichodesmium*. Further work in these areas is needed to extend our results to multiple taxa and other regions, and to quantify specific pathways of diazotrophic nitrogen incorporation into the food web.

REFERENCES

- Arfken, A. M., B. Song, and M. A. Mallin. 2015. Assessing hog lagoon waste contamination in the Cape Fear Watershed using Bacteroidetes 16S rRNA gene pyrosequencing. *Appl Microbiol Biotechnol* **99**: 7283–7293. doi:10.1007/s00253-015-6784-x
- Berman-Frank, I., Bidle, K. D., Haramaty, L., and Falkowski, P. G. The demise of marine cyanobacterium, *Trichodesmium* spp., via an autocatalyzed cell death pathway. *Limnology and Oceanography* **49**: 997-1005.
- Bergkvist, J., P. Thor, H. Henrik Jakobsen, S.-Å. Wängberg, and E. Selander. 2012. Grazer-induced chain length plasticity reduces grazing risk in a marine diatom. *Limnology and Oceanography* **57**: 318. doi:10.4319/lo.2012.57.1.0318
- Boling, W. B., G. A. Sinclair, and B. Wawrik. 2012. Identification of calanoid copepod prey species via molecular detection of carbon fixation genes. *Mar Biol* **159**: 1165–1171. doi:10.1007/s00227-011-1877-2
- Bombar, D., P. Moisander, J. Dippner, R. Foster, M. Voss, B. Karfeld, and J. Zehr. 2011. Distribution of diazotrophic microorganisms and nifH gene expression in the Mekong River plume during intermonsoon. *Marine Ecology Progress Series* **424**: 39–52. doi:10.3354/meps08976
- Bouvy, M., M. Pagano, and M. Troussellier. 2001. Effects of a cyanobacterial bloom (*Cylindrospermopsis raciborskii*) on bacteria and zooplankton communities in Ingazeira reservoir (northeast Brazil). *Aquatic Microbial Ecology* **25**: 215–227.
- Bronk, D. A., and D. K. Steinberg. 2008. Chapter 8 - Nitrogen Regeneration, p. 385–467. In *Nitrogen in the Marine Environment (2nd Edition)*. Academic Press.

- Capone, D. G. 2001. Marine nitrogen fixation: what's the fuss? *Current Opinion in Microbiology* **4**: 341–348. doi:10.1016/S1369-5274(00)00215-0
- Capone, D. G., J. A. Burns, J. P. Montoya, A. Subramaniam, C. Mahaffey, T. Gunderson, A. F. Michaels, and E. J. Carpenter. 2005. Nitrogen fixation by *Trichodesmium* spp.: An important source of new nitrogen to the tropical and subtropical North Atlantic Ocean: Nitrogen Fixation in the North Atlantic. *Global Biogeochemical Cycles* **19**: GB2024. doi:10.1029/2004GB002331
- Capone, D. G., J. P. Zehr, H. W. Paerl, B. Bergman, and E. J. Carpenter. 1997. *Trichodesmium*, a Globally Significant Marine Cyanobacterium. *Science* **276**: 1221–1229. doi:10.1126/science.276.5316.1221
- Carpenter, E. J., and D. G. Capone. 2008. Chapter 4 - Nitrogen Fixation in the Marine Environment, p. 141–198. *In* *Nitrogen in the Marine Environment* (2nd Edition). Academic Press.
- Carpenter, E. J., J. P. Montoya, J. Burns, M. R. Mulholland, A. Subramaniam, and D. G. Capone. 1999. Extensive bloom of a N₂-fixing diatom/cyanobacterial association in the tropical Atlantic Ocean. *Marine Ecology Progress Series* **185**: 273–283.
- Conroy, B. J., D. K. Steinberg, M. R. Stukel, J. I. Goes, and V. J. Coles. 2016. Meso- and microzooplankton grazing in the Amazon River plume and western tropical North Atlantic: Zooplankton grazing in the Amazon River plume. *Limnology and Oceanography* **61**: 825–840. doi:10.1002/lo.10261
- Cooley, S. R., and P. L. Yager. 2006. Physical and biological contributions to the western tropical North Atlantic Ocean carbon sink formed by the Amazon River plume. *Journal of Geophysical Research* **111**. doi:10.1029/2005JC002954

- Doney, S. C., M. Ruckelshaus, J. Emmett Duffy, and others. 2012. Climate Change Impacts on Marine Ecosystems. *Annual Review of Marine Science* **4**: 11–37. doi:10.1146/annurev-marine-041911-111611
- Dugdale, R. C., and J. J. Goering. 1967. Uptake of new and regenerated forms of nitrogen in primary productivity. *Limnol. Oceanogr.* **12**: 196–206.
- Eden, B. R., D. K. Steinberg, S. A. Goldthwait, and D. J. McGillicuddy. 2009. Zooplankton community structure in a cyclonic and mode-water eddy in the Sargasso Sea. *Deep Sea Research Part I: Oceanographic Research Papers* **56**: 1757–1776. doi:10.1016/j.dsr.2009.05.005
- von Elert, E., D. Martin-Creuzburg, and J. R. Le Coz. 2003. Absence of sterols constrains carbon transfer between cyanobacteria and a freshwater herbivore (*Daphnia galeata*). *Proc Biol Sci* **270**: 1209–1214. doi:10.1098/rspb.2003.2357
- Falcon, L. I., E. J. Carpenter, F. Cipriano, B. Bergman, and D. G. Capone. 2004. N₂ Fixation by Unicellular Bacterioplankton from the Atlantic and Pacific Oceans: Phylogeny and In Situ Rates. *Applied and Environmental Microbiology* **70**: 765–770. doi:10.1128/AEM.70.2.765-770.2004
- Foster, R. A., A. Subramaniam, C. Mahaffey, E. J. Carpenter, D. G. Capone, and J. P. Zehr. 2007. Influence of the Amazon River plume on distributions of free-living and symbiotic cyanobacteria in the western tropical north Atlantic Ocean. *Limnology and oceanography* **52**: 517–532.
- Foster, R. A., A. Subramaniam, and J. P. Zehr. 2009a. Distribution and activity of diazotrophs in the Eastern Equatorial Atlantic. *Environ Microbiol* **11**: 741–750. doi:10.1111/j.1462-2920.2008.01796.x

Foster, R. A., A. Subramaniam, and J. P. Zehr. 2009b. Distribution and activity of diazotrophs in the Eastern Equatorial Atlantic. *Environmental Microbiology* **11**: 741–750. doi:10.1111/j.1462-2920.2008.01796.x

Gannon, J. E., and S. A. Gannon. 1975. Observations on the Narcotization of Crustacean Zooplankton. *Crustaceana* **28**: 220–224.

Ger, K. A., L.-A. Hansson, and M. Lürling. 2014. Understanding cyanobacteria-zooplankton interactions in a more eutrophic world. *Freshw Biol* **59**: 1783–1798. doi:10.1111/fwb.12393

Gerphagnon, M., D. J. MacArthur, D. Latour, C. M. M. Gachon, F. Van Ogtrop, F. H. Gleason, and T. Sime-Ngando. 2015. Microbial players involved in the decline of filamentous and colonial cyanobacterial blooms with a focus on fungal parasitism. *Environ Microbiol* n/a–n/a. doi:10.1111/1462-2920.12860

Glibert, P. M., and D. A. Bronk. 1994. Release of dissolved organic nitrogen by marine diazotrophic cyanobacteria, *Trichodesmium* spp. *Applied and Environmental microbiology* **60**: 3996–4000.

Goebel, N. L., K. A. Turk, K. M. Achilles, and others. 2010. Abundance and distribution of major groups of diazotrophic cyanobacteria and their potential contribution to N₂ fixation in the tropical Atlantic Ocean: Diazotrophic cyanobacteria in the tropical North Atlantic. *Environmental Microbiology* **12**: 3272–3289. doi:10.1111/j.1462-2920.2010.02303.x

Goes, J. I., H. do R. Gomes, A. M. Chekalyuk, and others. 2014. Influence of the

Amazon River discharge on the biogeography of phytoplankton communities in the western tropical north Atlantic. *Progress in Oceanography* **120**: 29–40.

doi:10.1016/j.pocean.2013.07.010

Gorsky, G., M. J. Chrétiennot-Dinet, J. Blanchot, and I. Palazzoli. 1999. Picoplankton and nanoplankton aggregation by appendicularians: Fecal pellet contents of *Megalocercus huxleyi* in the equatorial Pacific. *J. Geophys. Res.* **104**: 3381–3390.

doi:10.1029/98JC01850

Gruber, N.. 2008. Chapter 1 - The Marine Nitrogen Cycle: Overview and Challenges, p. 1-50. In *Nitrogen in the Marine Environment (2nd Edition)*. Academic Press.

Grosse, J., D. Bombar, H. N. Doan, L. N. Nguyen, and M. Voss. 2010. The Mekong River plume fuels nitrogen fixation and determines phytoplankton species distribution in the South China Sea during low and high discharge season.

Limnology and Oceanography **55**: 1668–1680. doi:10.4319/lo.2010.55.4.1668

Guo, C., and P. A. Tester. 1994. Toxic effect of the bloom-forming *Trichodesmium* sp. (cyanophyta) to the copepod *Acartia tonsa*. *Natural Toxins* **2**: 222–227.

doi:10.1002/nt.2620020411

Hawser, S. P., J. M. O’neil, M. R. Roman, and G. A. Codd. 1992. Toxicity of blooms of the cyanobacterium *Trichodesmium* to zooplankton. *Journal of applied phycology* **4**: 79–86.

Hewson, I., S. R. Govil, D. G. Capone, E. J. Carpenter, and J. A. Fuhrman. 2004. Evidence of *Trichodesmium* viral lysis and potential significance for biogeochemical cycling in the oligotrophic ocean. *Aquat Microb Ecol* **36**: 1–8.

doi:10.3354/ame036001

- Hunt, B. P. V., S. Bonnet, H. Berthelot, B. J. Conroy, R. A. Foster, and M. Pagano. 2016. Contribution and pathways of diazotroph derived nitrogen to zooplankton during the VAHINE mesocosm experiment in the oligotrophic New Caledonia lagoon. Biogeosciences Discussions 1–33. doi:10.5194/bg-2015-614
- Kanagawa, T. 2003. Bias and artifacts in multitemplate polymerase chain reactions (PCR). *J. Biosci. Bioeng.* **96**: 317–323. doi:10.1016/S1389-1723(03)90130-7
- Kâ, S., J. M. Mendoza-Vera, M. Bouvy, G. Champalbert, R. N’Gom-Kâ, and M. Pagano. 2011. Can tropical freshwater zooplankton graze efficiently on cyanobacteria? *Hydrobiologia* **679**: 119–138. doi:10.1007/s10750-011-0860-8
- Landrum, J. P., M. A. Altabet, and J. P. Montoya. 2011. Basin-scale distributions of stable nitrogen isotopes in the subtropical North Atlantic Ocean: Contribution of diazotroph nitrogen to particulate organic matter and mesozooplankton. *Deep Sea Research Part I: Oceanographic Research Papers* **58**: 615–625. doi:10.1016/j.dsr.2011.01.012
- Legendre, L., and J. Michaud. 1998. Flux of biogenic carbon in oceans: size-dependent regulation by pelagic food webs. *Marine Ecology Progress Series* **164**: 1–11.
- Loick-Wilde, N., S. C. Weber, B. J. Conroy, D. G. Capone, V. J. Coles, P. M. Medeiros, D. K. Steinberg, and J. P. Montoya. 2016. Nitrogen sources and net growth efficiency of zooplankton in three Amazon River plume food webs. *Limnol. Oceanogr.* **61**: 460–481. doi:10.1002/lno.10227
- McClelland, J. W., C. M. Holl, and J. P. Montoya. 2003. Relating low $\delta^{15}\text{N}$ values of

zooplankton to N₂-fixation in the tropical North Atlantic: insights provided by stable isotope ratios of amino acids. Deep Sea Research Part I: Oceanographic Research Papers **50**: 849–861. doi:10.1016/S0967-0637(03)00073-6

Michaels, A. F., and M. W. Silver. 1988. Primary production, sinking fluxes and the microbial food web. Deep Sea Research Part A. Oceanographic Research Papers **35**: 473–490.

Moisander, P. H., R. A. Beinart, I. Hewson, A. E. White, K. S. Johnson, C. A. Carlson, J. P. Montoya, and J. P. Zehr. 2010. Unicellular Cyanobacterial Distributions Broaden the Oceanic N₂ Fixation Domain. Science **327**: 1512–1514. doi:10.1126/science.1185468

Montoya, J. P., E. J. Carpenter, and D. G. Capone. 2002. Nitrogen fixation and nitrogen isotope abundances in zooplankton of the oligotrophic North Atlantic. Limnology and Oceanography **47**: 1617–1628.

Montoya, J. P., C. M. Holl, J. P. Zehr, A. Hansen, T. A. Villareal, and D. G. Capone. 2004. High rates of N₂ fixation by unicellular diazotrophs in the oligotrophic Pacific Ocean. Nature **430**: 1027–1031. doi:10.1038/nature02824

Mulholland, M. R. 2007. The fate of nitrogen fixed by diazotrophs in the ocean. Biogeosciences **4**: 37–51. doi:10.5194/bg-4-37-2007

Nejstgaard, J. C., M. E. Frischer, P. Simonelli, C. Troedsson, M. Brakel, F. Adiyaman, A. F. Sazhin, and L. F. Artigas. 2008. Quantitative PCR to estimate copepod feeding. Mar Biol **153**: 565–577. doi:10.1007/s00227-007-0830-x

O’Neil, J. M. 1998. The colonial cyanobacterium *Trichodesmium* as a physical and

- nutritional substrate for the harpacticoid copepod *Macrosetella gracilis*. *Journal of plankton research* **20**: 43–59. doi:10.1093/plankt/20.1.43
- O’Neil, J. M., P. M. Metzler, and P. M. Glibert. 1996. Ingestion of $^{15}\text{N}_2$ -labelled *Trichodesmium* spp. and ammonium regeneration by the harpacticoid copepod *Macrosetella gracilis*. *Marine Biology* **125**: 89–96.
- O’Neil, J. M., and M. R. Roman. 1994. Ingestion of the cyanobacterium *Trichodesmium* spp. by pelagic harpacticoid copepods *Macrosetella*, *Miracia* and *Oculosetella*. *Hydrobiologia* **292**: 235–240. doi:10.1007/BF00229946
- Paerl, H. W., and T. G. Otten. 2013. Harmful Cyanobacterial Blooms: Causes, Consequences, and Controls. *Microbial Ecology* **65**: 995–1010. doi:10.1007/s00248-012-0159-y
- Pfannkuche, O., and K. Lochte. 1993. Open ocean pelago-benthic coupling: cyanobacteria as tracers of sedimenting salp faeces. *Deep Sea Research Part I: Oceanographic Research Papers* **40**: 727–737.
- Satinsky, B. M., B. C. Crump, C. B. Smith, and others. 2014. Microspatial gene expression patterns in the Amazon River Plume. *PNAS* **111**: 11085–11090. doi:10.1073/pnas.1402782111
- Scavotto, R. E., C. Dziallas, M. Bentzon-Tilia, L. Riemann, and P. H. Moisander. 2015. Nitrogen-fixing bacteria associated with copepods in coastal waters of the North Atlantic Ocean. *Environ Microbiol* **17**: 3754–3765. doi:10.1111/1462-2920.12777
- Schloss, P. D., S. L. Westcott, T. Ryabin, and others. 2009. Introducing mothur: Open-

- Source, Platform-Independent, Community-Supported Software for Describing and Comparing Microbial Communities. *Appl. Environ. Microbiol.* **75**: 7537–7541. doi:10.1128/AEM.01541-09
- Shoemaker, K. M., and P. H. Moisander. 2015. Microbial diversity associated with copepods in the North Atlantic subtropical gyre. *FEMS Microbiology Ecology* fiv064. doi:10.1093/femsec/fiv064
- Simonelli, P., C. Troedsson, J. C. Nejstgaard, K. Zech, J. B. Larsen, and M. E. Frischer. 2009. Evaluation of DNA extraction and handling procedures for PCR-based copepod feeding studies. *J. Plankton Res.* **31**: 1465–1474. doi:10.1093/plankt/fbp087
- Sohm, J. A., E. A. Webb, and D. G. Capone. 2011. Emerging patterns of marine nitrogen fixation. *Nature Reviews Microbiology* **9**: 499–508. doi:10.1038/nrmicro2594
- Steinberg, D. K., J. S. Cope, S. E. Wilson, and T. Kobari. 2008. A comparison of mesopelagic mesozooplankton community structure in the subtropical and subarctic North Pacific Ocean. *Deep Sea Research Part II: Topical Studies in Oceanography* **55**: 1615–1635. doi:10.1016/j.dsr2.2008.04.025
- Stukel, M. R., M. Décima, K. E. Selph, D. A. A. Taniguchi, and M. R. Landry. 2013. The role of Synechococcus in vertical flux in the Costa Rica upwelling dome. *Progress in Oceanography* **112–113**: 49–59. doi:10.1016/j.pocean.2013.04.003
- Subramaniam, A., P. L. Yager, E. J. Carpenter, and others. 2008. Amazon River enhances diazotrophy and carbon sequestration in the tropical North Atlantic Ocean. *PNAS* **105**: 10460–10465. doi:10.1073/pnas.0710279105
- Thompson, A., B. J. Carter, K. Turk-Kubo, F. Malfatti, F. Azam, and J. P. Zehr. 2014.

- Genetic diversity of the unicellular nitrogen-fixing cyanobacteria UCYN-A and its prymnesiophyte host. *Environ Microbiol* **16**: 3238–3249. doi:10.1111/1462-2920.12490
- Thompson, A. W., R. A. Foster, A. Krupke, B. J. Carter, N. Musat, D. Vaulot, M. M. M. Kuypers, and J. P. Zehr. 2012. Unicellular Cyanobacterium Symbiotic with a Single-Celled Eukaryotic Alga. *Science* **337**: 1546–1550. doi:10.1126/science.1222700
- Troedsson, C., P. Simonelli, V. Nägele, J. C. Nejstgaard, and M. E. Frischer. 2009. Quantification of copepod gut content by differential length amplification quantitative PCR (dla-qPCR). *Mar Biol* **156**: 253–259. doi:10.1007/s00227-008-1079-8
- Turk-Kubo, K. A., I. E. Frank, M. E. Hogan, A. Desnues, S. Bonnet, and J. P. Zehr. 2015. Diazotroph community succession during the VAHINE mesocosm experiment (New Caledonia lagoon). *Biogeosciences* **12**: 7435–7452. doi:10.5194/bg-12-7435-2015
- Turner, J. T. 2014. Planktonic marine copepods and harmful algae. *Harmful Algae* **32**: 81–93. doi:10.1016/j.hal.2013.12.001
- Villareal, T. A., C. G. Brown, M. A. Brzezinski, J. W. Krause, and C. Wilson. 2012. Summer Diatom Blooms in the North Pacific Subtropical Gyre: 2008–2009. *PLoS ONE* **7**: e33109. doi:10.1371/journal.pone.0033109
- Wiebe, P. H., K. H. Burt, S. H. Boyd, and A. W. Morton. 1976. A multiple opening/closing net and environmental sensing system for sampling zooplankton. *Journal of Marine Research* **34**: 313–326.

Wilson, S., and D. Steinberg. 2010. Autotrophic picoplankton in mesozooplankton guts: evidence of aggregate feeding in the mesopelagic zone and export of small phytoplankton. *Marine Ecology Progress Series* **412**: 11–27.

doi:10.3354/meps08648

Yeung, L. Y., W. M. Berelson, E. D. Young, and others. 2012. Impact of diatom-diazotroph associations on carbon export in the Amazon River plume. *Geophysical Research Letters* **39**: L18609. doi:10.1029/2012GL053356

Zehr, J. P. 2011. Nitrogen fixation by marine cyanobacteria. *Trends in Microbiology* **19**: 162–173. doi:10.1016/j.tim.2010.12.004

Zehr, J. P., J. B. Waterbury, P. J. Turner, J. P. Montoya, E. Omoregie, G. F. Steward, A. Hansen, and D. M. Karl. 2001. Unicellular cyanobacteria fix N₂ in the subtropical North Pacific Ocean. *Nature* **412**: 635–638. doi:10.1038/35088063

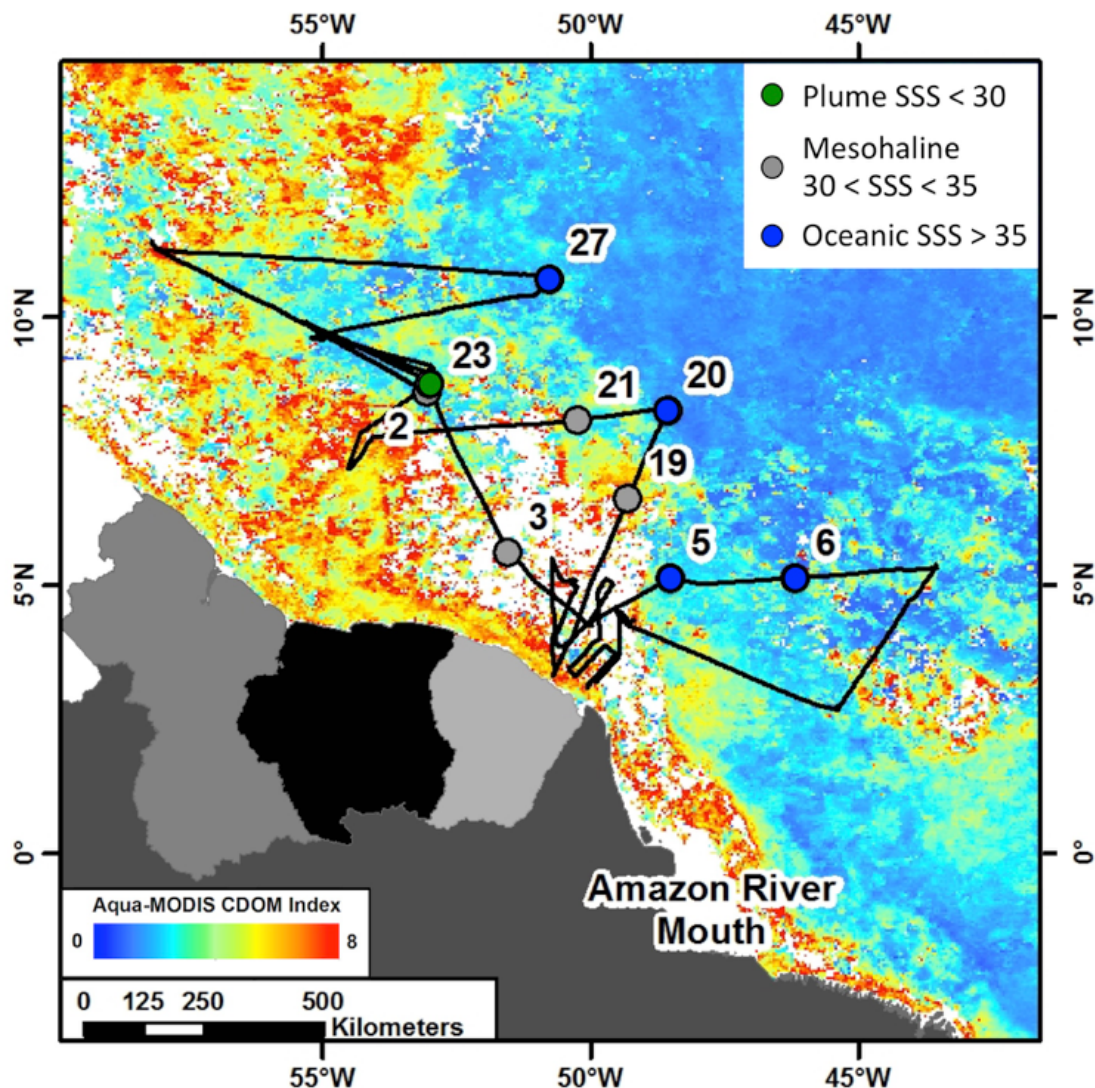


Figure 1. Cruise track from ANACONDAS cruise in May-June, 2010 with stations sampled for analyses used in this study labeled. Cruise track is overlaid on monthly averaged chromophoric dissolved organic matter (CDOM) concentration from Aqua-MODIS satellite data (oceancolor.gsfc.nasa.gov). Colors represent station categories based on sea surface salinity (SSS). Stations with SSS < 30 are considered “plume” and shown in green, stations with 30 < SSS < 35 are considered “mesohaline” and shown in grey and stations with SSS > 35 are considered “oceanic” and shown in blue.

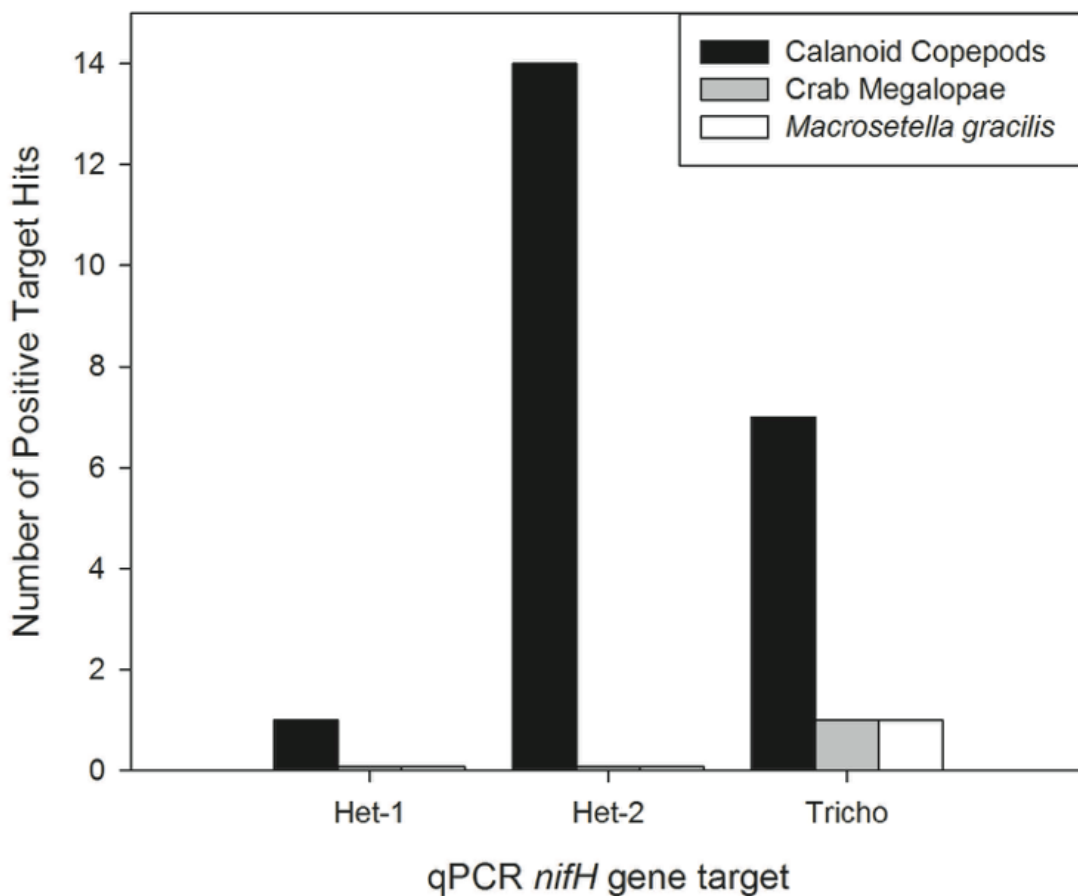


Figure 2. Number of positive qPCR target hits for calanoid copepods (n=50 assays of pooled individuals), crab megalopae (n=2 assays), and the harpacticoid copepod *Macrosetella gracilis* (n=13 assays). Het-1 targets the *Rhizosolenia-Richeliea* diatom diazotroph association (DDA), Het-2 targets the *Hemiallus-Richeliea* DDA, and Tricho targets *Trichodesmium*. Assays were run in triplicate and the numbers shown here represent samples with at least 2 of 3 replicates positive for the targets. Other taxa sampled (fish larvae, the decapod shrimp *Lucifer faxoni*, *Miracia* spp. harpacticoid copepods, and decapod larvae) presented no positive hits for any of the targets

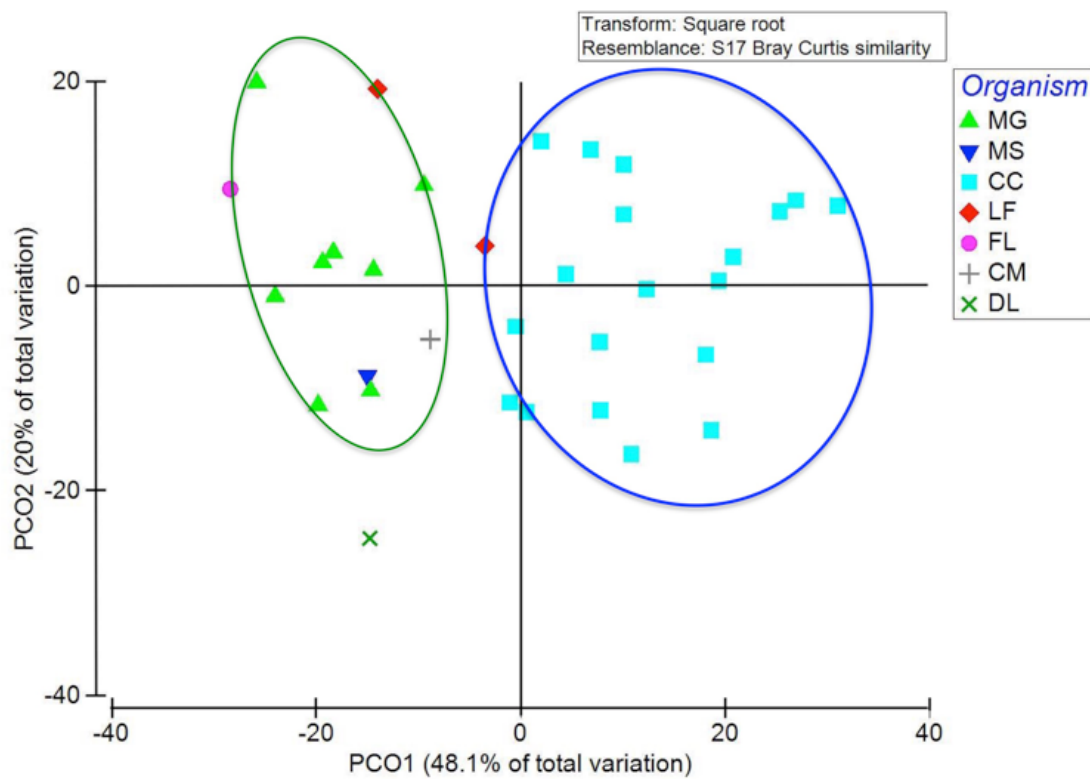


Figure 3. Principle coordinates analysis of 16S zooplankton microbial community shown by zooplankton taxonomic group. PCO1 and PCO2 explain 48.1% and 20% of the variation, respectively. Calanoid copepods (blue circle) and harpacticoid copepods including both *Macrosetella gracilis* and *Miracia* spp. (green circle) grouped. Organisms are: MG=*Macrosetella gracilis*, MS=*Miracia* spp., CC=calanoid copepod, LF=*Lucifer faxoni*, FL=fish larvae, CM=crab megalopae, and DL=decapod larvae.

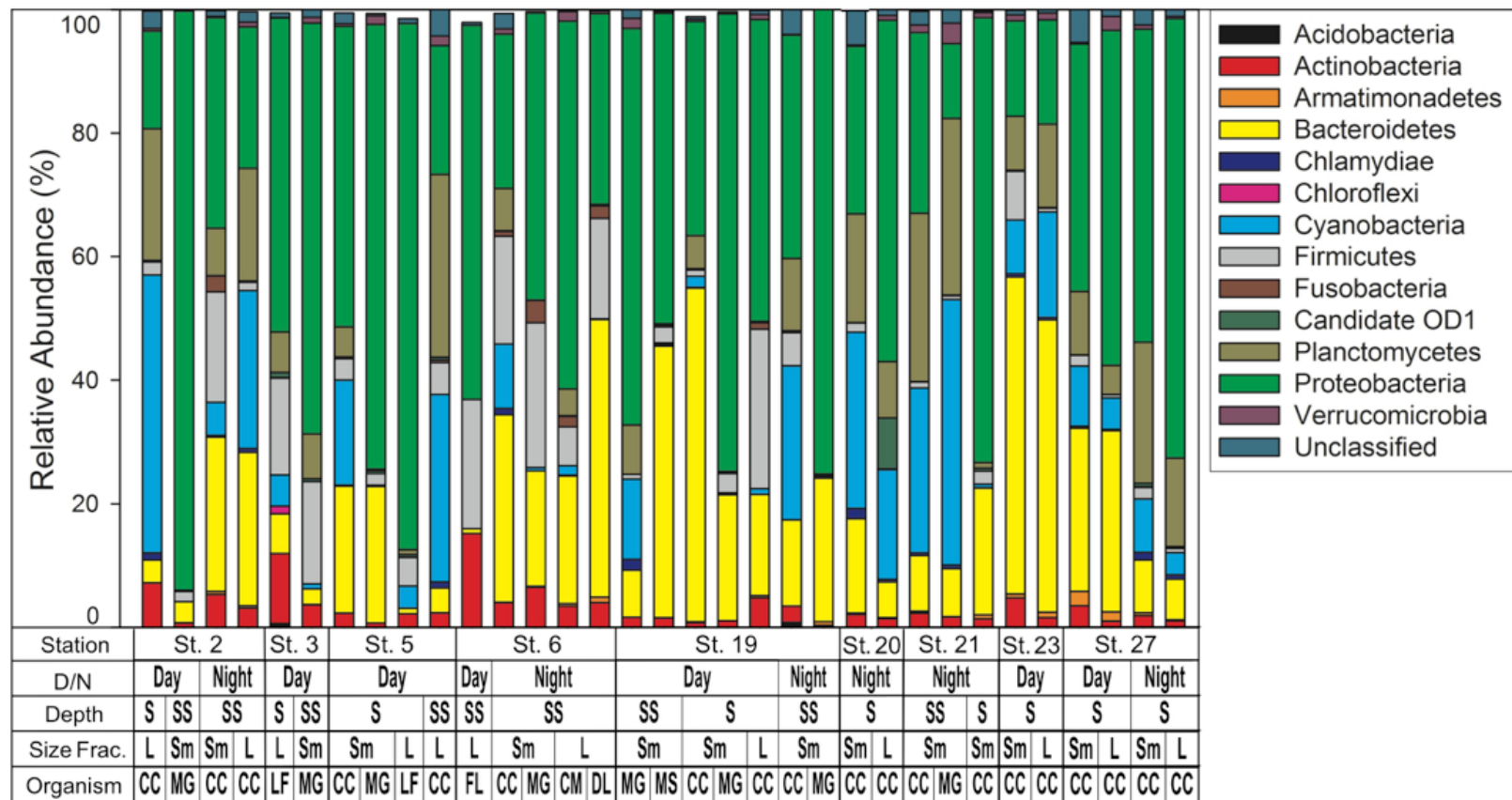


Figure 4. Bacterial community composition by phylum as determined by 16S next generation sequencing. Phyla are listed in key to right. Key below graph identifies each sample with categories as follows: D/N= day or night; Depth S=Surface 0-25m, SS=Sub Surface 25-50m; Size fraction L=1.0-2.0 mm, Sm=0.5-1.0 mm; Organism CC=calanoid copepod, MG=*Macrosetella gracilis*, MS=*Miracia* spp. LF=*Lucifer faxoni*, FL=fish larvae, CM=crab megalopae, and DL=decapod larvae.

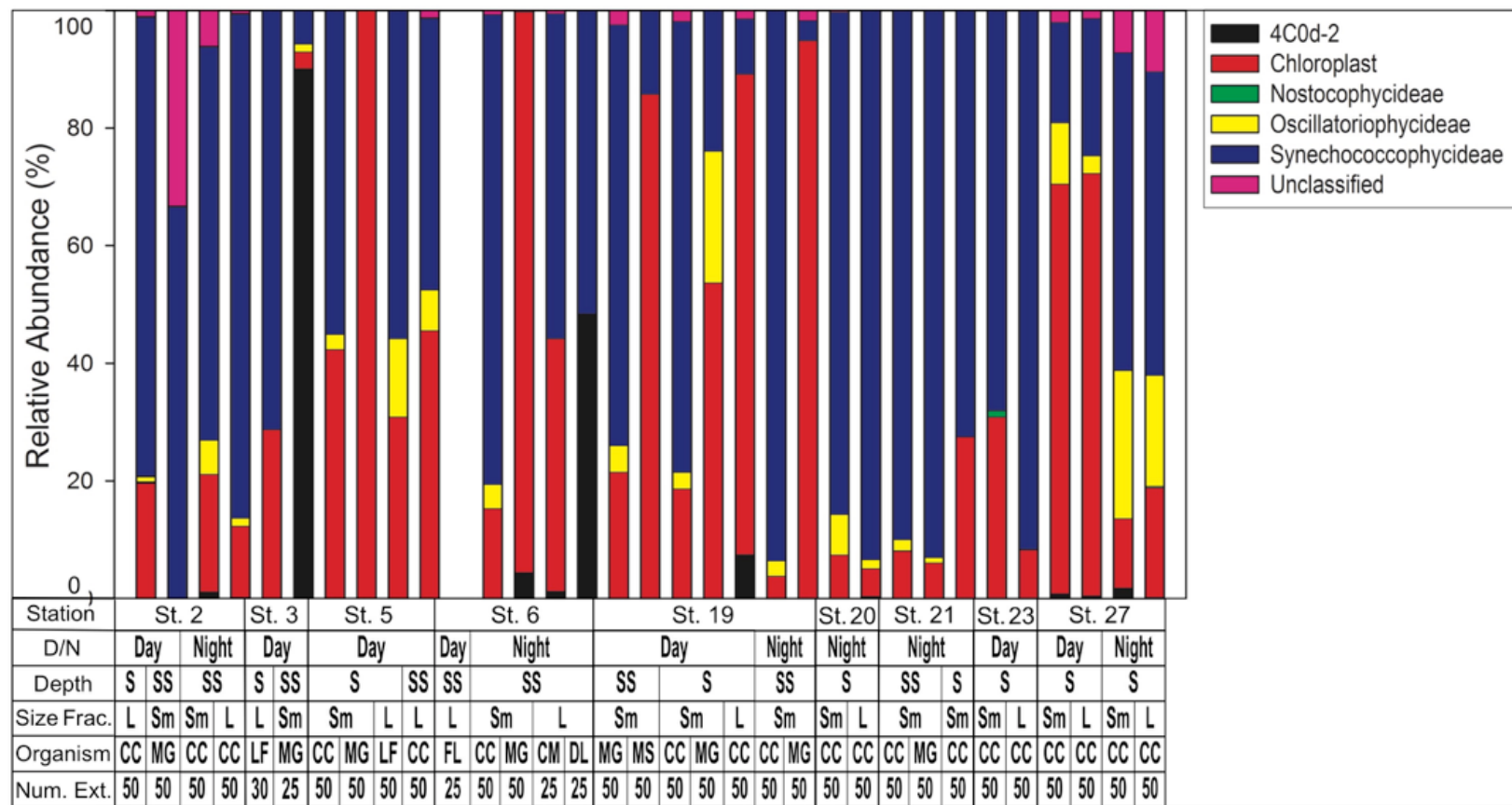


Figure 5. Cyanobacteria sequence composition by taxonomic class as determined by 16S next generation sequencing. Classes are listed in key to right. Note chloroplasts are included in the Green Genes database although not technically cyanobacteria. 4C0d-2 are closely related to cyanobacteria but recently proposed candidates for the new phylum melanabacteria. Key below graph identifies each sample with categories as follows: D/N= day or night; Depth S=Surface 0-25m, SS=Sub Surface 25-50m; Size fraction L=1.0-2.0 mm, Sm=0.5-1.0 mm; Organism CC=calanoid copepod, MG=*Macrosetella gracilis*, MS=*Miracia* spp. LF=*Lucifer faxoni*, FL= Fish Larvae, DL=Decapod Larvae, CM=Crab Megalopae; Num Ext.=animals per extraction.

Table S1. List of samples utilized in qPCR assays targeting het-1 (*Rhizosolenia*-*Richelia* DDA) and het-2 (*Hemiaulus*-*Richelia* DDA) and *Trichodesmium* spp., and estimated number of *nifH* gene copies/organism. Samples are identified by station, collection time D=Day N=Night, size fraction, organism and number of individuals pooled in each DNA extraction. Samples which resulted in detection of only 1 of 3 replicates are indicated as dnq = detected not quantifiable. Samples with 2 of 3 or 3 of 3 replicates are reported as *nifH* gene copies per organism for the respective targets. Numbers in parentheses indicate replicates out of 3 reported with 3 of 3 reported in bold. bd indicates below detection or samples which had no amplification detected. *Macrosetella gracilis* and *Miracia* spp. are harpacticoid copepods, the decapod larvae were members of the family Thalassinidae. Not Run indicates samples which were not assayed for a particular target.

St.	D/N	Depth Interval (m)	Size Fraction (mm)	Organism	Number Extracted	het-1 <i>nifH</i> copies/organism	het-2 <i>nifH</i> copies/organism	<i>Trichodesmium nifH</i> copies/organism
2	D	0-25	0.5-1.0	Calanoid Copepods	50	bd	2.91 (2)	bd
2	D	0-25	0.5-1.0	<i>Macrosetella gracilis</i>	25	bd	bd	bd
2	D	0-25	1.0-2.0	Calanoid Copepods	50	bd	dnq (1)	bd
2	D	25-50	0.5-1.0	Calanoid Copepods	50	bd	bd	bd
2	D	25-50	0.5-1.0	<i>Macrosetella gracilis</i>	50	bd	bd	bd
2	D	25-50	1.0-2.0	Calanoid Copepods	50	bd	bd	bd
2	N	25-50	0.5-1.0	Calanoid Copepods	50	Not Run	bd	bd
2	N	25-50	1.0-2.0	Calanoid Copepods	50	Not Run	bd	dnq (1)
3	D	0-25	0.5-1.0	Calanoid Copepods	50	bd	bd	Not Run
3	D	0-25	1.0-2.0	Calanoid Copepods	20	bd	bd	Not Run
3	D	0-25	1.0-2.0	<i>Lucifer faxoni</i>	30	bd	bd	Not Run
3	D	25-50	0.5-1.0	Calanoid Copepods	50	bd	bd	Not Run
3	D	25-50	0.5-1.0	<i>Macrosetella gracilis</i>	25	bd	bd	Not Run
3	D	25-50	1.0-2.0	Calanoid Copepods	50	bd	bd	Not Run
5	D	0-25	0.5-1.0	Calanoid Copepods	50	bd	11.57 (3)	dnq (1)
5	D	0-25	0.5-1.0	<i>Macrosetella gracilis</i>	50	bd	dnq (1)	bd
5	D	0-25	1.0-2.0	Calanoid Copepods	25	bd	2.11 (2)	bd
5	D	0-25	1.0-2.0	<i>Lucifer faxoni</i>	50	bd	bd	bd

St.	D/N	Depth Interval (m)	Size Fraction (mm)	Organism	Number Extracted	het-1 <i>nifH</i> copies/organism	het-2 <i>nifH</i> copies/organism	<i>Trichodesmium nifH</i> copies/organism
5	D	25-50	0.5-1.0	Calanoid Copepods	50	bd	5.87 (3)	bd
5	D	25-50	0.5-1.0	<i>Macrosetella gracilis</i>	50	bd	bd	dnq (1)
5	D	25-50	1.0-2.0	Calanoid Copepods	50	bd	3.31 (3)	bd
6	D	0-25	0.5-1.0	Calanoid Copepods	50	bd	dnq (1)	dnq (1)
6	D	0-25	0.5-1.0	<i>Macrosetella gracilis</i>	50	bd	bd	dnq (1)
6	D	0-25	1.0-2.0	Calanoid Copepods	50	bd	bd	bd
6	D	25-50	0.5-1.0	Calanoid Copepods	50	bd	1.61 (2)	bd
6	D	25-50	1.0-2.0	Calanoid Copepods	50	bd	bd	bd
6	D	25-50	1.0-2.0	Crab Megalopae	25	bd	bd	4.03 (3)
6	D	25-50	1.0-2.0	Fish Larvae	25	bd	bd	bd
6	N	0-25	0.5-1.0	Calanoid Copepods	50	bd	bd	bd
6	N	0-25	0.5-1.0	<i>Macrosetella gracilis</i>	50	bd	bd	1.88 (2)
6	N	0-25	1.0-2.0	Calanoid Copepods	50	bd	bd	bd
6	N	25-50	0.5-1.0	Calanoid Copepods	50	bd	dnq (1)	bd
6	N	25-50	0.5-1.0	<i>Macrosetella gracilis</i>	50	bd	bd	bd
6	N	25-50	1.0-2.0	Calanoid Copepods	50	bd	bd	bd
6	N	25-50	1.0-2.0	Crab Megalopae	25	bd	bd	dnq (1)
6	N	25-50	1.0-2.0	Decapod Larvae	25	bd	bd	bd
19	D	0-25	0.5-1.0	Calanoid Copepods	50	bd	bd	dnq (1)
19	D	0-25	0.5-1.0	<i>Macrosetella gracilis</i>	50	bd	bd	bd
19	D	0-25	0.5-1.0	<i>Miracia spp.</i>	50	bd	bd	bd
19	D	0-25	1.0-2.0	Calanoid Copepods	50	bd	bd	bd
19	D	25-50	0.5-1.0	Calanoid Copepods	50	bd	3.23 (3)	3.00 (2)
19	D	25-50	0.5-1.0	<i>Macrosetella gracilis</i>	50	bd	bd	bd
19	D	25-50	1.0-2.0	Calanoid Copepods	50	bd	bd	bd

St.	D/N	Depth Interval (m)	Size Fraction (mm)	Organism	Number Extracted	het-1 <i>nifH</i> copies/organism	het-2 <i>nifH</i> copies/organism	<i>Trichodesmium nifH</i> copies/organism
19	N	0-25	0.5-1.0	Calanoid Copepods	50	dnq (1)	11.03 (3)	1.64 (2)
19	N	0-25	1.0-2.0	Calanoid Copepods	50	0.10 (2)	16.76 (3)	dnq (1)
19	N	0-25	1.0-2.0	Fish Larvae	25	bd	bd	bd
19	N	25-50	0.5-1.0	Calanoid Copepods	50	bd	12.9 (3)	bd
19	N	25-50	0.5-1.0	<i>Macrosetella gracilis</i>	50	bd	bd	bd
19	N	25-50	1.0-2.0	Calanoid Copepods	50	bd	dnq (1)	2.90 (2)
19	N	25-50	1.0-2.0	Fish Larvae	25	bd	bd	bd
20	N	0-25	0.5-1.0	Calanoid Copepods	50	bd	8.42 (3)	dnq (1)
20	N	0-25	1.0-2.0	Calanoid Copepods	50	bd	bd	bd
20	N	25-50	0.5-1.0	Calanoid Copepods	50	bd	dnq (1)	bd
20	N	25-50	1.0-2.0	Calanoid Copepods	50	bd	dnq (1)	bd
21	N	0-25	0.5-1.0	Calanoid Copepods	50	bd	dnq (1)	bd
21	N	0-25	1.0-2.0	Calanoid Copepods	50	bd	bd	bd
21	N	25-50	0.5-1.0	Calanoid Copepods	50	bd	7.59 (2)	bd
21	N	25-50	0.5-1.0	<i>Macrosetella gracilis</i>	50	bd	bd	bd
21	N	25-50	1.0-2.0	Calanoid Copepods	50	bd	bd	bd
23	D	0-25	0.5-1.0	Calanoid Copepods	50	bd	dnq (1)	bd
23	D	0-25	1.0-2.0	Calanoid Copepods	50	bd	13.61 (2)	bd
23	D	25-50	0.5-1.0	Calanoid Copepods	50	bd	bd	bd
23	D	25-50	1.0-2.0	Calanoid Copepods	50	bd	bd	bd
27	D	0-25	0.5-1.0	Calanoid Copepods	50	bd	2.33 (3)	2.17 (2)
27	D	0-25	0.5-1.0	<i>Macrosetella gracilis</i>	50	bd	bd	dnq (1)
27	D	0-25	1.0-2.0	Calanoid Copepods	50	bd	bd	2.21 (3)
27	D	25-50	0.5-1.0	Calanoid Copepods	50	bd	bd	bd
27	D	25-50	1.0-2.0	Calanoid Copepods	50	bd	dnq (1)	2.20 (2)

27	N	0-25	0.5-1.0	Calanoid Copepods	50	bd	bd	dnq (1)
27	N	0-25	1.0-2.0	Calanoid Copepods	50	bd	dnq (1)	1.12 (2)
27	N	25-50	0.5-1.0	Calanoid Copepods	50	bd	bd	bd
27	N	25-50	1.0-2.0	Calanoid Copepods	50	bd	bd	bd

Table S2. TaqMAN oligonucleotides used in qPCR assays. The numbers in parenthesis designate the target positions relative to the aligned nucleotide sequence of *Azotobacter vinelandii* (accession number AY351672).

Target	Forward Primer 5'-3'	Probe	Reverse Primer 5'-3'	Source
<i>Trichodesmium</i>	GACGAAGTATTGAAG CCAGGTTTC (217-241)	CATTAAGTGTGTTGAATCT GGTGGTCCTGAGC (246-278)	CGGCCAGCGCAACC TA (284-300)	Church et al. (2005b)
Rhizosolenia-Richeliea (DDA) Het-1	CGGTTCCGTGGTGTA CGTT (105-124)	TCCGGTGGTCCTGAGCCTG GTGT (133-155)	AATACCACGACCCG CACAAAC (158-177)	Church et al. (2005a)
Hemiallus-Richeliea (DDA) Het-2	TGGTTACCGTGATGT ACGTT (106-124)	TCTGGTGGTCCTGAGCCTG GTGT (133-155)	AATGCCCGACCCAG CACAAAC (133-155)	Foster et al. (2007)

Table S3. Summary of samples and results from the NGS study. Sample collection information is reported, including station, the time of day (day or night), depth interval of collection (m) and size fraction (mm), the total number of sequences, cyanobacteria sequences, and the percentage of total sequences represented by cyanobacteria for respective samples.

Station		Depth Interval (m)	Size Fraction (mm)	Organism	Total Sequences	Cyanobacteria Sequences	Percent Cyanobacteria
n	Day/Night						
2	Day	0-25	1.0-2.0	Calanoid Copepods	27,987	12,585	44.97
2	Day	25-50	0.5-1.0	<i>Macrosetella gracilis</i>	14,747	3	0.02
2	Night	25-50	0.5-1.0	Calanoid Copepods	75,024	4,005	5.34
2	Night	25-50	1.0-2.0	Calanoid Copepods	111,459	28,506	25.58
3	Day	0-25	1.0-2.0	<i>Lucifer faxoni</i>	4,204	212	5.04
3	Day	25-50	0.5-1.0	<i>Macrosetella gracilis</i>	8,665	71	0.82
5	Day	0-25	0.5-1.0	Calanoid Copepods	45,771	7,775	16.99
5	Day	0-25	0.5-1.0	<i>Macrosetella gracilis</i>	37,313	64	0.17
5	Day	0-25	1.0-2.0	<i>Lucifer faxoni</i>	6,026	217	3.60
5	Day	25-50	1.0-2.0	Calanoid Copepods	42,326	12,844	30.35
6	Day	25-50	1.0-2.0	Fish Larvae	3,287	0	0.00
6	Night	25-50	0.5-1.0	Calanoid Copepods	24,709	2,577	10.43
6	Night	25-50	0.5-1.0	<i>Macrosetella gracilis</i>	115,046	582	0.51
6	Night	25-50	1.0-2.0	Crab Megalopae	82,420	1,259	1.53
6	Night	25-50	1.0-2.0	Decapod Larvae	41,497	33	0.08
19	Day	0-25	0.5-1.0	Calanoid Copepods	16,601	2,152	12.96
19	Day	0-25	0.5-1.0	<i>Macrosetella gracilis</i>	52,389	155	0.30
19	Day	0-25	1.0-2.0	Calanoid Copepods	54,674	999	1.83
19	Day	25-50	0.5-1.0	<i>Macrosetella gracilis</i>	33,822	67	0.20
19	Day	25-50	0.5-1.0	<i>Miracia sp.</i>	40,999	371	0.90
19	Night	25-50	0.5-1.0	Calanoid Copepods	7,259	1,808	24.91
19	Night	25-50	0.5-1.0	<i>Macrosetella gracilis</i>	35,323	59	0.17
20	Night	0-25	0.5-1.0	Calanoid Copepods	34,193	9,771	28.58

20	Night	0-25	1.0-2.0	Calanoid Copepods	91,767	16,297	17.76
21	Night	0-25	0.5-1.0	Calanoid Copepods	69,605	18,572	26.68
21	Night	25-50	0.5-1.0	Calanoid Copepods	69,076	29,706	43.00
21	Night	25-50	0.5-1.0	<i>Macrosetella gracilis</i>	46,608	254	0.54
23	Day	0-25	0.5-1.0	Calanoid Copepods	70,097	6,100	8.70
23	Day	0-25	1.0-2.0	Calanoid Copepods	86,336	14,753	17.09
27	Day	0-25	0.5-1.0	Calanoid Copepods	93,353	9,075	9.72
27	Day	0-25	1.0-2.0	Calanoid Copepods	126,192	6,437	5.10
27	Night	0-25	0.5-1.0	Calanoid Copepods	67,591	5,856	8.66
27	Night	0-25	1.0-2.0	Calanoid Copepods	114,001	4,133	3.63
Total					1,750,367	197,298	11.27

CHAPTER 5

Summary and Concluding Remarks

The Amazon River plume supports large-scale blooms of diatom diazotroph associations (DDAs) in the western tropical North Atlantic (WTNA) due to input of silicon and phosphorus (Subramaniam et al. 2008). Plume-associated DDA blooms have been observed for nearly two decades (Carpenter et al. 1999; Carpenter 2002; Foster et al. 2007; Goes et al. 2014), but to understand the fate of these blooms it is necessary to investigate the secondary production in the WTNA as well. My research is the first to investigate the effect of the Amazon River plume on mesozooplankton community composition in the WTNA (Chapter 2). Furthermore, I provide measurements of grazing for meso- and microzooplankton (Chapter 3) and show direct consumption of DDAs, *Trichodesmium*, and unicellular cyanobacteria by zooplankton (Chapter 4).

A number of studies in river plumes show that the physical processes associated with the mixing of fresh and saltwater, as well as enhancement of primary production, act to aggregate zooplankton and support distinct zooplankton communities (Govoni et al. 1989; Grimes and Finucane 1991; Dagg 1995; Morgan et al. 2005). My research is the first to show distinct mesozooplankton communities along the Amazon River plume salinity gradient. In spring, total mesozooplankton and copepod abundance was positively correlated with sea surface salinity (SSS), while in the fall both were negatively correlated with SSS. This was due to a seasonal change in abundance at the salinity end-members (low salinity plume and oceanic stations) but not the mesohaline plume stations where DDAs occur. Furthermore, the distribution patterns for the coastal decapod shrimp *Lucifer faxoni*, decapod and fish larvae, and euphausiids suggest that the plume functions as an “extended” estuary into the WTNA, and may be utilized as a nursery habitat for some taxa.

Mesozooplankton grazing showed a seasonal lag pattern of low grazing in the spring and elevation in the fall. Impact of mesozooplankton grazing on Chl-*a* in the surface 150m was 2.3% and 7.1% of Chl *a*, for spring and fall respectively. This seasonal difference in grazing was even more apparent when grazing impact was limited to the surface 25 m of the water column when fall (20.1%) was much higher than spring (2.5%). The concentration of mesozooplankton grazing in surface waters associated with the plume supports the “extended” estuary function of the plume by providing an area of concentrated high primary production that they graze. Similar seasonal patterns of grazing have been observed in the Mississippi River plume (Dagg 1995), suggesting that other large river plumes may act as an “extended” estuaries. Furthermore, a suggested shift in food web structure highlights the importance of the Amazon River plume for biogeochemical cycling. Stations with SSS<33 had a short, coastal “export” food web dominated by mesozooplankton grazing compared to those with SSS>33 which had a microzooplankton dominated “retention” food web. Since low salinity regions occur beyond the shelf break, these low salinity and mesohaline export food webs could enhance carbon export to depth.

Results from the molecular analysis indicate that copepods directly consume DDAs, *Trichodesmium*, and other unicellular cyanobacteria (e.g., *Synechococcus*). Prior work utilized stable isotopes which can identify the source of nitrogen, and showed incorporation of diazotrophic nitrogen into mesozooplankton (Montoya et al. 2002; Landrum et al. 2011; Loick-Wilde et al. 2016). However, stable isotope methodology doesn’t demonstrate direct consumption of diazotrophs, as N₂ may be incorporated into the food web through the microbial loop before incorporation into mesozooplankton.

Similarly, work by Conroy et al. (2016) relied on pigment analysis which cannot differentiate the Chl-*a* source in copepod guts. The molecular results are thus novel in that they are the first report of direct DDA consumption. Also novel is the first direct evidence of *Trichodesmium* grazing by calanoid copepods. This finding is important given the abundance of *Trichodesmium* in the tropical and subtropical oceans, with previous studies suggesting harpacticoid copepods were the only significant grazers on *Trichodesmium* (Hawser et al. 1992; O’Neil and Roman 1994; O’Neil et al. 1996; O’Neil 1998).

Similar to other river plumes, the Amazon River supports enhanced secondary production of zooplankton, likely through a combination of enhanced primary production (i.e., bottom up control) and physical aggregation processes. Given the predicted changes of the Amazon River hydrological cycle with climate change (Gloor et al. 2013), our measurements of mesozooplankton abundance and grazing provide an important baseline for future comparison. Future research should examine if the lag in mesozooplankton grazing and abundance, observed only in low salinity plume waters, occurs over a consistent time frame (i.e., from peak discharge into seasonal retroflection). Loick-Wilde et al. (2016) suggest that the inshore low salinity plume waters may act as seed populations for DDA blooms in the mesohaline plume waters. If that is the case, then the mesozooplankton response to the phytoplankton accumulations may not be a single annual event. Instead, it may occur throughout the year in quick pulses in response to periodic advection of the inshore diatom populations into offshore waters. Most observations of the DDA blooms have occurred during spring (Foster et al. 2007; Subramaniam et al. 2008; Goes et al. 2014) but Carpenter et al. (1999) reported a DDA

bloom during a fall cruise to the WTNA. Future sampling should investigate whether the mesozooplankton grazing and abundance patterns we observed in fall and spring similarly occur from fall to winter or winter to spring. Furthermore, future research should quantify direct grazing on DDAs and *Trichodesmium* by copepods and other mesozooplankton taxa through controlled experiments and further application of the molecular methods developed here. Ideally, development of DDAs and *Trichodesmium* cultures would allow for controlled laboratory experiments to measure grazing rates as well as develop a gut degradation rate for DDA and *Trichodesmium* target DNA. Lastly, my results are useful for improvement of biogeochemical models of the region (Cooley et al. 2007; Stukel et al. 2014), as well as in other river plumes, or areas where expansive DDA blooms are observed (Foster et al. 2009; Grosse et al. 2010).

REFERENCES

- Carpenter, E. J. 2002. Marine Cyanobacterial Symbioses.pdf. *Biology and Environment: Proceedings of the Royal Irish Academy* **102B**: 15–18.
- Carpenter, E. J., J. P. Montoya, J. Burns, M. R. Mulholland, A. Subramaniam, and D. G. Capone. 1999. Extensive bloom of a N₂-fixing diatom/cyanobacterial association in the tropical Atlantic Ocean. *Marine Ecology Progress Series* **185**: 273–283.
- Conroy, B. J., D. K. Steinberg, M. R. Stukel, J. I. Goes, and V. J. Coles. 2016. Meso- and microzooplankton grazing in the Amazon River plume and western tropical North Atlantic. *Limnology and Oceanography* **61**: 825–840. doi:10.1002/lo.10261
- Cooley, S. R., V. J. Coles, A. Subramaniam, and P. L. Yager. 2007. Seasonal variations in the Amazon plume-related atmospheric carbon sink: SEASONALITY OF CO₂ IN AMAZON PLUME. *Global Biogeochemical Cycles* **21**: n/a–n/a. doi:10.1029/2006GB002831
- Dagg, M. J. 1995. Copepod grazing and the fate of phytoplankton in the northern Gulf of Mexico. *Continental Shelf Research* **15**: 1303–1317. doi:10.1016/0278-4343(94)00086-3
- Foster, R. A., A. Subramaniam, C. Mahaffey, E. J. Carpenter, D. G. Capone, and J. P. Zehr. 2007. Influence of the Amazon River plume on distributions of free-living and symbiotic cyanobacteria in the western tropical north Atlantic Ocean. *Limnology and oceanography* **52**: 517–532.
- Foster, R. A., A. Subramaniam, and J. P. Zehr. 2009. Distribution and activity of diazotrophs in the Eastern Equatorial Atlantic. *Environmental Microbiology* **11**: 741–750. doi:10.1111/j.1462-2920.2008.01796.x

- Gloor, M., R. J. W. Brienen, D. Galbraith, and others. 2013. Intensification of the Amazon hydrological cycle over the last two decades: AMAZON HYDROLOGIC CYCLE INTENSIFICATION. *Geophysical Research Letters* **40**: 1729–1733. doi:10.1002/grl.50377
- Goes, J. I., H. do R. Gomes, A. M. Chekalyuk, and others. 2014. Influence of the Amazon River discharge on the biogeography of phytoplankton communities in the western tropical north Atlantic. *Progress in Oceanography* **120**: 29–40. doi:10.1016/j.pocean.2013.07.010
- Govoni, J. J., D. E. Hoss, and D. R. Colby. 1989. The spatial distribution of larvalfishes about the Mississippi River plume. *Limnol. Oceanogr.* **34**: 178–187. doi:10.4319/lo.1989.34.1.0178
- Grimes, C. B., and J. H. Finucane. 1991. Spatial distribution and abundance of larval and juvenile fish, chlorophyll and macrozooplankton around the Mississippi River discharge plume, and the role of the plume in fish recruitment. *Marine ecology progress series*. Oldendorf **75**: 109–119.
- Grosse, J., D. Bombar, H. N. Doan, L. N. Nguyen, and M. Voss. 2010. The Mekong River plume fuels nitrogen fixation and determines phytoplankton species distribution in the South China Sea during low and high discharge season. *Limnology and Oceanography* **55**: 1668–1680. doi:10.4319/lo.2010.55.4.1668
- Hawser, S. P., J. M. O’neil, M. R. Roman, and G. A. Codd. 1992. Toxicity of blooms of the cyanobacterium *Trichodesmium* to zooplankton. *Journal of applied phycology* **4**: 79–86.
- Landrum, J. P., M. A. Altabet, and J. P. Montoya. 2011. Basin-scale distributions of

- stable nitrogen isotopes in the subtropical North Atlantic Ocean: Contribution of diazotroph nitrogen to particulate organic matter and mesozooplankton. Deep Sea Research Part I: Oceanographic Research Papers **58**: 615–625.
doi:10.1016/j.dsr.2011.01.012
- Loick-Wilde, N., S. C. Weber, B. J. Conroy, D. G. Capone, V. J. Coles, P. M. Medeiros, D. K. Steinberg, and J. P. Montoya. 2016. Nitrogen sources and net growth efficiency of zooplankton in three Amazon River plume food webs. Limnol. Oceanogr. **61**: 460–481. doi:10.1002/lno.10227
- Melle, W., B. Ellertsen, and H. R. Skjoldal. 2007. Zooplankton: the link to higher trophic levels, p. 203–226. *In* The Norwegian Sea Ecosystem. Trondheim: Tapir Academic Press.
- Montoya, J. P., E. J. Carpenter, and D. G. Capone. 2002. Nitrogen fixation and nitrogen isotope abundances in zooplankton of the oligotrophic North Atlantic. Limnology and Oceanography **47**: 1617–1628.
- Morgan, C. A., A. De Robertis, and R. W. Zabel. 2005. Columbia River plume fronts. I. Hydrography, zooplankton distribution, and community composition. Mar. Ecol.-Prog. Ser. **299**: 19–31. doi:10.3354/meps299019
- O'Neil, J. M. 1998. The colonial cyanobacterium *Trichodesmium* as a physical and nutritional substrate for the harpacticoid copepod *Macrosetella gracilis*. Journal of plankton research **20**: 43–59. doi:10.1093/plankt/20.1.43
- O'Neil, J. M., P. M. Metzler, and P. M. Glibert. 1996. Ingestion of $^{15}\text{N}_2$ -labelled *Trichodesmium* spp. and ammonium regeneration by the harpacticoid copepod *Macrosetella gracilis*. Marine Biology **125**: 89–96.

- O'Neil, J. M., and M. R. Roman. 1994. Ingestion of the cyanobacterium *Trichodesmium* spp. by pelagic harpacticoid copepods *Macrosetella*, *Miracia* and *Oculosetella*. *Hydrobiologia* **292**: 235–240. doi:10.1007/BF00229946
- Sommer, U., R. Adrian, L. De Senerpont Domis, and others. 2012. Beyond the Plankton Ecology Group (PEG) Model: Mechanisms Driving Plankton Succession. *Annual Review of Ecology, Evolution, and Systematics* **43**: 429–448. doi:10.1146/annurev-ecolsys-110411-160251
- Steinberg, D. K., and R. H. Condon. 2009. Zooplankton of the York River. *Journal of Coastal Research* 66–79. doi:10.2112/1551-5036-57.sp1.66
- Stukel, M. R., V. J. Coles, M. T. Brooks, and R. R. Hood. 2014. Top-down, bottom-up and physical controls on diatom-diazotroph assemblage growth in the Amazon River plume. *Biogeosciences* **11**: 3259–3278. doi:10.5194/bg-11-3259-2014
- Subramaniam, A., P. L. Yager, E. J. Carpenter, and others. 2008. Amazon River enhances diazotrophy and carbon sequestration in the tropical North Atlantic Ocean. *PNAS* **105**: 10460–10465. doi:10.1073/pnas.0710279105
- Sundby, S., K. F. Drinkwater, and O. S. Kjesbu. 2016. The North Atlantic Spring-Bloom System—Where the Changing Climate Meets the Winter Dark. *Front. Mar. Sci.* 28. doi:10.3389/fmars.2016.00028
- Winder, M., and J. E. Cloern. 2010. The annual cycles of phytoplankton biomass. *Philos Trans R Soc Lond B Biol Sci* **365**: 3215–3226. doi:10.1098/rstb.2010.0125

VITA

BRANDON JUDD CONROY

Born in Portsmouth, VA on January 16, 1987. Graduated from Brookville High School and the Central Virginia Governor's School for Science and Technology in 2005. Earned a Bachelor of Science in Biology with a concentration in Environmental Biological Conservation from the University of Virginia in 2009. Worked as research assistant in Dr. Donald Anderson's laboratory at Woods Hole Oceanographic Institution from 2009-2010. Entered graduate school at the Virginia Institute of Marine Science, College of William and Mary under advisor Dr. Deborah K. Steinberg in 2010.